Potential Assessment and Feasibility Analysis of Solar PV - Genset Stand-Alone Hybrid Power System with Energy Management for Rural Area

(The Case Study on Jarso Kebele in Konso, Southwest Ethiopia)

By Ollata Kalano Robayo

A Thesis Submitted to the Department of Electrical Power and Control Engineering

School of Electrical Engineering and Computing

Presented in Partial Fulfillment of the Requirement for the Degree of Master's in Electrical Power and Control Engineering (Specialization in **Power Electronics**)

Office of Graduate Studies

Adama Science and Technology University

Adama, Ethiopia

September, 2019

Potential Assessment and Feasibility Analysis of Solar PV - Genset Stand-Alone Hybrid Power System with Energy Management for Rural Area

(The Case Study on Jarso Kebele in Konso, Southwest Ethiopia)

By: Ollata Kalano

Advisor: Molla Biweta (Ph.D.)

A Thesis Submitted to the Department of Electrical Power and Control Engineering

School of Electrical Engineering and Computing

Presented in Partial Fulfillment of the Requirement for the Degree of Master's in Electrical Power and Control Engineering (Specialization in **Power Electronics**)

Office of Graduate Studies

Adama Science and Technology University

Adama, Ethiopia

September, 2019

Approval of Board of Examiners

We, the undersigned, members of the Board of Examiners of the final open defense by ________________________________ have read and evaluated his thesis entitled "**Potential Assessment and Feasibility Analysis of Solar PV - Genset Stand-Alone Hybrid Power System with Energy Management for Rural Area (The Case Study on Jarso Kebele in Konso, Southwest Ethiopia)**" and examined the candidate. This is, therefore, to certify that the thesis has been accepted in partial fulfillment of the requirement of the Degree of Master's in Electrical Power and Control Engineering (Specialization in **Power Electronics**).

____________________	__________	__________
Advisor	Signature	Date
____________________	__________	__________
Chairperson	Signature	Date
____________________	__________	__________
Internal Examiner	Signature	Date
____________________	__________	__________
External Examiner	Signature	Date

Declaration

I hereby declare that this MSc Thesis is my original work and has not been presented for a degree in any other university, and all sources of material used for this thesis have been duly acknowledged.

Name: ____

Signature: ____

This MSc Thesis has been submitted for examination with our approval as thesis advisors.

Name of Advisor: ______________________________

Signature:_________________________________

Date of submission: ________________

Advisors approval sheet

To: Electrical Power and Control Engineering department

Subject: Thesis Submission

This is to certify that the thesis entitled **"Potential Assessment and Feasibility Analysis of Solar PV - Genset Stand-Alone Hybrid Power System with Energy Management for Rural Area (The Case Study on Jarso Kebele in Konso, Southwest Ethiopia)"** submitted in partial fulfillment of the requirements for the degree of Master's in Electrical Power and Control Engineering (Specialization in **Power Electronics**), the Graduate program of the department of Electrical Power and Control Engineering, and has been carried out by **Ollata Kalano** Id. No **PR15368/10**, under my supervision. Therefore, I recommend that the student has fulfilled the requirements and hence hereby he can submit the thesis to the department.

__________________________ __________________ ___________________

Name of major Advisor Signature Date

Acknowledgments

First and foremost, praises and thanks to the God, the Almighty, for His showers of blessings throughout my thesis work to complete the research successfully.

I would like to start, by expressing my deepest gratitude to my professional assistance, thesis advisor Dr. Molla Biweta, for his guidance support, and constant supervisions. He went to great lengths so I can achieve my goals and become the researcher that I am today. This MSc. study would not have been possible without them. For that, I am forever grateful.

I would like to express my sincere gratitude to Dr. Ongaya Oda who has always been there for me, helping me during the most difficult times. Special thanks go to my family, especially my wife, father, mother, brothers and friend, Kassahun Berisha whose endless support helped me get through this tiring experience.

I would like to say thanks to my friends and research colleagues, Mr. Hamza Gadisa , Mr. Assefa sefu, Mr. Assaye Fetene, and Mr. Shukri Abdujebar for their constant encouragement.

I thank the School of Electrical and Computing Engineering, ASTU for their support to do this work. I thank Mr. Hinsermu Alemayehu department head of Electrical Power and Control Engineering for his genuine support to complete this thesis successfully.

Finally, my thanks go to all the people who have supported me to complete the research work directly or indirectly.

Abstract

A most of Sub – Saharan African countries the access of electricity supply is extremely antiquated compared to developed countries. When comparing Ethiopia with other African countries, the overall electric access and the electric supplying system is very low. Most of the Ethiopian rural areas do not have access to electrical energy and the urban areas are not satisfied with the present energy supply. Accordingly, Jarso Kebele, Kondo village is one of a rural community found in southwest Ethiopia, which the access of grid electric supply extinction is not available yet. Therefore, this thesis aims to undertake the feasibility analysis of Solar PV – Genset hybrid power system with energy management to come up with the best level of techno–economic availability and configuration for electric supplying to this rural village. The study conducted by sizing of all components of hybrid system analytically and modeled in the MATLAB / SIMULINK program to simulate a real PV system behavior, then a P&O MPPT technique, output results has a good performance than direct method. Also, the PLC-based energy management system has been designed to optimize the off-grid system. The model of Solar PV, diesel generator and battery storage were developed by Homer software for optimization and sensitivity analysis. Using the developed model the overall simulation results obtained were arranged based on the feasibility of power supply system has in ascending order to their total net present cost (Total NPC). The obtained simulation results show that the majority of the power is produced from Solar PV. The optimization simulation result describes total NPC of $154,090, and cost of energy (COE) of $0.298/kWh is minimum best competitive cost of the hybrid power system to electrify the community.

Finally, this investigation identified that the hybrid system PV/diesel generator/battery is cost-effective and environmentally friendly compared with PV/Genset, Genset/battery, and only diesel generator in categories optimization results for the community.

Keywords: *Hybrid, Solar, Diesel Generator, Energy Storage, MPPT, MATLAB, PSIM PLC, and HOMER Software.*

Table of Contents

List of Figures

List of Tables

List of Abbreviations

AC	Alterative Current
BDC	Bi-Directional Converter
CC	Cycle charging
COE	Cost of Energy
CFL	Compact fluorescent lumps
D	Duty ratio
DC	Direct Current
DG	Diesel Generator
DOA	Days of Autonomy
DOD	Depth of Discharge
EAPP	Eastern Africa Power Pool
EEPCo	Ethiopian Electric Power Corporation
EMR	Electricity Match Rate
FC	Fossil Cell
GDP	Growth Domestic Program
GTP	Growth and Transformation Plan
HES	Hybrid Energy System
HOMER	Hybrid Optimization Model for Electric Renewable
HPS	Hybrid Power System
LCD	Liquid crystal display
LED	Light emitting diode
LF	Load following
LPF	Low Pass Filter
MCU	Microcontroller
MEM	Match Evaluation Method
MOSPO	Multi-Objective Particle Swarm Optimization

MPPT	Maximum Peak Power Tracking
PC	Personal Computer
PID	Proportional Integration Differentiation
PLC	Programmable Logic Control
PV	Photovoltaic
P&O	perturbs and observations
NASA	National Aeronautics and Space Administration
NMA	National Metrological Agency
NPC	Net Present Cost
RES	Renewable Energy System
SNNPR	Southern Nation Nationalities and People Region
TV	Televisions
UEAP	Universal Electricity Access Program
UNEP	United Nations Environment Program
USB	Universal serial bus
VRLA	Valve regulated lead-acid

List of Symbols

C_b	Capacity of battery
GWh	Giga watt hour
I_{mp}	Maximum peak current
I_{sc}	Short circuit current
KW	Kilo watt
KWh	Kilo watt hour
KV	Kilo Volts
MW	Mega Watts
P_{mp}	maximum peak power
R_S	series Resistance
R_{SH}	Shunt Resistance
V_{mp}	Maximum peak voltage
V_{oc}	Open circuit voltage
W	Watt
W/m^2	Watt per square meter
η_B	Efficiency of Battery
η_{CC}	Efficiency of charge controller
η_{inv}	Efficiency of inverter
η_{mo}	Efficiency of module
η_{Rec}	Efficiency of rectifier
θ_z	zenith angle
ϕ	Latitude of the location
δ	Declination angle
ω	Solar hour angle

CHAPTER 1

INTRODUCTION

1.1 Background

At the current rates of consumption, the reserves of oil and gas would be adequate to meet the demand for only another 41 and 67 years, respectively [1]. In addition to this, environmental problems are growing dramatically due to a combination of several factors. These factors include an increase in world population, energy consumption, and industrial activity. Solutions to such environmental challenges require a policy aimed at long-term sustainable and clean development. In this respect, renewable energy resources appear to be one of the most efficient and effective solutions.

It is now a globally accepted reality that electrical energy is fundamental for social and economic development. Also, a research done by the United Nations Environment Program (UNEP), describes that an estimated 1.7–2.0 billion people in the world have no the access of electricity services from the grid, and thus majority of which live in underdeveloped rural areas [2] [3]. The statistic shows that population growth is mostly in developing countries where most of the people live in remote, rural areas. The extension of the utility grid is complicated and expensive due to geographical, economic and social barriers. Up to now, mostly diesel generators are used for rural electrification. This is not a good solution because of fuel cost and maintenance cost is expensive and unfriend with environment. In such conditions, an option is to utilize locally accessible sustainable power sources (e.g. PV, wind, hydro biomass tidal geothermal and so on) and implement modular, expandable and task-oriented system concepts that guarantee cost-effective and sustainable resources of energy, especially for remote and rural areas.

Ethiopia is located in the eastern part of Africa between 3^o to 15^o north and 33^o to 48^o east. With the landmass of 1.14 million square kilometers in third goliaths and second populace countries in the Sub – Saharan African with an assessed population of around 99 million [4]. As United Nation Development Program (UNDP, 2015) report the positioned Ethiopia 173^{th} in the human advancement list with per capital normal pay of 619.10 $ and around 30% of the population underneath neediness line [5]. Moreover, the growth rate population per year is increasing 2.3% and an average annual GDP growth rate around 10% fast-growing for a decade [6].

The access of electricity in Ethiopia is one of the lowest by any standard, with only 25% of households connected and 56% of electricity coverage by Ethiopian Electric Power Corporation (EEPCo) in 2017. The electricity grid is from Hydropower 3810 MW, Wind 324MW, Geothermal 7MW, and Diesel 143MW. The total electric generation capacity of 4284MW and cross-border interconnection with Djibouti and Sudan at 230KV level is a power flow up to 90 MW and 250MW respectively. Moreover, interconnection with Kenya 2,000MW, 500KV (construction to be completed in 2019).

Table 1.1 the total renewable energy sources potential currently available in Ethiopia [7] [8].

Types of source	Amount
Hydropower	45,000 MW
Solar energy potential	(annual average daily irradiation) 5.5 kWh /m^2 /day
Geothermal potential	5,000 to 10,000 MW
Wind energy	>1000 GW(average wind speed of ≥7 m/s , 50 m above ground level)
Wood	3.9388751808 10^{12} MW/year
Agricultural waste	52.7527926 to 70.3370568 MW/year
Oil shale	889.76376852 GW
Coal	1055.055852 GW

The development of Ethiopia's renewable energy sector has been one of the leading new drivers of economic growth in the country. The bulk of the country's 2.26 GWh energy generation capacity comes from hydroelectricity, which accounts for 86% of the country's total capacity. The government of Ethiopia more focuses on private investment in its renewable energy sector as vital for the success by an achievements Growth and Transformation Plan (GTP), which aims to reshape the country into a middle-income state by 2025. Considering the high amount of solar irradiation Ethiopia receives, averaging at 5.2 kWh/m^2/day the development of solar PV projects in Ethiopia is a highly remunerative opportunity for investors.

Renewable energy technologies are more dominantly the solution for clean and abundant energy gathered from self- renewing resources such as the sun, wind, water, animal and plants. Renewable energy sources offer more important energy compared to conventional energy sources. The advantage of the renewable generation system reduces the use of expensive fuels, allows for the clearness generation of electric power and friend with environments and improve the standard living of many people in rural areas. The main drawback of the solar system is that naturally variable solar radiation causes power and voltage fluctuation problem at the load side. These kinds of problems can be solved by using suitable power converters and control strategies.

The electricity system can be either grid or off-grid. Stand-alone (off-grid) system is the type of system, which is not connected to the main utility grid. The stand-alone system operates independently, that makes system more reliable and the best application for remote areas. Among the conventional energy sources, the hybrid of wind and solar energy system are considered an ideal solution for rural electrification due to abundant solar radiation and significant wind distribution availability around the rural societies in Ethiopia. This thesis deals the production of electrical energy from solar–diesel generator hybrid with battery bank system and energy management for Jarso Kebele in Konso, Southwest Ethiopia.

1.2 Statement of the Problem and motivation

It is known that energy consumption for any country's development takes the first rank. But, most of the developing countries like Ethiopia, the number of people and energy consumption do not match. Most of the Ethiopian rural areas do not have access to electrical energy and the urban areas are not satisfied with the present energy supply. Remote area, due to the lack of electricity, the community has exerted a negative impact on the socio-economy condition, health, education sectors, environments, and politics. Additionally, due to the lack of electricity in rural areas, women invests their time and their potential to collect firewood, to fetch water, cooking food for their family and other activities. For these reasons, the opportunity for learning has not given to women in societies. Jarso Kebele in SNNPR, Konso Woreda is one of such rural communities. The community of Jarso mostly uses traditional biomass for cooking food and Kerosene for heating and lightning. To overcome the above problems, the hybrid solar energy, diesel generator and battery storages source used as the best optional solution for the selected area. The motivation of this research is the potential existence of solar radiation is very high to overcome the problem of the community by the power supplying an alternative for "Jarso" local Kebele in Konso, southeast Ethiopia district area.

1.3 Objective

1.3.1 General objective

The main aim of this thesis is to overcome the problem of electricity in Jarso Kebele by studying the potential assessment and feasibility analysis of solar – Genset standalone hybrid power system with energy management by using MATLAB/SIMULINK, HOMER software and PSIM PLC simulator.

1.3.2 Specific objective

The specific objectives of this study are to:

- potential evaluation and assess the feasibility solar radiations of the selected site.
- determine community loads and based on result selecting a suitable size of diesel generator, PV module, battery, charge controller, and inverter.
- estimate the size of PV array, battery storages, charge controller, and inverter.
- estimate and analyze the optimal system configuration and develop appropriate dispatch strategy and manage, control, and monitor the energy supply of each sources using programmable logic control (PLC).
- model and simulate of hybrid solar–diesel generator standalone with batter system for a selected suitable location.

1.4 Scope of the project

This thesis work is delimited to studying the potential assessment and feasibility analysis of the solar–diesel standalone hybrid system with energy management for Jarso Kebele in Konso, southwest Ethiopia. More specifically, it has only focus on simulation while hardware implementation is out of the scope due to installation cost. From various renewable energy sources, it has only consider solar energy.

1.5 Significance of the project

The significance of this thesis is improving the living standard of the rural areas, which are not electrified from the national grid. To that end, a PV – diesel generator - batter's hybrid power supply system to solve the problems of the societies like TV, lighting, supplying refrigerators, mobile charges, etc.

1.6 Methodology

To design the hybrid solar–diesel with batteries energy-saving system, the following issues have been considered:

- Doing literature review and identify the research problems: The related literature review on hybrid system applicable for rural area electrification are considered. These include journal transactions, journal article, conference papers and books
- Identified the place where high potentials solar radiation is available
    - ✓ Estimating solar energy depending on climatic data obtaining from NASA surface meteorological online sources, solar resource data from global solar radiation and Solar Energy database for the selected site indicates that the annual solar radiation
    - ✓ Estimating socioeconomic for the selected site in simulation
- Developed a mathematical model for a solar system and an algorithm for MPPT of solar panels
- Developed a model design of PV/Diesel/battery hybrid system with energy management and charge controller for the selected site by using MATLAB, PSIM PLC simulator and analyzing optimization and sensitivity using the HOMER software simulation.

1.7 Thesis organizations

Chapter one discusses the background, the statements of problem, objective, the significance of the study, methodology and the overall thesis work.

Chapter two describes the literature review including different hybrid system related works.

Chapter three described the estimation of the feasibility of solar radiation collected different sources, community daily loads and sizing of each component needed for the hybrid system and energy managements.

Chapter four has been described the modeling system

Chapter five has been described the simulation results and discussion system and,

Chapter six presents conclusion and recommendations of this thesis.

CHAPTER 2

LITERATURE REVIEW AND THEORETICAL BACKGROUND

2.1 Theoretical Background

Over the last few years, many types of research have been done on the Hybrid power system. Under this chapter, the renewable energy technologies that are used for remote electrification in the world is described. However, the solar PV energy technology is the major of this study as it is widely available and abundant, especially in the region which selected for the case study area and the other renewable energy discussed for the comparison purposes and to understand the solution that is available and have been design the off-grid electrification for the area.

2.1.1 Solar Photovoltaic

The conversion of solar radiation directly into electricity occurs by the photovoltaic effect, which first observed by Becquerel in 1839. It quite generally explained as the emergence of an electric voltage between two electrodes attached to a solid or liquid system upon brightly light onto this system. Energy conversion devices, that utilized to convert sunlight to electricity by the use of the photovoltaic effect, are called solar cells. Single converter cell is called a solar cell and many solar cells become form solar module or several photovoltaic module combinations of such cells designed to increase the electric power output is called solar array and the name ‘Photovoltaic Arrays’. These arrays, composed of several thousand individual cells, can function as central electric power stations, converting sunlight into electrical energy for distribution to residential users, commercial and industrial. Solar cells in much smaller schemes are common, referred to as panels or solar cell panels. Practically, all photovoltaic devices connecting with a P-N junction in a semiconductor device across which the photovoltage is created. The solar panels mainly consist of Silicon with A semiconductor material, is most, commonly used. [9]

2.1.1.1 Operation Principle of Solar Cell or Photovoltaic Cell

A solar cell is a combination of two different layers of silicon p-type and n-type. When a negative type semiconductor is connected to a positive type semiconductor, the electrons near to the junction jump from N region to P region and, similarly the holes close to the junction jump from

P region to N region this phenomenon create a depletion layer. Therefore, the electrons will be in the P region at a depletion layer and the holes in the n region at a depletion layer an electric field formed in this depletion layer because of the movement of holes and the electrons. Depletion layer also called the space charge region, which prevents the migration of charge carriers from the side located to the other side. When a semiconductor exposed to sunshine, the photons smash the electrons of the silicon atoms, and drive out it, making extra free electrons and extra free holes. The electric field makes the direction of the electron movement to the negative side while the direction of the flow of the gap to the positive side, this called a photo generation of charge carriers and happens during negative and positive type semiconductors. The separation which results from the formation of positive and negative charges during the junction is known as voltage or potential difference. Where the negative charge is accumulated along with one position and the positive charge on the other position of the solar cell, a potential difference between these sides of the solar cell formed is around 0.5 V as shown in Figure 2.1 [10]. This potential difference in a solar cell depends on the material and does not depend on the area of the cell. Figure 2.1 a) shows a solar cell structure and working principle and b) shows the configuration of a solar panel.

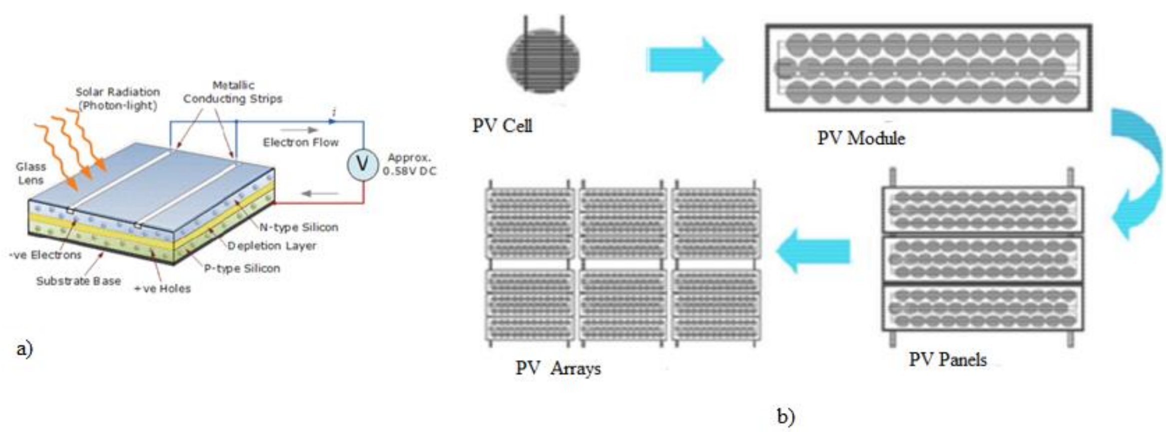

Figure 2.1 a) Solar cell components and its working principle b) configuration of a solar pane [11].

2.1.1.2 Types of Solar PV Cells

The electricity generation depends on the size of the PV cell, the conversion efficiency, and sunlight intensity of the local area. Based on [9] the material two categories of PV cells are used in most of today's commercial PV modules: thin-film and crystalline silicon.

I. **Mono-crystalline PV Cells:** Monocrystalline PV cell is the first generation of all PV cells that made from single crystals, that has high heat resistance ability and most efficient than both polycrystalline PV cell and thine film PV cell but consume more time to manufacture and more expensive. This technology can convert 1000W/m^2 solar radiation to approximately 140W of electricity in PV cell surface area of 1m^2 [12].

II. **Polycrystalline PV Cells:** That made from a combination of the multi-crystalline PV cell, which is the most efficient of the mainstream PV products, most widely used cells nowadays. This technology can convert 1000W/m^2 solar radiation to approximately 130W of electricity in PV cell surface area of 1m^2 [12]. Size of poly-crystalline solar panel is larger than mono-crystalline panel to get the same wattage because the mono-crystalline is more efficient per area than the multi-crystalline. So when comparing the two PV panels in terms of size to get high power output, single-crystalline is good in usefulness.

III. **Thin Film PV Cells:** It is a second-generation PV cell, which made from real crystals rather the silicon is deposited on stainless steel, plastics or glass to form the solar module. These types of PV cells are much less efficient than the above two but the production process costs less. The inefficiency shows that larger panels of this type required producing the same power as the mono or polycrystalline panels. They have efficiency from 5% to 13% and their lifespan is about 15-20 years.

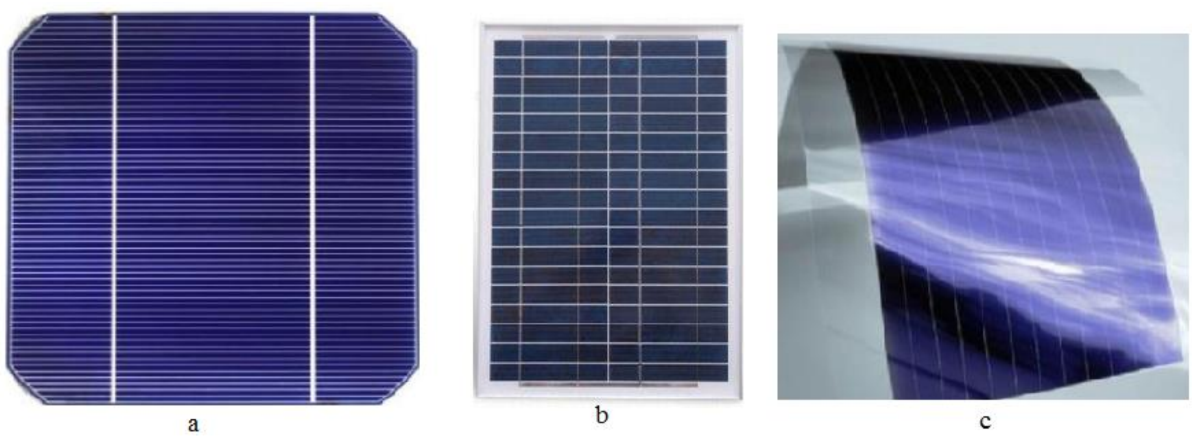

Figure 2.2 Types PV cell a) Mono-crystalline b) Poly-crystalline c) Amorphous [13]

2.1.1.3 Solar Cell Characteristics

The current-to-voltage characteristic and power-to-voltage characteristics of a solar cell are non-linear, which make it difficult to determine the maximum power point. It is directly to find the maximum power point (MPPT) on a linear curve as maximum power is transferred at the midpoint of the current-voltage characteristic. A typical I-V characteristic of a solar cell is shown in Fig 2.3.

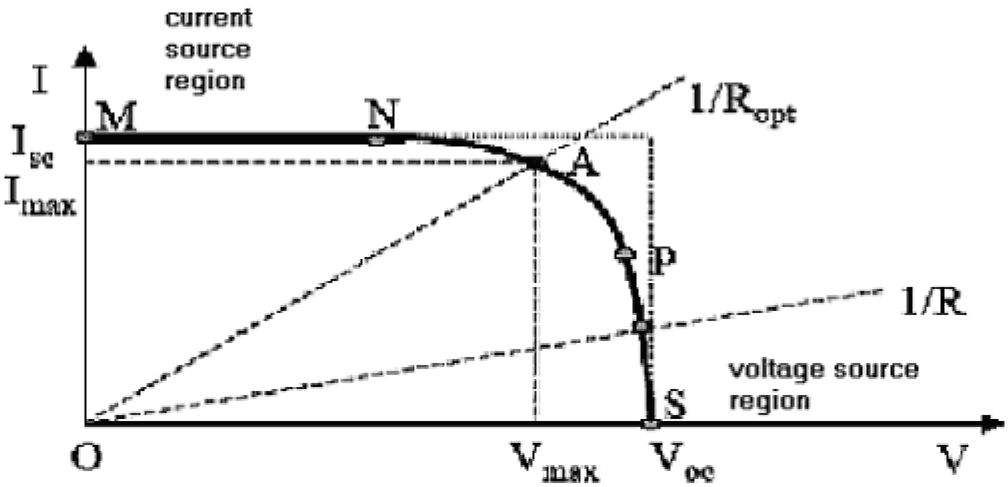

Figure 2.3 V-I characteristics of solar cell [14]

For a solar cell, the non-linear relationship means the maximum power point has to be obtained by calculating the product of the current and output voltage. To extract maximum power from the solar cell, the solar cell must always be operated at or very close to where the product of the voltage and output current is the highest. This point is referred to as the maximum power point (MPP) and it is located around the 'bend' or 'knee' of the I-V characteristic [15].

Irradiance is a characteristic related to the amount of Sun energy reaching the earth, and under ideal conditions, it is measured as 1000 W/m^2 at the equator. The sun energy on the earth is highest around the equator when the sun is directly overhead. Some important magnitudes related to irradiance include the spectral irradiance, radiation, and irradiance. Spectral irradiance is the power received by a unit surface area at a particular wavelength, while irradiance is the integral of the spectral irradiance extended to all wavelengths of interest. Radiation is the time integral of the irradiance extended over a given period [16].

Majority of solar cells have high capacitance associated with their forward-biased p-n junctions because the charged carriers are much closer together. The unwanted capacitance increases as the size of the solar cell and junction area increases. The I-V curve of the solar cell can be determined by taking fast I-V measurements, which is done by applying a constant voltage and measuring the resulting current for the device being tested. However, the high capacitance makes it difficult to get fast I-V measurements. [17]

The short circuit current is estimated by the incident light intensity and it is inversely proportional to the applied voltage. The total circuit voltage and incident light determine the external circuit current.

2.1.1.4 Non-Linear characteristics of PV's

Photovoltaics have nonlinear behavior, where the performance and output power are direct changes by the difference of the operating conditions (temperature and solar irradiance. Figures 2.4 a, b, show the effect of changing the temperature and 2.5 a, b, show the effect of changing solar irradiance on PV's output current, voltage, and power).

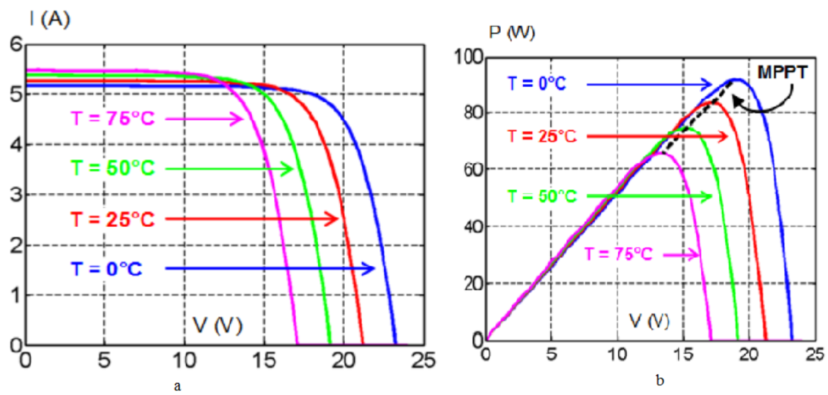

Figure 2.4 Effect of temperature changes on a) I-V curves b) P-V curves [18]

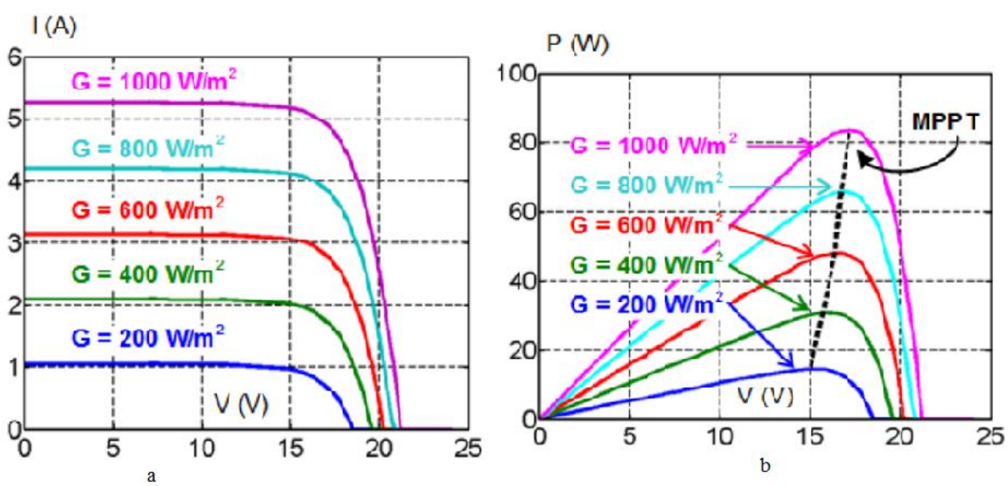

Figure 2.5 Effect of solar irradiance changes on a) I-V curves b) P-V curves [18]

As seen from the above figures 2.4 and 2.5 that the output power of PV's is directly proportional to the amount of solar irradiance reducing on it and inversely proportional with its temperature. Figures 2.4 and 2.5 show that with the variation of the solar irradiance and the temperature the point at which maximum power can gain also changes, it means that the array terminal voltage must be varied using DC-DC converters to track the maximum power point. Maximum power point tracking methods have discussed in details in chapter 3 section 3.4.6.

2.1.2 Stand-alone System Components

In this thesis, the stand-alone power system as a results of solar photovoltaic and diesel generator with battery bank storage. Photovoltaic panel and the Diesel generator are highly complementary to each other. A Photovoltaic system does not cause fuel utilization and expenses kept up commonly low. Diesel generators cause expenses of operating [19], however, can create energy request. The mix of energy sources permits the continuous cover of power demand (electric power generation utilizing photovoltaic generators when the climate is sunny and Diesel generators when the climate is dark). Be that as it energy generation isn't altogether sustainable and for applications in remote locales, transportation and fuel costs and the ecological expenses are high [19].

Figure 2.6 distinguishes various vital parts that make up an essential stand-alone PV system. The system comprises of the PV array itself, batteries for the capacity of storage, a charge controller, an inverter, and system control, alongside various disconnect switches. A backup generator was possibly being incorporated into the system.

The PV array conveys control through it's going with combiner box to a controller. The controller has three essential capacities. Its MPPT keeps the PVs working at their most efficient operating point. Its charge control function secures the batteries by shutting off charging current when completely charged and by disconnecting the batteries from the DC loads when it detects a low-voltage condition.

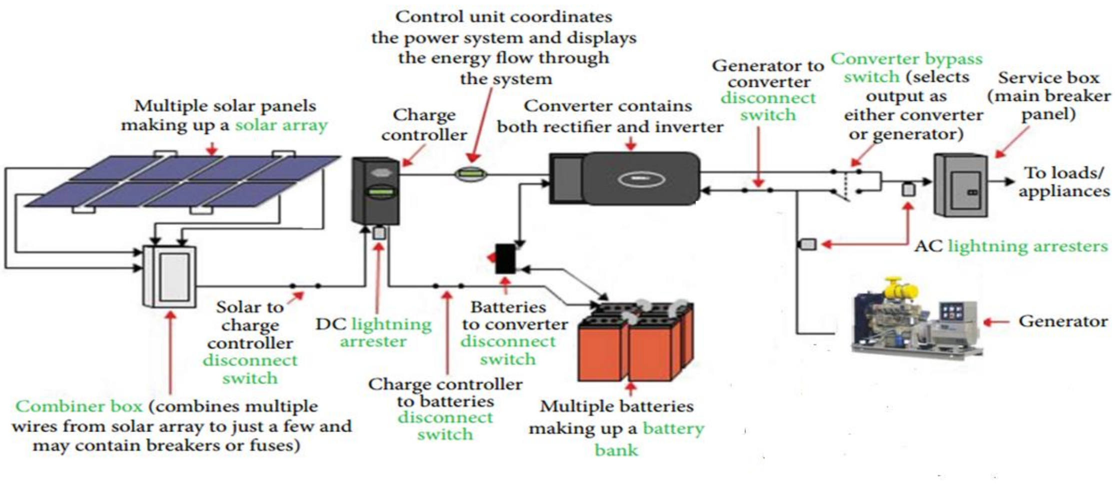

Figure 2.6 Block diagram of PV – Diesel generator hybrid system [20]

2.1.2.1 Solar PV module array

The PV modules are mostly available in wattage rating of 3 Wp to 300 Wp. A PV module is characterized by several parameters including Isc, Voc, Im, Vm, Wp (Pmax or Pm), FF and h. The main parameters useful for the practical application are Im, Vm and Pm.

In a PV power plant, the PV modules connected in series are referred to as PV modules string. A solar PV array is a combination of PV modules in series and parallel. This due to increase or decrease the parameters of the PV system to meet the required load.

To increase the generating capacity without changing the array voltage, strings of modules, which connected in parallel. Figure 2.7 a) shows an example of a PV string and b) shows a PV array connected in a series string.

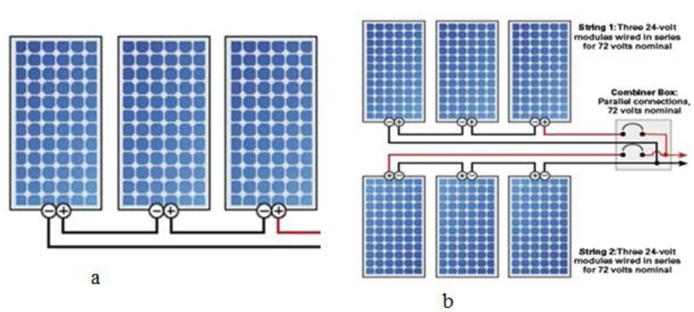

Figure 2.7 a) shows of a PV string and b) shows a PV array connected in a series string. [21]

2.1.2.2 Battery

The Battery is another important element in a stand-alone PV power system. The battery is important in such a system because of the fluctuating behavior of the output delivered by the PV arrays. Thus, during high solar radiation, the PV system is directly supplying the load, the excess electrical energy being stored in the battery. During the night, or during a period of low solar irradiation, energy supplied to the load from the battery [22].

- **Types of batteries**

There are two basic types of batteries, thus are Primary batteries (disposable batteries), which designed to use once and discarded and secondary batteries (rechargeable batteries), which designed to be recharged and utilized multiple times.

Most of the batteries used today for hybrid power system are from the rechargeable type [23]. There are several kinds of rechargeable batteries. Among them, as shown in Table 2.1: NiCd (Nickel Cadmium), NiMH (Nickel Metal Hydride), Lead-acid, and Lithium-Ion (Li-Ion).

Table 2.1 Common rechargeable battery types

Parameters	**NiCd**	**NiMH**	**Lead-Acid**	**Lithium-Ion**
Nominal cell voltage (V)	1.2	1.2	2.1	3.6
Energy density (Wh/kg)	40-60	30-80	30-40	150-250
Specific power (W/kg)	150	250-1000	180	180
Charge/discharge efficiency (%)	70%-90%	66%	70%-92%	99%+
Self-discharge rate in (%/month)	20%	30%	3%-4%	5%-10%
Cycle durability[3]	1500	500-1000	500-800	1200-10000

[3]The total number of cycles a battery is capable of producing before it fails.

As shown in Table 2.1, Lithium-Ion battery has many advantages than other rechargeable batteries, such as [24] [25].

- **Batteries for Photovoltaic (PV) Systems**

The batteries used for PV systems must be a rechargeable battery, ought to have a long life expectancy, permit deep discharge, effectively adjusted and have high limits and low self-discharge. Lead-acid batteries are a rechargeable battery, normally, they have 500 to 800 charge-dis charge cycles, they have limits in the range of 1 to 12000 Ah and life - the time is of around 2 to 3 years. The lead-acid battery performs very well for a wide range of temperatures, from – 15 °C to 60 °C. The replacement and maintenance of lead-acid batteries are simple. All these factors make lead-acid batteries a good choice for PV applications. Different types of lead-acid batteries were accessible. In general, the lead-acid batteries are into two classifications:

1. Liquid vented
2. Sealed or VRLA (Valve Regulated Lead-Acid) It is of two types:
    - Absorbed glass mat (AGM) battery
    - Gel battery (gel cell)

Liquid vented batteries generally used in automobiles. When a battery is charged and discharged, the hydrogen and oxygen gas produced due to chemical reactions.

Sealed or valve regulated lead-acid (VRLA) batteries do not have any gap from where the gases delivered in the charge-discharge cycle can exit as if there should arise an occurrence of fluid vented batteries. The VRLA batteries structured in a way that hydrogen and oxygen created in the battery recombined again to deliver water. The valve gave in the battery to direct the weight inside the battery. Since during the charge-discharge cycle no water is lost, no refilling of water is required for sealed or VRLA batteries. They are free from maintains. Subsequently, the sealed Lead-Acid Deep cycle battery is the perfect decision utilized broadly in the PV frameworks. Deep cycle batteries can be deep cycle permitting to utilize a large portion of its capacity (i.e., ~50% of its capacity) [26]

2.1.2.3 Charge controller

Charge controller placed between batteries and solar module. Also, have the following function;

- **Protection against battery overcharging:** the controller regulates the energy coming from the module, depending on the battery's state of charge. When there is a lot of suns and the battery reaches full charge, the controller reduces the current flowing into the battery to protect it from overcharging.

- **Protection against battery over-discharging:** if energy demand is high and the modules are not able to replace the energy being consumed (at night, for example), the controller detects when the battery state of charge is too low and disconnects the load.
- **System monitoring and performance:** depending on the model, the controller can provide the basic information about the state of the system, monitoring the voltage, current, and the state of charge of the battery, via LED lights or an LCD screen.

Figure 2.8 shows the Diagram displaying the functional principle of reverse current diodes, deep-discharge protection and overcharge protection in a PV system

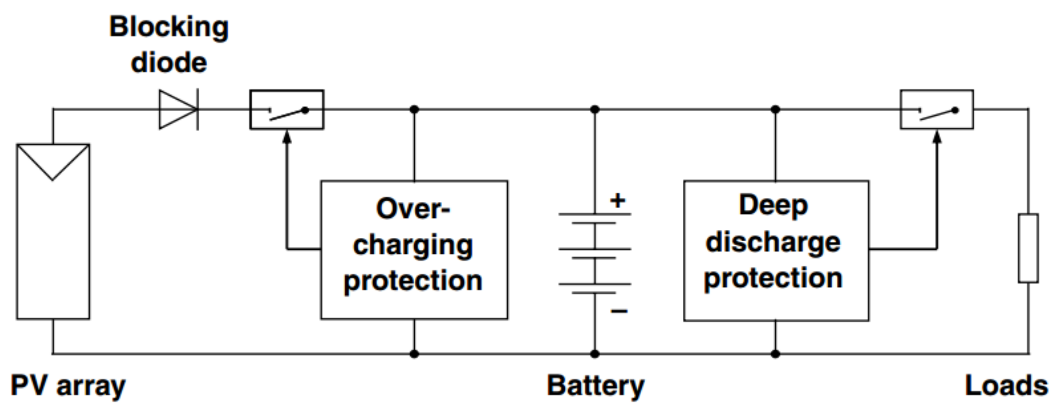

Figure 2.8 Diagram of deep-discharge and overcharge protection in a PV system

The overcharge protector-switching threshold should be set high enough that it does interfere with the normal operation of the charge controller or solar tracker.

Charge controllers usually charged batteries in four phases:

- **Initial charge:** when the battery voltage reaches a certain level, the controller allows all the available current from the module to flow in until the battery reaches an 80% state of charge.
- **Current** coming from the modules until it reaches a 100% state of charge.
- **Float charge:** once the battery completely charged, the controller only lets a very small current pass through to the batteries, to maintain the state of charge at 100%.

- **Equalization of charge:** a function in certain controllers, only to use with flooded lead-acid batteries that have liquid electrolyte. The process consists of a controlled overcharging, to reduce acid stratification and sulphation inside the battery, as well as to level out the voltage in the different cells of the battery.

The relationship between the current and the voltage during the three phases of the charge cycle can be as shown in figure 2.9 below.

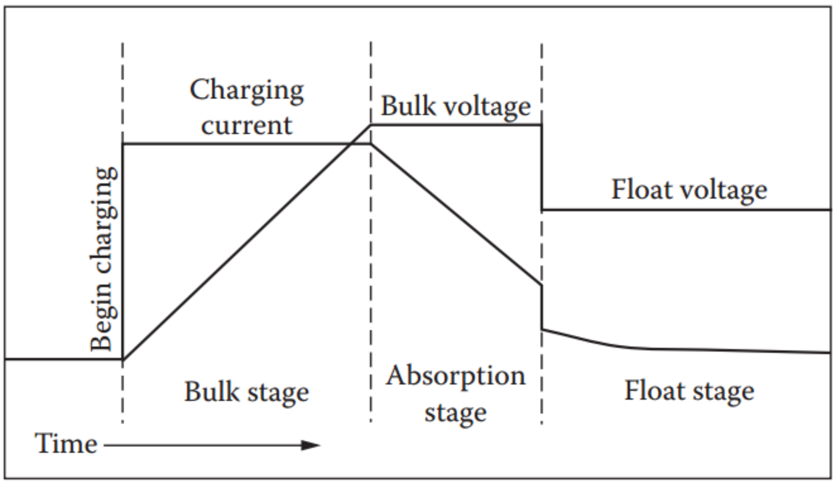

Figure 2.9 Three-stage battery charge control [27] [28].

- **Type of Charge Controller**

Virtually all charge controllers contain a feature to prevent the array from overcharging the battery. The controller monitors the battery state of charge and reduces or terminates solar charge as the battery gets fully charged. Charge regulation technology has improved dramatically since the 1990s, so it is worth shopping around to find a modern unit. There are four general types of charge controllers (though they may share features), categorized by the method by which they regulate charge from the module to the battery as described below:

I. **Series and Parallel or shunt:** Both connections are simple and cheap controller but the series connection is generally not used in PVS systems now a day and parallel connection well suited to small SPV systems. Series charge controller connected in series between the module and the battery while shunt controller connected in parallel between the module and battery as shown in figure 2.10 a) and b) respectively.

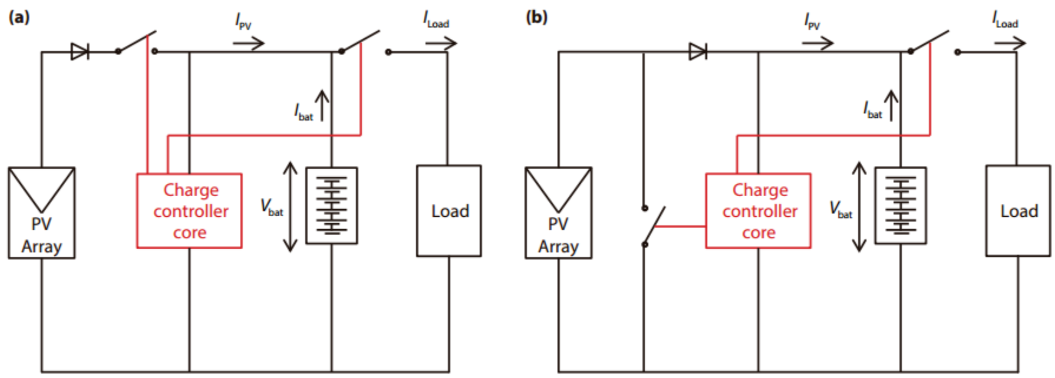

Figure 2.10 Basic circuit scheme of (a) a series and (b) a shunt charge controller

II. **Pulse Width Modulation (PWM):** they emit pulses of charge to the battery. The "width" or intensity of the pulses depends on the battery's state of charge. The width of the pulses decreases progressively as the battery charges. It is a well-proven technology and PWM controllers are usually cost-effective and reliable.

III. **Maximum Power Point Tracking (MPPT):** these have a continuous current converter, which enables them to work at the maximum power point of the module. The voltage at P_{max} is usually much higher than the charging voltage of a system of the battery. Utilize DC-to-DC conversion electronics to 'track' the maximum power point of the module or array I-V curve. By keeping the charge voltage at the maximum power point, MPPT controllers gain an extra 10–35 percent output from the array. MPPT trackers also can accept higher voltages from the module, meaning that they can use modules with a higher voltage (i.e. 24V or higher) and convert the power to 12V (or the rated battery voltage). MPPTs tend mostly to use in large systems, where getting the most out of the array results in significant cost gains for the system. [29].

2.1.2.4 Inverters for solar PV system

An inverter is a device that converts DC voltage into AC voltage. An alternating current (AC) is that which flows in both positive and negative directions, while the direct current (DC) is a current that flows in only one direction. There are two basic types of inverters based on the type of sources input sources; Current Source (CSI) and Voltage source (VSI). Voltage/current source implies that the voltage/current level does not change instantly as the result of switching. Photovoltaic source and Batteries source can be used as voltage sources.

Figure 2.11 Block diagram of Inverter [26]

An inverter may be single-phase or three-phase (half-bridge, full-bridge) but single-phase half and full-bridge voltage source inverter is used for low-range power applications. The inverter aims is to provide a three-phase voltage source, where the amplitude, frequency, and phase of the voltages to be controlled. And, this thesis discussed three-phase inverters with the controlling techniques and selects the best one based on the performance parameter.

- **Sinusoidal pulse width Modulation (SPWM) in Three-Phase VSI**

  As in the single-phase voltage source inverters PWM technique can be used in three-phase inverters, in which three sine waves phase shifted by 120°with the frequency of the desired output voltage is compared with a very high-frequency carrier triangle, the two signals are mixed in a comparator whose output is high when the sine wave is greater than the triangle and the comparator output is low when the sine wave or typically called the modulation signal is smaller than the triangle.

2.1.2.5 Filters for photovoltaic system

The results from inverter and diesel generator have connected to a low pass filter to supply a pure sinusoidal output voltage to the load. The factors such as voltage current and efficiency harmonics constraints, weight, volume, and cost should be taken into consideration when selecting the optimal filter design [30]. Also, the saturation of the inductor core should be avoided [31]. There are different filters topologies of sine wave inverter. These topologies include L filter, LC filter, and LCL filter.

Interims of voltage to current conversion L filter have high-quality performance but the damping of the high frequency (HF) noise is weak. The LC filter has better performance in case of current to voltage conversion (CSI) and noise damping but the filter capacitor may be unsafe to line voltage harmonics, which generates more currents. The LCL filter has similar good properties with the LC and the L filters. Moreover, the damping of high-frequency noise is good due to the extra inductance, and the capacitor is no more exposed to line voltage distortion. On the other word, LCL can sometimes cost more than other topologies and is inherently unstable due to resonance [32]. For reducing oscillations and unreliable conditions of the LCL filter, a damping resistor (Rd) is placed in series with the filter capacitor. Damping resistor is reliable compared to the other, but system decrease efficiency and it increases the losses of the system, but the advantage of LCL filter overcome, other types of filter are the reasons that made this filter are used in the proposed inverter circuit.

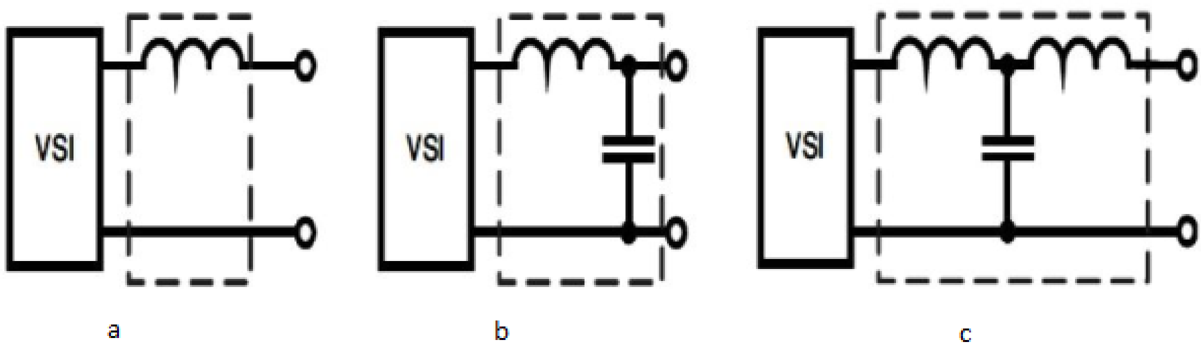

Figure 2.12 a) L b) LC c) LCL-filter [33]

There are some important factors that should be considered when design LCL filter which comprise such as: Inverter output ripple current, Inverter to load inductor ratios and filter capacitance maximum power variations.

2.1.2.6 DC-DC Converter Used for the MPPT System

An MPPT is used to extracting the maximum power from the solar PV module and transferring that power to the required load. A dc-dc converter used for the transfer maximum power from the solar PV module to supply the load. Without dc-dc converter no MPPT systems are designed, consider dc-dc converter acts as an interface between the load and the module as in Fig.2.13.

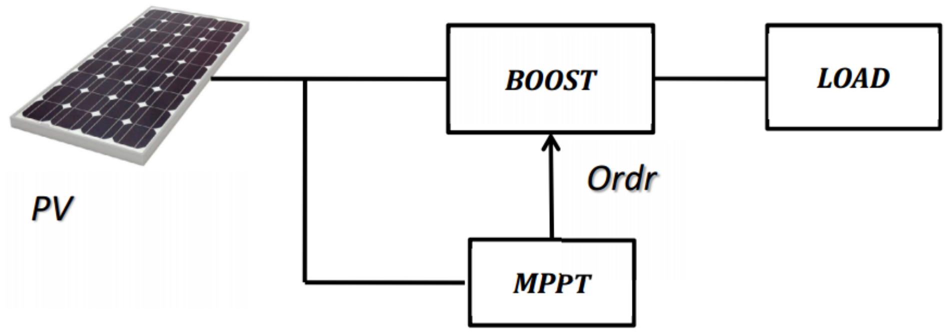

Figure 2.13 Block diagram of typical MPPT system

Typically, the converter used is based on the method of the system PV panel. If the converter and PV system is not connected to power grid it is called off-grid system. At no-load state, the energy generated from PV panels is usually stored in batteries. If the energy consumption begins, the converter starts to deliver the energy to the load through the inverter. If the level of power obtained from PV panels is higher than the system can offer, the converter starts to draw the energy from batteries [34].

There are many circuit configurations for switch converters. However, the most popular are boost converter (step-up converter), buck converter (step-down converter), buck-boost converter (CUK).

I. Boost Converter

The DC-DC boost converter is also known as the step-up converter. It can be used in the cases when the output voltage greater than the input voltage, essentially functioning like a reversed buck converter. The practical application which uses a boost type converter appear in grid systems. Fig. 2.14 [35].

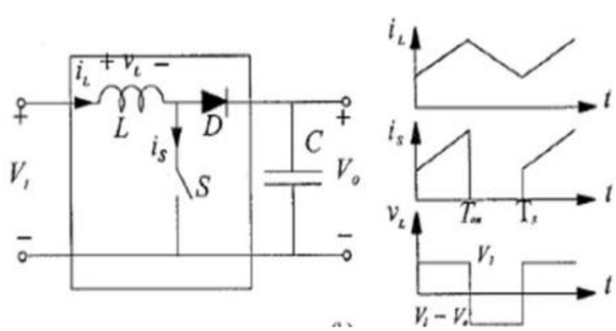

Figure 2.14 Equivalent circuit of a boost converter

II. Bidirectional dc to dc Converter

A conventional buck-boost converter can management the power flow in one direction only but power can flow in both the direction in the bidirectional converter. Bidirectional dc-dc converters are the device used for the purpose of step-down or step-up the voltage range with the capability of flow power in either forward directions or in a backward direction. Bidirectional dc-dc converters work as a regulator of power flow of the DC bus voltage in both the direction. These energy storage devices store the surplus energy during low load demand and provide backup in case of system failure and when the output of energy system changes due to weather conditions. Thus, bidirectional dc-dc converters are needed to allow power flow in both forward and backward the directions. A conventional dc-dc converter can be converted into a bidirectional converter using the bidirectional switch by using a diode in anti-parallel with MOSFET or IGBT allowing current flow in both the direction using controlled switching operation.

This scheme is a basic circuit of bidirectional dc-dc converter Fig.2.15. It is the anti-parallel combination of buck-boost converters. During the boost operation, Q1 is conducting according to the duty cycle whereas Q2 will not conduct in this mode. In buck mode, Q2 will conduct according to the duty cycle and Q1 will not conduct in this mode. Given topology is a non-isolated half-bridge BDC topology and it is designed by the combination of boost converter connected antiparallel with buck converter [36] [37]. This topology is simple and has greater efficiency [38].

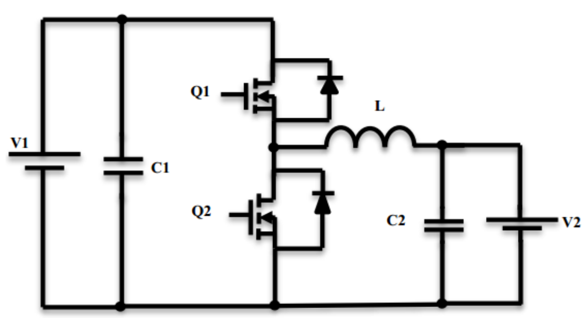

Figure 2.15 Basic circuit of bidirectional dc-dc converter [39]

2.1.2.7 Diesel Generator Model

Diesel generators used as backup the power supply during sudden increment in energy demand or when the power from batteries is not sufficient. The diesel generator described by its efficiency defined as the proportion of the electrical power provided to the proportionate energy of the fuel used to produce it. The fuel utilization of a diesel generator can describe by amounts relating to various purposes of motor operation.

- **The Main comports and Diesel Generator Sets Characteristics**

The main parts of a diesel generator are the internal combustion engine, usually air- or water-cooled; the electric generator usually of synchronous type; the mechanical coupling; the support chassis; the battery for generator start-up; the fuel tank; the starter motor; the command panel, etc. The main characteristics of a diesel generator set are rated voltage, rated power, the number of phases, rated frequency, etc.

The diesel generator sets are usually, designed to run at 3000 rpm or 1500 rpm at a frequency of 50 Hz. The primary movers (shaft) are internal combustion engines equipped with mechanical regulators to remain the imposed speed, integrated with the injection pump and adjusted to get the result of the output frequency of about 50 Hz for rated load and 52 Hz without load.

The proper operation of a diesel generator set is estimated to a great extent by two main components, the voltage regulator and the speed regulator.

The speed regulator designed to keep constant the internal combustion engine speed by changing the quantity of fuel consumed by the motor. The direct result of this speed regulation is a stable frequency of voltage at the generator terminals (since the frequency is proportional to the generator speed). A constant frequency requires good precision and very short response time from the speed regulator. The speed regulator starts regulating when various electric loads are connected or disconnected at the generator terminals.

2.2 Review of other works of hybrid power system

Hybrid systems generally refer to the combination of any two or more than two input sources, here solar PV can be integrated with Diesel Generator, Wind Turbines, Bio-mass, solar PV with wind and hydropower or any other renewable on non-renewable energy sources. Solar PV systems will generally use a battery bank to store energy output from the panels to accommodate a pre-defined period of the small value of solar radiation or sunshine, there may still be exceptional periods of poor weather when another source is required to secure power production. PV-hybrid systems combine a PV module with another power sources typically a diesel generator, but occasionally another renewable supply such as a wind turbine, hydropower. Usually size the PV generator to meet the baseload demand, with the alternate supply being called into action only when essential. This scheme offers all the essential of PV in respect of minimum operation and maintenance costs but additionally ensures a secure supply.

Hybrid systems can also be a sensible approach in situations where occasional demand peaks are significantly higher than the baseload demand. It makes little sense to size a system to be able to meet demand entirely with PV if, for example, the normal load is only 10 % of the peak demand. Similarly, a diesel generator-set sized to meet the peak demand would be operating at inefficient part-load for most of the time. In such a situation, a PV-diesel hybrid would be a good compromise. Figure 2.16 shows the single line diagram of the Solar PV hybrid system.

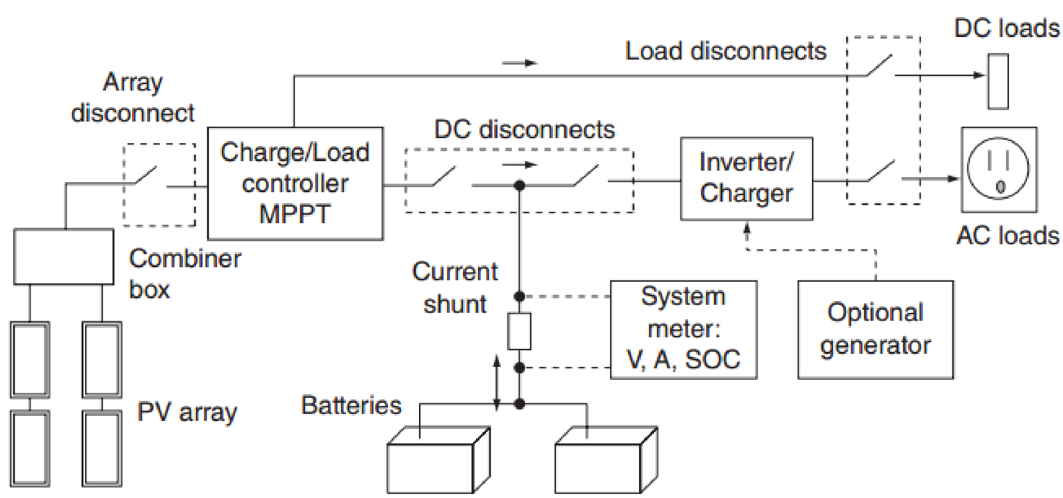

Figure 2.16 A single line diagram of the stand-alone PV system [40]

2.2.1 Solar PV/Wind Hybrid power system

Mengesha A. [41] describes this his thesis “Techno-Economic Assessment of Wind Energy to Supply the Demand for Electricity for Residential Community in Ethiopia”. He selected three sites for the project Moyale, Nagele and Mehalemeda. To analyze the optimization process and identifying the potential of wind area and optimize cost-effective wind energy system He used HOMER software. Depending up the calculated load appliances the optimization process is done for hundreds of households.

In the International Journal of Engineering Research and General Science, there is another hybridization of PV/Wind entitled “Feasibility of Solar Wind Hybrid Renewable Energy in India.”

[42]. In the work, the hybrid power system combined the solar array and wind turbine. The hybrid system is designed to convenient and cost-effective which not only reduces the dependency of the grid but also improve the reliability of the community.

Chaitanya M. and K. Ravi K. [43] proposed a hybrid wind-solar energy system with battery energy storage for an isolated system. The hybrid system is proposed to generate 10KW from wind and solar and 4KW from external to meet the load. The dynamic modeling and simulation of the hybrid using Matlab/Simulink. They also present the hybrid system power controlled to give the maximum output under the different condition to meet to the load. They describe the concept and principle of the hybrid system and its control. The present simulation results to evaluate the performance and power reliability of the hybrid system.

A.K.Pradhan et al, discuss the Off–Grid Renewable Hybrid Power Generation System for a Public Health Center for Rural Village [44]. The off-grid hybrid energy system combines of photovoltaic panels, wind generator, bi-directional converters and battery storage (energy storage during excess energy). The hybrid system produces energy, wind for 24 hrs, and solar panels produce during the day that means from 6 AM to 6 PM. The system modeled by HOMER simulation for techno-economic analysis for selected sites.

Anumeha A. et al. [45] discussed a hybrid power system (HPS) which consists of a wind turbine, solar array together with storage batteries power electronics devices in this work. An inventory of connection that made for wind generates AC power and solar generates DC power. The modeled of the hybrid, power generation system using MATLAB/SIMULINK blocks and the results of the system analyzed.

Mohammad – Ali [46] describes the modeling and sizing optimization of the hybrid photovoltaic/wind power generation system. Under this work, he describes the methods used to decrease the impact global warming due to fossil fuel the option for the solution is replacing the renewable especially solar and wind energies in the case of fossil fuel energy. The sizing of the renewable energy the Multi-objective optimization procedure uses MOPSO for the design of hybrid solar/ wind power generation. To calculate the size of optimal the match evaluation method (MEM) developed on the availability of energy supply/demand and electricity match rate (EMR) for the evaluation criteria to the size of the proposed hybrid system in lowest cost.

2.2.2 Solar PV/Diesel Hybrid power system

Zelalem Girma [47] presents in his paper hybrid renewable energy design for rural electrification in Ethiopia. Zelalem describes the hybrid system power that generates energy from solar energy, batteries and diesel generator used as a backup. The hybrid system model is simulated using HOMER software to determine the optimal and control stratagem of the system. The system generally designed to produces energy for two hundred households by consuming 279KWh/day and 64KW peak power demand with an average of five members per household.

B. Tudu et al. [48] Present stand-alone hybrid renewable energy system – an alternative to increased energy demand. Their system consists of solar power, diesel generator and battery for the feasibility and sensitivity analysis using Homer software simulation. Optimized net present cost and cost of energy for the system obtained and the detailed study regarding the power output from the resources, unmet load scenario, and sensitivity analysis carried out.

Chowdhury, et. al, [49] describes "economic feasibility of a PV/diesel HPS in various climatic zones within South Africa at different climatic zone". The integrated system is to achieve the desired output, most economically viable solution, continuous power supply, to reduce greenhouse and to the optimization of systems. The types of upcoming renewable and low-carbon generation technologies are being preferred for such systems depending on their availability and economic viability in these countries. Moreover, HPSs are also being preferred to improve the overall energy efficiency of the system and to get a judicious generation mix, which would minimize the operating cost of the system. Rural communities in South Africa endure poor access to electricity mostly due to the lack of grid-connected power lines. It is, therefore, the ideal place to conduct a study on the economic feasibility of introducing HPSs for typical residential loads for the rural community in South Africa.

2.2.3 Wind /PV/Diesel Hybrid Power System

The paper by **Md Saleh .et.al** [50], entitled "Design, Simulation and Stability Analysis of Wind /PV/Diesel Hybrid Power System using ETAP" and published in the American Journal of Modern Energy, indicates that the hybrid power system, stability analysis of steady-state and transient stability described in details. The model proposed for hybrid power system consists of a solar array, wind turbine, backup diesel generator, and energy storage or battery bank. The ETAP software simulation developed the model.

In the world, more than 1.3 billion peoples do still not get access to electricity. From this, more than 95% of them have located in Sub – Saharan Africa and developing Asian countries, and almost 2.6 billion peoples still now use traditional energy. More than 76.7% of the Ethiopian population is life without electricity [51].

The other relevant work, [52] is the model of the converter and multi-level inverter described. The system modeled by using MATLAB/SIMULINK.

Gelama Boneya and Getachew Bekele conducted research and concluded that more than 80% of the Ethiopian population lives without electricity [53].

Sen and Bhattacharya [16] describe a hybrid system design can to solve the problem of the interdependence of renewable energies and increase the reliability of supply. In their research for electrification of remote villages, they carry out a case study of an Indian village using HOMER software and find that hybrid system ae technically and economically viable in many locations.

Ersan K. et al. presented the design and implementation of a renewable energy monitoring system [54]. The hybrid system parameter for monitoring defined to the analysis of voltage and current for real-time tracking property introduced in this work. The energy generated from the solar array, the wind turbine coupled over dc – bus and the batteries have connected to the system for current and voltage rate. In this work hardware, implementation presented by using voltage sensor, a microcontroller (MCU), personal computer (PC) and over the universal serial bus (USB) to save the database and to be observing the system instantly. The proposed system for monitoring to observe is coded Microsoft visual studio.

Tarlochan K. Ravi S. described Designing Rural Electrification Solutions Considering Hybrid Energy System. In this works, the hybrid power system consists of a solar PV system, small hydropower, natural gas based on generator and battery storage as a backup. The model developed by HOMER software for analyzing the sensitivity and performance as well as the optimal of the system design. Load estimation for the community is calculated on each particularly purpose [55].

CHAPTER 3

FEASIBILITY ANALYSIS, LOAD ESTIMATION, SYSTEM SIZING, and ENERGY MANAGEMENTS

3.1 Solar potential energy in Ethiopia

Ethiopia receives 4.55 to 6.5 kWh/m^2/day annual average of solar insolation throughout the country [56]. This varies significantly during the year, ranging from a minimum of 4.55kWh/m^2/day in July to a maximum of 6.55kWh/m^2/day in February and March. Other works of literatures describe the yearly average radiation to be in the range from 4.25 kWh/m^2 in the areas of the Gambella regional state (western Ethiopia), to 6.25 kWh/m^2 around Adigrat in the Tigray regional state (northern Ethiopia) [57]

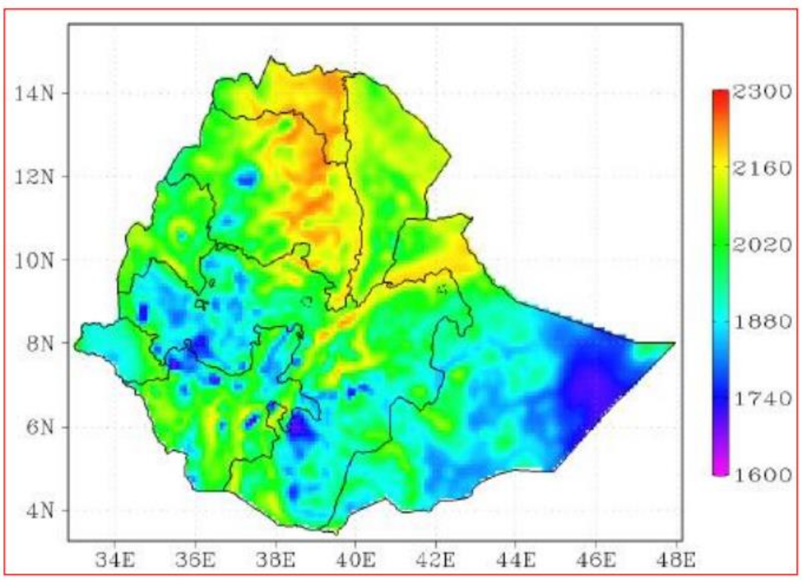

Figure 3.1 Distribution of Average Annual Total Solar Radiation of Ethiopia, kWh/d/m^2 (1980~2009) [58].

3.2 Estimation of Solar Radiation

For any solar-based system design, the most important factors are the position of the sun in the sky, the slope, and orientation of a collecting surface, and obstruction and reflection properties of neighboring structures. Figure 3.2 shows the geometry describing the orientation of a collector and the position of the sun in the sky. Generally the geometry of solar collector describes the angles such as inclination, zenith, and solar azimuth in figure 3.2.

A point on the earth's surface is expressed by its latitude and longitude. The angle between the collector surface and the horizontal is called slope, β (with $0^0 < \beta < 90^0$ for a surface facing towards the equator; $90^0 < \beta < 180^0$ for a surface facing away from the equator). Surface azimuth angle, γ is the angle between the normal to the surface and the local longitude meridian, projected on the horizontal plane. In either hemisphere, γ equals 0^0 for a surface facing due south, 180^0 due north, 0^0 to 180^0 for a surface facing westward and 0^0 to - 80^0 eastward. For a horizontal surface, γ is always 0^0.

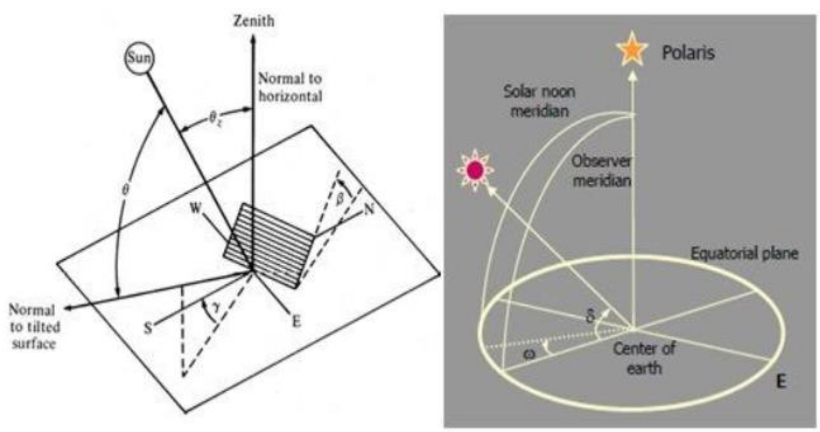

Figure 3.2 Geometry of solar collector and location of sun relative to earth [59]

Location of the sun in the sky, relative to a point on the ground, can be defined in terms of two angles, the solar altitude, α_s (or its complement the solar zenith angle, θ_z) and the solar azimuth γ_s. Solar altitude, α_s angle of the solar beam to the horizontal. Solar azimuth, γ_s is the angle between the solar beam and the longitude meridian projected on the horizontal plane. Sign convention is the same as for surface azimuth angle (γ). Solar altitude and solar azimuth are functions of location (latitude, ϕ), time of the year (declination angle, δ) and time of the day (hour angle, ω). Solar declination angle (δ) is the angle between the earth's equatorial plane and the earth sun line. Solar hour angle ω is the angle Earth has rotated since solar noon. The relation between these angles is given below [58] [60] [59]

$$\delta = 23.45 \sin\left(360 \frac{284+n_d}{365}\right) \quad (3.1)$$

Where δ = solar declination angle (^{0}), n_d = day number of the year starting at January 1st as 1

$$\omega = (12 - t_l)15^0 \quad (3.2)$$

Where t_l = local solar time in hours, ω = solar hour angle (^{0})

$$\sin(\alpha_s) = \sin(\phi)\sin(\delta) + \cos(\phi)\cos(\delta)\cos(\omega) \quad (3.3)$$

Where α_S = solar altitude (^{0}), ω = latitude (^{0})

$$\sin(\gamma_s) = \frac{\cos(\delta)\sin(\omega)}{\cos(\alpha_s)} \quad (3.4)$$

Where γ_s= solar azimuth (^{0})

The sunset/sunrise angle is given by

$$\omega_s = cos^{-1}(-\tan(\phi)\tan(\delta)) \quad (3.5)$$

The angle of incident θ_i is the angle between the solar beam and normal to the solar panel which is given by:

$$\cos(\theta i) = \sin(\delta)\sin(\phi)\cos(\beta) - \sin(\delta)\cos(\phi)\sin(\beta)\cos(\gamma) + \cos(\delta)\cos(\phi)\cos(\beta)\cos(\omega) + \cos(\delta)\sin(\phi)\sin(\beta)\cos(\gamma)\cos(\omega) + \cos(\delta)\sin(\beta)\sin(\gamma)\sin(\omega) \quad (3.6)$$

The intensity of solar radiation incident per unit area exposed normally to the sun's rays at the average sun-earth distance (about $1.5x10^{11}$m), measured outside the earth's atmosphere is called the solar constant, G_{sc} (1366 W/m^2) [60] [61]. The intensity of radiation received outside the earth's atmosphere varies as the inverse square of the earth-sun distance and can be expressed in relation to the time of the year. The extraterrestrial irradiance on a surface at normal incidence (G_{on}) expressed as:

$$G_{on} = G_{sc}\left[1 + 0.03cos\,\frac{2\pi n_d}{365}\right] \quad (3.7)$$

The extraterrestrial irradiance incident on a horizontal plane at an arbitrary angle of incidence given by,

$$G_o = G_{on}\cos(\theta_z) \quad (3.8)$$

Where θ_z = zenith angle (angle between the sun and the vertical line from a point on earth) which equals to the incident angle of a horizontal surface at the point of interest.

The whole daily extraterrestrial radiation, H_o from the sunrise to the sunset can be calculated as follows:

$$H_o = \frac{24 \times 3600 \times G_{sc}}{\pi}\left(1 + 0.033 \times \cos\left(\frac{360N}{360}\right)\right) \times \left(cos\phi\, cos\delta\, sin\omega_s + \frac{\pi\omega_s}{180} sin\emptyset\; sin\delta\right) \qquad (3.9)$$

Where N is Day number starting from January 1st as 1, G_{SC} is equals to 1366 W/m^2, the solar constant, ϕ = Latitude of the location (15^0), δ = Declination angle (^{0}) given by equation (3.1), ω_s = Sunset hour angle (^{0}).

Ideally, the data required to predict the solar potential of any site are several years of measurements of irradiance on the proposed collector plane. These are rarely available, so the required data must be estimated from meteorological data available either (i) from the site, or (ii) from some nearby site having similar irradiance, or (iii) from an official solar atlas or database [59]. Here, the sunshine duration data from the nearby station used to estimate the monthly average solar radiation using the following angstrom type equation 3.6, 3.7, 3.8 and 3.9.

$$\frac{H}{H_o} = a + b\frac{n}{N_s} \qquad (3.10)$$

Where H = monthly average daily radiation on horizontal surface (MJ/m^2), H_o = monthly average daily extraterrestrial radiation on a horizontal surface (MJ/m^2)

N_s = the maximum possible daily hours of bright sunshine given by equation

n = monthly average daily number of hours of bright sunshine.

a and b are regression coefficients is calculated by the given formula [58] [62] [63].

$$a = -0.110 + 0.235cos\emptyset + 0.323\left(\frac{n_s}{N_s}\right) \qquad (3.11)$$

$$b = 1.449 - 0.533cos\emptyset - 0.694\left(\frac{n_s}{N_s}\right) \qquad (3.12)$$

The day length, N_s, is the maximum possible daily sunshine hour is given by equation 3.13

$$N_S = \frac{2}{15} \times \omega_s \tag{3.13}$$

Table 3.1 Recommended average days for months and values of n by months [63]

Months	n for ith day of the month	For the average day of the month		
		Date	**n, day of year**	**δ declination (^{0})**
January	i	17	17	-20.92
February	31+i	16	47	-12.95
March	59+i	16	75	-2.42
April	90+i	15	105	9.33
May	120+i	15	135	18.79
June	151+i	11	162	23.09
July	181+i	17	198	21.18
August	212+i	16	228	13.45
September	243+i	15	258	2.22
October	273+i	15	288	-9.60
November	304+i	14	318	-18.91
December	334+i	10	344	-23.05

3.3 Feasibility analysis of solar radiation for selected site

The assessment of the potential for solar radiation of the selected has been done by taking the data from different sources. These are Global solar radiation, NASA and the National metrological service agency of Ethiopia. In the first approach, the data are taken from the national metrological service Agency is analyzed using equation 3.7 and 3.8 based on the sunshine duration data collected over the past four consecutive years. The sunshine duration data taken from the National Metrological agency of Ethiopia given in table 3-2. The measurements were taken for four consecutive years starting from 2014. As it is seen in the table, the data for years 2014, 2015, 2016 and 2017. However, 2015 and 2017 measurements are incomplete. Hence, only the 2014- and 2016-year data taken to convert into MJ/m^2 using equation 3.7. This result then compared with the data collected from NASA and an average of 22 years recorded global weather database found to be nearly equal. Region: SNNPR, Station: Konso.

Table 3.2 Average Daily sunshine of Konso

Years	**Jan**	**Feb**	**Mar**	**Apr**	**May**	**Jun**	**Jul**	**Aug**	**Sept**	**Oct**	**Nov**	**Dec**
2014	8.5	6.0	7.0	7.6	6.8	6.6	3.3	4.7	6.3	7.4	9.7	10.2
2015	10.4	8.6	8.8	7.4	5.3	5	5	6.4	7.9	6.5	NA	NA
2016	10.2	9.2	6	8.1	6	4	5.3	5.8	8.6	8.7	9.7	9.6
2017	10.2	7.2	6.9	7.4	4.8	4.2	4.3	6.7	7.5	NA	NA	NA
Average value of **(n)**	**9.35**	**7.6**	**6.5**	**7.85**	**6.4**	**5.3**	**4.3**	**5.25**	**7.45**	**8.05**	**9.7**	**9.9**

Therefore, the analysis for the monthly average solar radiation is then calculated using the values of the regression coefficients and H_O, which can be calculated using equation 3.7. The result of the analysis shown below in table 3-2 is the monthly average solar radiation in MJ/m^2 and KWh/m^2 for the sunshine duration average measured of 2014 and 2016. The symbols used in table 3-2 represent the measured and calculated values, which used to analyze the extraterrestrial radiation (i.e. Ho) and the solar radiation for the location. n and ϕ represent measured sunshine duration and the latitude angle of the area respectively. However, the symbols δ, ωs, and Ns indicates the calculated values for declination angle, sunset angle and day length which are obtained using equations 3.1, 3.4 and 3.8 respectively. The average 2014 and 2016 monthly solar radiation data of the year with full measured hours of bright sunshine shown in table 3.3. This table also shows monthly and annual average solar radiation in MJ/m^2 and KWh/m^2 of Konso.

$$\mathbf{1\ MJ/m^2 = 0.2778\ kWh/m^2}$$

Table 3.3 Estimation of the 2014 and 2016 average solar radiation in MJ/m^2 and KWh/m^2

Months	**n**	**Φ**	**δ**	**ωs**	**Ns**	**Ho (MJ/m^2)**	**a**	**b**	**H (MJ/m^2)**	**KWh/m^2**
January	9.35	15	-20.92	84.12	11.22	29.54	0.39	0.36	20.43	5.7
February	7.6	15	-12.95	86.47	11.53	32.25	0.12	0.48	14.07	3.9
March	6.5	15	-2.42	89.52	11.94	35.72	0.29	0.56	21.25	5.9
April	7.85	15	9.33	92.52	12.34	38.4	0.33	0.49	24.72	6.9
May	6.4	15	18.79	95.23	12.70	39.5	0.28	0.58	22.61	6.3
June	5.3	15	23.09	96.56	12.87	39.73	0.25	0.65	20.57	5.7
July	4.3	15	21.18	95.96	12.79	39.66	0.23	0.70	18.46	5.1
August	5.25	15	13.45	93.67	12.49	39.04	0.26	0.64	20.75	5.8
September	7.45	15	2.22	90.60	12.08	36.96	0.32	0.50	23.30	5.5
October	8.05	15	-9.60	87.40	11.65	33.38	0.34	0.45	21.77	6.1
November	9.7	15	-18.91	84.73	11.30	29.62	0.40	0.34	20.49	5.7
December	9.9	15	-23.05	83.45	11.13	27.72	0.41	0.32	19.26	5.4

The assessment of the potential for solar radiation of the selected area done by taking data from different sources. These are the National Metrological Service Agency of Ethiopia (NMSA), NASA, and NASA surface meteorology and solar global horizontal radiation monthly average values over 22 years, period (July 1983 – June 2005)**.** At the first approach, the data taken from the National Metrological Service Agency is analyzed using a mathematical approach based on the sunshine duration collected on the past four consecutive years starting from 2014 to 2016. The sunshine duration data are taken from the National Metrological Agency of Ethiopia, Konso branch, converted into solar radiation using Angstrom Radiation-Sunshine Relation [58]. Therefore, for calculating the radiation in KWh/m^2 from the sunshine duration, the values for the regression coefficients ɑ and b are also calculated based on the formula given equation 3.9 and 4.0 [58] [64]. Finally, this result is compared with the data taken from NASA, NMSA, and it is found that the annual average solar radiation obtained from NASA surface meteorology and solar global horizontal radiation monthly average values over 22 years' period (July 1983 – June 2005) is 5.7

KWh/m^2, 6.0 KWh/m^2 and 5.76 KWh/m^2 respectively. For this study, the calculated monthly average daily radiation summarized in Table 3.4 used for modeling the hybrid system. The monthly average solar radiation of Konso data taken from NASA, NMSA and NASA surface meteorology and solar global horizontal radiation monthly average values over 22 years' period (July 1983 – June 2005) is shown in Table 3.4. Where NMSA1 is the form of average sunshine monthly values period (July 1983 – June 2005).

Table 3.4 Monthly average solar radiation at the Konso from different sources

Average Solar energy	**Months**												
	Jan	**Feb**	**Mar**	**Apr**	**Ma y**	**Ju n**	**Jul y**	**Au g**	**Se p**	**Oc t**	**No v**	**De c**	**Ann u**
Reflected **(**kWh/m^2)	6.4	6.6	6.3	5.7	5.6	5.3	4.9	5.3	5.6	5.6	5.9	6.2	**5.8**
Direct **(**KWh/m^2)	7.4	7.3	6.2	5.2	5.3	4.8	4.2	4.5	5.2	5.1	6.3	7.3	**5.7**
Global **(**KWh/m^2)	6.2	6.5	6.3	5.8	5.6	5.3	5.0	5.3	5.8	5.5	5.8	6.0	**5.8**
NMSA **1** **(**KWh/m^2)	5.7	3.9	5.9	6.9	6.3	5.7	5.1	5.8	5.5	6.1	5.7	5.4	**5.7**
NMSA **2** **(**KWh/m^2) 2	6.8	6.4	6.2	5.8	5.7	6.2	6.7	6.7	6.6	6.5	6.6	6.5	**6.4**
Average monthly (KWh/m^2)	**6.5**	**6.1**	**6.2**	**5.9**	**5.7**	**5.5**	**5.2**	**5.5**	**5.7**	**5.8**	**6.3**	**6.3**	**5.9**

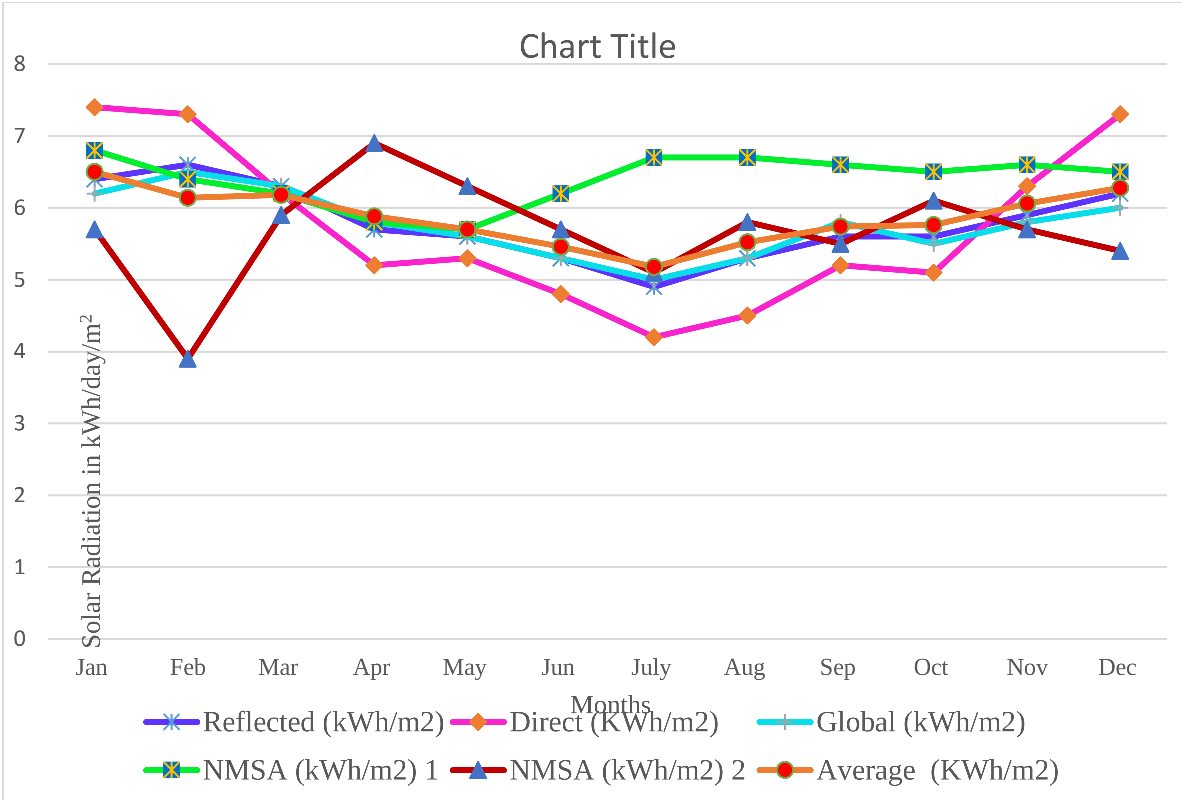

Figure 3.3 Average monthly solar radiation in kWh/d/m^2 using excel

3.4 Estimating the Load

To design an off-grid hybrid power system for a specific area community the establishment of information's like the daily load profile of the community, climatic/weather data of the sites, the initial cost of the components, cost of diesel fuel and project lifetime, etc are the important parameters to consider. It commonly is known that the load factor in a rural community is lower than urban areas; therefore, it is necessary to keep the load factor from being poor when designing an energy system with balancing the cost of energy per Kilowatt-hour. Load estimation approached based on the electric appliances used by each sector, with no attention given for their efficiency. Renewable sources power generation systems cannot generate the exact amount of energy to meet the load demand, either they produce excess electricity or below the demand. Thus instead of calculating the estimated load of the community by the efficiency factor of each appliance, it is better to allow excess electricity production from the system. The initial point to know in calculating the load is deciding which appliance, as well as the rural family household, assumed the current and future situation of the local community, as well as the countries energy system must use.

Under this project three of Jarso villages namely Kondo, paripata and Anatatim are consider where Kondo is the central village both elementary school and clinic center are available.

Under this case, solar PV/diesel hybrid with energy is considered. In this project, the community of the village electric load demand divided into three major categories like:

- The household/domestic sector which includes (lighting, Radio and mobile charge)
- Community load for Elementary school consists of (Lighting, fans, TV, desktop computer, printer, fans, and refrigerator).
- Clinic health center which includes (Lighting, fans, TV, desktop computer, personal computer, Microscope, printer, and refrigerator).

The design process for stand-alone systems begins with an estimate of the daily loads that are to provide for analysis. As with all design processes, several of produces may be required. Various produce will follow in which trade-offs are made between more expensive, but more efficient, appliances and devices in exchange for fewer PVs and batteries. Lifestyle adjustments need to be considered in which some loads are to, treated as essentials that must provide for, and others are luxuries to use only when conditions allow. A key decision involves whether to use all dc loads to avoid the inefficiencies associated with inverters, or whether the convenience of an all ac system is worth the extra cost, or perhaps a combination of the two is best. Another important decision is whether to include a generator back-up system. Design steps is shown in fig 3.4.

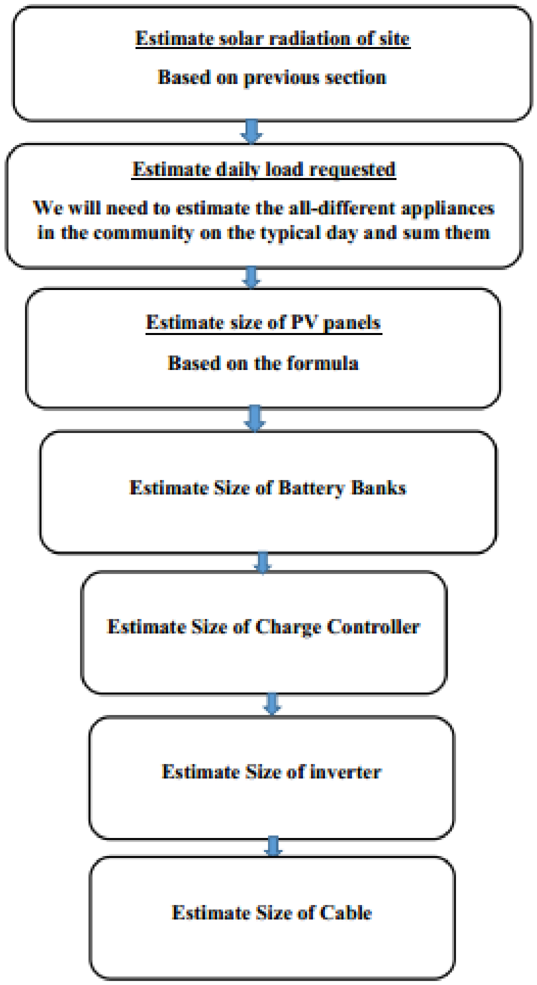

Figure 3.4 Flowchart of estimating the size of a system

- **Estimation of Primary Load**

The Primary load is the load that should meet by the energy providing system, as it requires immediately. Here the electricity load consumption in each household considered to the same and constant throughout the year. The load determination of the village performed for 245 household numbers with an average of five family members per household; that depicts a population number of 1225. The rural economic situation of the country is below the poverty line and thus in this energy system design, the selection of appliances was reflected for the low wattage for the affordability of the provided electric energy. The electricity load estimation made according to the following approach.

$$Weekly\ Energy\ consumption\ (kWh)(E_{week}) = \frac{n_{app} \times P_{rate} \times Hrs_{week}}{1000 \times 7days} \quad (3.14)$$

Where. E_{week} is energy required per week, n_{app} is number of appliance, and P_{rate} is power rating,

3.4.1 Load required for Elementary School

For any community Quality education is essential for Scio-economic development of one country. Under this study in each household's family, at least three members are considered as school attending age. Thus 12 classrooms, 2 administration offices, 2 staff offices and with 2 toilet rooms for students and 1 toilet room for staff are proposed for this study. For each class rooms 4 units of 36W CFL, 2 units of 36W CFL for each administration and staff offices, 1 unit of 36W CFL for each toilets rooms, 1 unit of 200W desktop computer for each administration offices, a common 1 unit of 150W printer and 1 unit 350W photocopy machine for offices, 1 units 60W of fan for each offices and a common 1 unit of 100W refrigerator for administration offices is required. Additional, 4 units of 36W CFL for the school surroundings lighting is also proposed. As noticed above during the daytime no need for electricity for the classrooms since the sunlight can brighten the classes through the glass windows. Thus, the computers and printer at day times will utilize most of the electricity, which is very small. The largest load of the school will have recorded on the evening times when evening classes would be accompanying. The desktop computer is to be functioning for 8:00 hours from 8:00-12:00 and from 13:00-17:00, a photocopy which will operates 2:00 from 9:00 to 10:00 and 14:00 to15:00, and printer, 150W is to be run for an average of 1 hour from 15:00-16:00, following all typing will be completed. An assumption taken that evening classes would conduct from 18:00-21:00 hours. However, the number of evening students would expect not to be more than three classes. During the weekends, evening classes have been conducted in the daytime from 8:00 to 12:00 and at the same time, students can have tutorial classes. The annual break of the academic year for schools is during July and August and the semester break is in January. The total daily electricity consumed by the school except for January, July, and August is shown below in table 4.1. [65].

Table 3.5 School Daily and Weekly Electricity Load Consumption

Appliance	Qty	Capacity (wattage)	Daily Duty Cycle (Hrs/day)	Daily Duty Cycle (day/week)	Daily load Wh/day	KWh/day	Weekly load (KWh/week)	Peak Load (Wh/Day)	Peak Load (KWh/Day)
Lighting	63	36	4	5	9072	9.072	6.48	2268	2.268
Fans	4	60	4	5	960	0.96	0.6857143	240	0.24
Desktop Computers	2	200	8	5	3200	3.2	2.2857143	400	0.4
Printer	1	150	2	5	300	0.3	0.2142857	150	0.15
32" LCD television	1	90	8	7	720	0.72	0.72	90	0.09
Photocopy	1	350	2	5	700	0.7	0.5	350	0.35
Refrigerator	1	100	5	5	500	0.5	0.3571429	100	0.1
Other loads	2	100	2	7	400	0.4	0.4	200	0.2
Total		**1086**			**15852**	**15.852**	**11.64286**	**3798**	**3.798**

3.4.2 Load required for Domestic/households

For an each individual household, the electricity demand considered energy-saving lamps, radio or cassette recorder, 10% of the household may use Refrigerators and TV. The individual households assumed of 11W energy-saving lamps, 2 units for residential rooms lighting, which is to be operational for 6:00 hours, on average from 18:00-00:00 hour. A radio of 5W, which will operate for 4 hours from 8:00 to 10:10 and from 19:00 to 20:00, suggested. A refrigerator operates for 4:00 hours from 11:00 to 14:00, a 19"LCD TV operates for 8:00 hours at 08:00, 09:00, 12:00, 13:00, and from 18:00 to 21:00. Finally, 10% of the total daily load to become to the other loads, be considered for the community. The electricity load demand estimated for a single household for weekdays only being calculated, as follows and summarized in table 3.6.

Table 3.6 Households Daily and Weekly Electricity Load Consumption

Appliance	Qty	Capacity (wattage)	Daily Duty Cycle (Hrs/day)	Daily Duty Cycle (day/week)	Daily load Wh/day	KWh/day	Weekly load (KWh/week)	Peak Load (Wh/Day)	Peak Load (KWh/Day)
Lighting	490	11	4	7	21560	21.56	21.56	5390	5.39
Radio	245	5	4	7	4900	4.9	4.9	1225	1.225
Refrigerator	25	100	4	7	10000	10	10	2500	2.5
19" LCD TV	25	40	8	7	8000	8	8	1000	1
Mobile Charger	245	4	6	7	5880	5.88	5.88	980	0.98
Sum		**160**			**50340**	**50.34**	**50.34**	**11095**	**11.095**
Other loads				7	5034	5.034	5.034	719.1429	0.71914286
Total					**55374**	**55.374**	**55.374**	**11814.14**	**11.8141428**

3.4.3 Load for Health Clinic

Health clinic connected close to a gathering of communities is fundamental administration center, which is equipped with simple delivery services and minor diseases to treat surrounding communities. The health center would hope to fill in as a health facility, which will serve pharmacy drug, follow up of the health state of the residents including pregnant everyday health condition. The basic illnesses that require extraordinary treating were not be served in this health center rather will be alluded to the near-by very much prepared centers or medical clinics.

The main possible appliances that draw electric power in this clinic are low energy light bulbs, fan, television, computer, printer, laboratory microscope, and refrigerator. The health center will have 4 reception rooms, 1 delivery rooms, 1 laboratory room, 2 offices, 1 pharmacy room, 2 toilet rooms for employee and 2 toilet rooms for customary are proposed in this study. Each reception, offices rooms, laparotomy, and pharmacy room, the delivery room is lighted with 2 units of 15W energy-saving lamps, and toilet rooms are lighted with 1 unit of 15W energy-saving lamps, for which would work for 12 hours and 4 units of 15W energy-saving lamps for external lighting for 12 hours. It is also proposed to be equipped with 1 unit of 30W microscope to work for 7:00 hours per day from 8:00-14:00 on top of this from 15:00-16:00, 1 unit of 60W fan for each reception, laboratory, delivery, and for offices which is expected to operates for 5:00 hours per day from 11:00 -16:00, 1 unit of 90W 32" LCD television which is expected to work for 12:00 hours per day from 08:00-20:00 hours, 1 unit of 100W refrigerator operating for 24:00 hours, 1 unit 200W desktop computer working for 8:00 hours from 8:00-12:00 and 13:00-17:00 hour, 1 unit 65W printer working for 1:00 hour per day from 14:00-15:00, fan which will operates from 11:00 to 16:00. The highest electrical energy load of the health center will be gained from the lighting, which is 4.68 KWh. Thus, the daily energy consumption by the health center is 14.57 KWh and it is presented below in table 3.7.

Table 3.7 Health Clinic Daily and Weekly Electricity Load Consumption

Appliance	Qty	Capacity (wattage)	Daily Duty Cycle (Hrs/day)	Daily Duty Cycle (day/week)	Daily load Wh/day	KWh/day	Weekly load (KWh/week)	Peak Load (Wh/Day)	Peak Load (KWh/Day)
Lighting	26	15	12	7	4680	4.68	4.68	390	0.39
Fan	9	90	5	7	4050	4.05	4.05	810	0.81
Desktop Computers	1	200	8	7	1600	1.6	1.6	200	0.2
Printer	1	150	1	7	150	0.15	0.15	150	0.15
Refrigerator	1	100	24	7	2400	2.4	2.4	100	0.1
Microscope	1	30	7	7	210	0.21	0.21	30	0.03
32" LCD television	1	90	12	7	1080	1.08	1.08	90	0.09
Other load	2	100	2	7	400	0.4	0.4	200	0.2
Total		**775**	**71**	**56**	**14570**	**14.57**	**14.57**	**1970**	**1.97**

$$Total\ \ daily\ \ \ load\ of\ Kondo = load\ School + \ load\ Households + load\ of Health \tag{3.15}$$

$$= 15.852 + 55.374 + 14.57$$

$$= \mathbf{85.8}\ \boldsymbol{KWh/day}$$

By assuming the overall losses of the hybrid stand-alone power system (solar PV losses, diesel generator losses, battery, controller, controller, and transmission system losses) (30%) [66]

$$Total\ \ daily\ \ energ\ consumed\ by\ a\ load = total\ load\ of\ Kondo + loss\ energy \tag{3.16}$$

$$= 85.8\ KWh/day \times 1.3$$

$$= \mathbf{111.54}\ \boldsymbol{KWh/day}$$

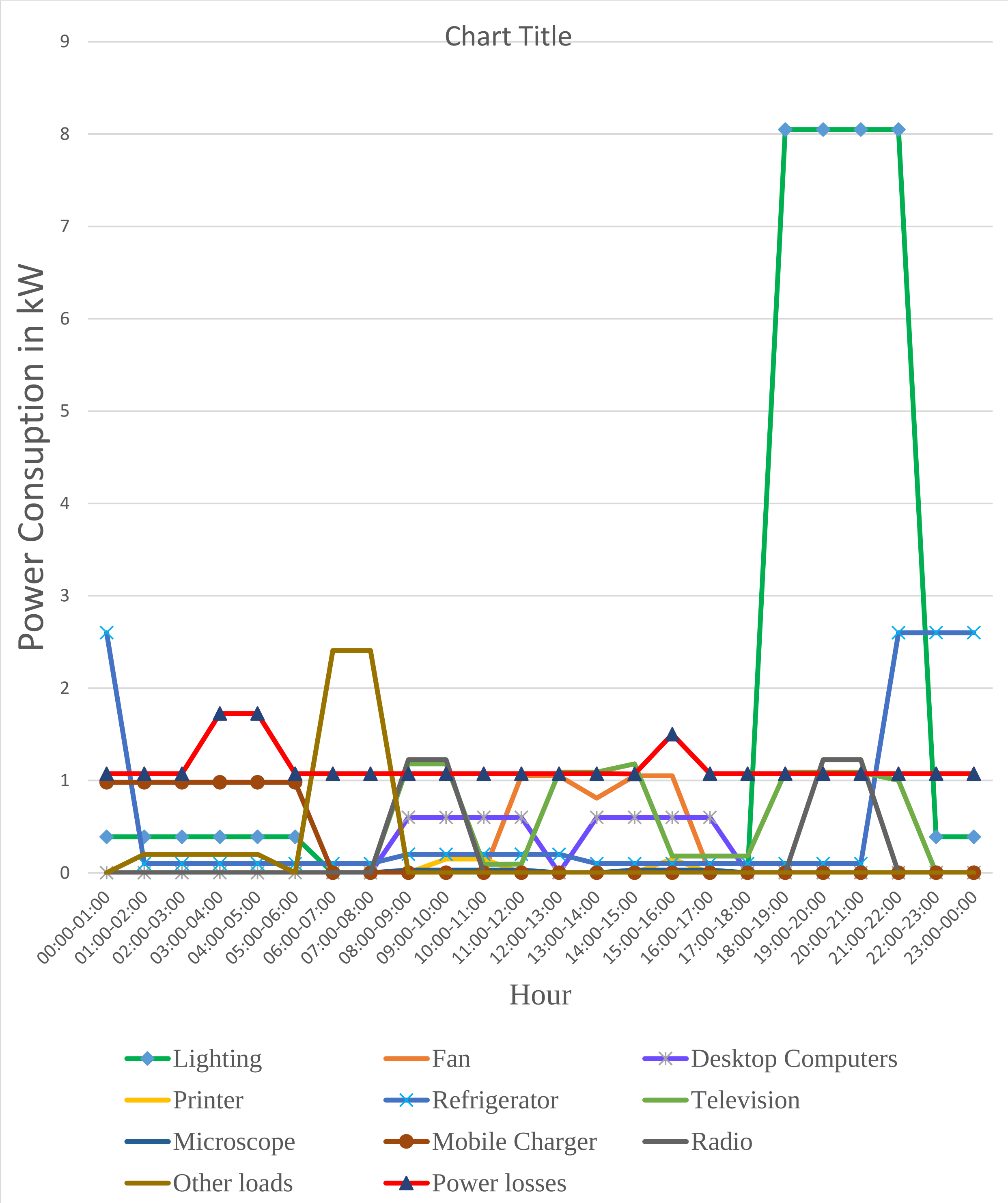

Figure 3.5 Daily Electricity Load Consumption

Table 3.8 Daily load of Kondo

Appliance	00:00-01:00	01:00-02:00	02:00-03:00	03:00-04:00	04:00-05:00	05:00-06:00	06:00-07:00	07:00-08:00	08:00-09:00	09:00-10:00	10:00-11:00	11:00-12:00
Lighting	0.39	0.39	0.39	0.39	0.39	0.39	0	0	0	0	0	0
Fan	0	0	0	0	0	0	0	0	0	0	0	1.05
Desktop Computers	0	0	0	0	0	0	0	0	0.6	0.6	0.6	0.6
Printer	0	0	0	0	0	0	0	0	0	0.15	0.15	0
Refrigerator	2.6	0.1	0.1	0.1	0.1	0.1	0.1	0.1	0.2	0.2	0.2	0.2
Television	0	0	0	0	0	0	0	0	1.18	1.18	0.09	0.095
Microscope	0	0	0	0	0	0	0	0	0.03	0.03	0.03	0.03
Mobile Charger	0.98	0.98	0.98	0.98	0.98	0.98	0	0	0	0	0	0
Radio	0	0	0	0	0	0	0	0	1.225	1.225	0	0
Other loads	0	0.2	0.2	0.2	0.2	0	2.4079	2.4079	0	0	0	0
Power losses	1.0725	1.0725	1.0725	1.725	1.725	1.0725	1.0725	1.0725	1.0725	1.0725	1.0725	1.0725
Load per each Hrs	**5.0425**	**2.7425**	**2.7425**	**3.395**	**1.67**	**2.5425**	**3.5804**	**3.5804**	**4.3075**	**4.4575**	**2.1425**	**3.0475**

Appliance	12:00-13:00	13:00-14:00	14:00-15:00	15:00-16:00	16:00-17:00	17:00-18:00	18:00-19:00	19:00-20:00	20:00-21:00	21:00-22:00	22:00-23:00	23:00-00:00
Lighting	0	0	0	0	0	0	8.0488	8.0488	8.0488	8.0488	0.39	0.39
Fan	1.05	0.81	1.05	1.05	0	0	0	0	0	0	0	0
Desktop Computers	0	0.6	0.6	0.6	0.6	0	0	0	0	0	0	0
Printer	0	0	0	0.15	0	0	0	0	0	0	0	0
Refrigerator	0.2	0.1	0.1	0.1	0.1	0.1	0.1	0.1	0.1	2.6	2.6	2.6
Television	1.09	1.09	1.18	0.18	0.18	0.18	1.09	1.09	1.09	1	0	0
Microscope	0	0	0.03	0.03	0.03	0	0	0	0	0	0	0
Mobile Charger	0	0	0	0	0	0	0	0	0	0	0	0
Radio	0	0	0	0	0	0	0	1.225	1.225	0	0	0
Other loads	0	0	0	0	0	0	0	0	0	0	0	0
Power losses	1.0725	1.0725	1.07	1.5	1.0725	1.0725	1.0725	1.0725	1.0725	1.0725	1.0725	1.0725
Load per each Hrs	**3.4125**	**3.6725**	**4.03**	**3.61**	**1.9825**	**1.3525**	**10.3113**	**11.5363**	**11.5363**	**12.7213**	**4.0625**	**4.0625**
Total	**111.54KWh/day**											

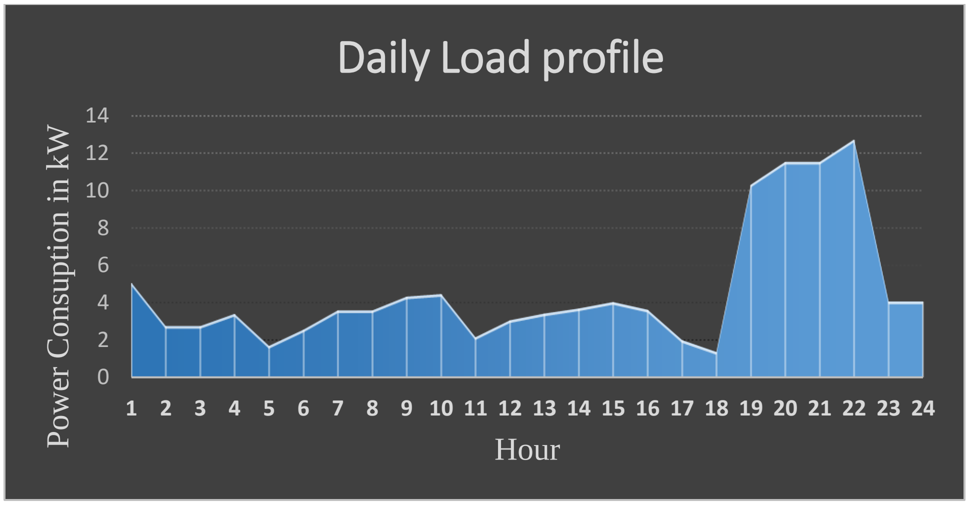

Figure 3.6 Daily load curve for the Kondo Village

3.5 Sizing of System Components

By considering each component of the system independently, the preliminary sizes of the PV-arrays, Genset, Battery bank, Controller, and power converters discussed below.

3.5.1 Sizing of Diesel Generator

Based on daily energy required for the community, this project case study, the size of the diesel generator may generate 6.5 kW for a time duration for four consecutive hours, which is 26 KWh/day from 19:00 to 22:00.

The diesel generator can be model by a polynomial of first or second demand [67] [68], in Eq. 3.17.

$$V = a \times P^2 + b \times P + k \tag{3.17}$$

Where a, b, and k are the constant, V is the volume of fuel consumed, P is the electric power.

The curve cuts the y-axis in v = k, which corresponds to no-load operation. The slope of line b represents the increase in consumption with the load, but near the nominal operating point, the increase in consumption is not linear. This is due to the influence of Diesel motor efficiency. Making measurements, that have made it possible to fit the values of the parameters a, b and k.

Once we have sized the required electricity units from Diesel Genset, amount of required Diesel will be calculated by using the thumb rule that 350 ml of Diesel is used to generate 1 kWh of electricity [69] [70].

$$Value\ of\ liters\ used\ per\ day = \frac{Generator\left(\frac{KWh}{day}\right) \times 350ml}{1KWh} \tag{3.18}$$

$$= \frac{26\frac{KWh}{day} \times 350}{1\ KWh}$$

$$= \mathbf{9100\frac{ml}{day}} = \mathbf{9.1\ l/day} \quad where\ (1l = 1000ml)$$

3.5.2 PV System Array Sizing

Solar Photovoltaic array designing and selection has done by choosing the month with lowest available radiation. To calculate the panel generation factor, the lowest monthly $KWh/m^2/day$ value is the one available, (From Jarso site the minimum radiation is on July month **5.2kWh/m²/day**, on table 3.4). That is equivalent to 5.2 hours or PSH of $1000W/m^2$ sunlight every day.

- **Solar Cell Modeling**

The output-terminal current (I) is equal to the light-generated current I_L, less the diode-current I_D and the shunt-leakage current I_{SH}. The series resistance RS represents the internal resistance to the current flow, and depends on the p-n junction depth, the impurities, and the contact resistance. The shunt resistance R_{SH} is inversely related to leakage current to the ground. In an ideal PV cell, R_S= 0 (no series loss), and $R_{SH} = \infty$ (no leakage to ground). In a typical high quality one square inch silicon cell, R_S = 0.05 to 0.09 ohm and R_{SH} = 316 to 518 ohms. The PV conversion efficiency is sensitive to small variations in R_S, but is insensitive to variations in R_{SH}. A small increase in R_S can decrease the PV output significantly.

The simplified equivalent circuit of a solar cell consists of a diode and a current source, which switched in parallel. The current source generates the photocurrent I_{Ph}, which is directly proportional to the solar irradiance G. The p-n transition area of the solar cell is equivalent to a diode.

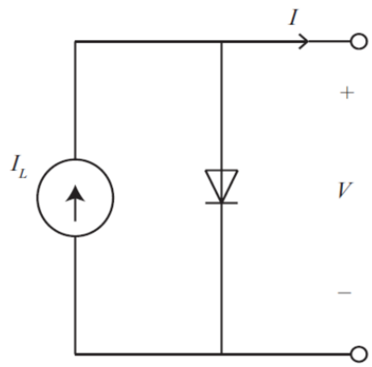

Figure 3.7 Equivalent circuit of a solar cell [38]

The V-I equation of the simplified equivalent circuit could be derived from Kirchhoff's current law

$$I = I_{ph} - I_D = I_{ph} - I_S(\exp\left(\frac{V}{mV_T}\right) - 1) \quad (3.19)$$

Where, I_{ph} is Photocurrent, I_D is diode current, I_S is saturation current, m is diode ideal factor, VT is (k*T)/q is Thermal voltage (25.7 mV at 25°C), k = Boltzmann Constant=1.3824*e-23, q = charge of an electron=1.60*e-19 coulombs, T is absolute température, V is output voltage of the solar cell and I is output current through the solar cells.

The simplified equivalent circuit does not give an optimal representation of the electrical process at the solar cell. In real solar cells, a voltage loss on the way to the external contacts could observed. This voltage loss could be expressed by a series resistor R_S.

Furthermore, leakage currents could have observed, which a parallel resistor R_P could describe. (Fig. 3.8).

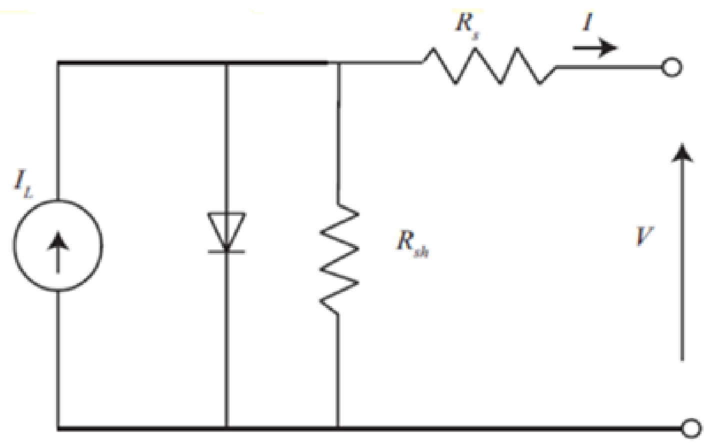

Figure 3.8 Equivalent circuit for one diode mode of a solar cell [71]

Derived from Kirchhoff´s first law the equation for the extended I-V curve could achieve.

$$I = I_{Ph} - I_D - I_P \tag{3.20}$$

$$I_P = {V_D}/{R_P} = \left\{ \frac{(V + IR_S)}{R_P} \right\} \tag{3.21}$$

$$I = I_{Ph} - \left\{ I_S \left(\exp\left(\frac{q(V + IR_S)}{mkTN_S} \right) - 1 \right) \right\} - \left(\frac{V + IR_S}{R_P} \right) \tag{3.22}$$

Where: I_{Ph} is the photo current; I_D I is the Diode current, R_S is the cell's series resistance and R_P is the shunt resistance

The power output of a PV system is determined by the type and area of the PV material and the incident solar radiation.

Mathematically, it can be expressed by equation [2.5].

$$P_{pv} = A_c \eta_{mp} \eta_e GT \tag{3.13}$$

Where: P pv= power output of PV array

Ac=the array area

η_{mp} =the maximum power point efficiency of the array (≈14%)

η_e =the efficiency of power conditioning equipment (≈90%)

GT = the incident solar radiation on the array. The solar cell described above is the basic building block of the PV power system. For obtaining high power, mathematically such cells are connected in parallel and series circuits on a panel (module). The solar array or panel is then made from a group of several modules electrically connected in series-parallel combinations to generate the required voltage, current and power.

The practical PV cells also contain parasitic elements, series resistance (R_s) and shunt resistance (R_{sh}). The presence of shunt resistance is due to impurities near the p-n junction and series resistance is due to high resistance of metal contacts, interconnections and, semiconductor material. The higher value of shunt resistance is desirable and thus it increases the performance of PV cell and the lower value of series resistance increases the output power of PV cell as shown in Figure 3.9.

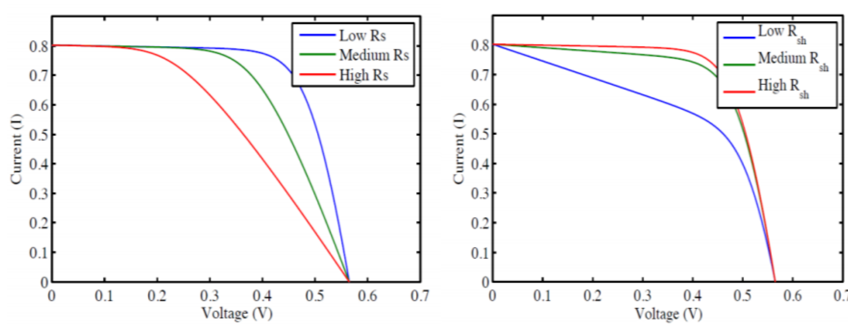

Figure 3.9 The series and shunt resistance effect on V-I curve of a solar cell [72].

The presence of shunt and series resistance in the V-I characteristics of PV cell given by:

$$I = I_L - I_O \left[\exp\left(\frac{(v+TR_S)q}{nkT}\right) - 1\right] - \frac{v+TR_{Sh}}{R_{sh}} \quad (3.27)$$

➢ **Temperature and Irradiance effect on PV cell**

The performance of PV cell affected by ambient factors such as temperature and irradiance. This section describes the dependency of both factors on the performance of PV cell. The short circuit current has an almost linear relationship to irradiance on the cell. The increase in irradiance increases the short circuit of PV cell and vice versa [73].

$$I_{sc}(G) = \left(\frac{G}{G_o}\right).I_{sc}G_o \tag{3.28}$$

Where, G_o is reference level of irradiance and G is the incident irradiance on PV cell. The dependency of irradiance and temperature also illustrated in Figure 3.10 apparently, the environment temperature affects the operational performance of PV cell. The increase in temperature slightly increases the open circuit current due to narrow bandgap but it decreases the short circuit voltage significantly. The dependency of crystalline silicon-based solar cell on temperature is given as [73]

$$I_{sc}(T) = I_{sc.REF} + 0.006\frac{A}{K}(T - T_{REF}) \tag{3.29}$$

And the dependency of open circuit voltage on temperature is expressed as [73]

$$V_{oc}(T) = \frac{E_{go}}{q} - \frac{kT}{q}ln(\frac{BT^{\gamma}}{I_{sc}}) \tag{3.30}$$

Where γ is temperature dependent on parameter of dark saturation current, *B* is constant and independent of temperature, Ego is the linearly extrapolated zero temperature band gap energy of the semiconductor [74]. The rough estimation of the increase of every degree centigrade of silicon cell decreases the output power by 0.5%. The dependency of temperature and irradiance on the V-I characteristics of PV cell is shown in Figure 3.10.

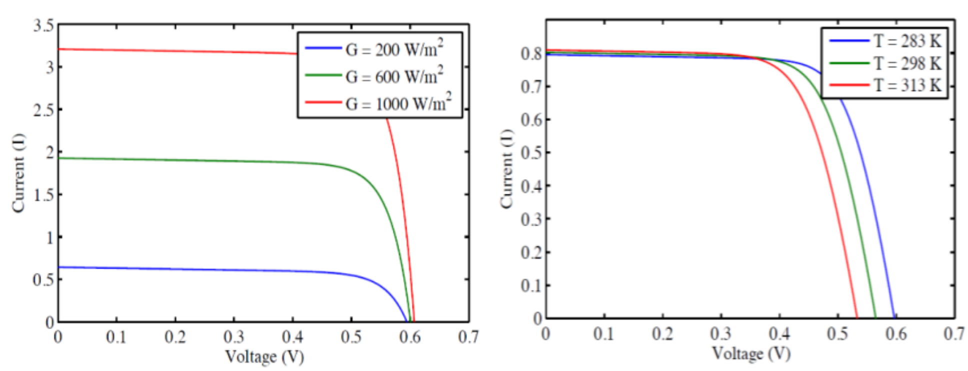

Figure 3.10 The irradiance and temperature effect on V-I characteristics of PV cell [75].

For this task estimation, the system will be powered by 24V DC, 240W PV module that accessible module in the market. The initial step toward estimating the PV array is to determine the daily energy load demand from the array. The required energy gained is then, divided by the insolation or sun peak hour of month's out of every day for Jarso to get the peak power. Then peak power divided by the selected module wattage to obtain to several modules required. At last, many parallels and series modules arrangement can then be determined to give the array size. Based on the individual cost of the module (M_{cost}), the total cost of the PV modules (M_{cost}) can then be determined. Where, k is mismatch factor of the solar PV modules expressed in percentage. Table 3.9 determination procedure of sizing and cost summary of the PV array.

Table 3.9 Sizing and Cost Estimate Summary of PV Array

Required Information		
Solar Module: Perform Poly240W, Vrm = Vmp = 30.4V, $V_{nominal} = 24V$ Irm = Imp = 8.0 A, Isc_m = 8.52A, M_{cost} = \$365, $k = 60\%$		
Rated output watt – peak of PV module (Wpv) =240		
System Voltage (V_{sys}) = 48V		
Total required PV array voltage at maximum power point ($V_{arr\ m}$) = 410.3 V		
Insolation (PSH) = 5.2 KWh/day		
Daily Energy Demand (Ed) = 85796 Wh/day		
Battery Efficiency (η_b) = 0.85		
Inverter Efficiency (η_i) = 0.9		
Charge Controller Efficiency (η_{cc}) = 0.9		
Parameter Being Determined	**Working Formula**	**Computed Parameter Value**
Required Daily Energy Demand (E_{rd})	$E_{rd} = \frac{E_d}{\eta_b \eta_i \eta_{cc}}$	124.412 KWh/day

Average Peak Power (Pave,peak)	$P_{av\_peak} = \frac{E_{rd}}{PSH \times k}$	301.17 KWh/day ≅ 32000 Wh/day
Total Number of Modules (Ntm)	$N_{tm} = \frac{P_{av\_peak}}{W_{PV}}$	132
Number of Series Modules (Nsm)	$N_{sm} = \frac{V_{arr\ m}}{V_{mp}}$	11
Number of Parallel Modules (Npm)	$N_{pm} = \frac{N_{tm}}{N_{sm}}$	12
Maximum power of PV array (P_{ma})	$P_{ma} = V_m \times I_m \times N_{pm}$	32 kW
Total Cost of Array (Acost)	$A_{cost} = N_{tm} \times M_{cost}$	$48180

3.5.3 Battery sizing

The ampere-hour capacity (CAh) and watt-hour capacity (CWh) of a battery bank required to supply a load for a certain period (day) when energy from renewable resources is not available can be specified as follows [76] [77].

To size the battery bank, the estimated energy storage is first determined. The obtained energy value is then, divided by the allowable depth of discharge of the battery to give a safe energy storage value of the required battery bank. At this point, the particular battery be used is selected and using its specifications, the capacity of the entire battery bank in Ampere-hours is computed, and subsequently, the total number of batteries in the bank is computed. Finally, the number of batteries in series and parallel branches of the bank are determined and an estimate of the cost of the battery bank ($B_{b\text{-}cost}$) made from the knowledge of the cost the selected single battery (B_{cost}). The procedure for sizing the battery bank and cost estimate described in Table 3.10.

Table 3.10 Sizing and Cost Estimate Summary of Battery Bank

Required Information
Number of Days of Autonomy (DOA) = 1 Day **Battery:** PV200**,** C_{batt} = 200 Ah, V_{batt} = 12 V, V_{dc} = 48V, D_{disch} = 50% , B_{cost} = $450

Parameter Being Determined	Working Formula	Computed Parameter Value
Estimated Energy Storage (E_{stored})	$E_{stored} = E_d \times DOA$	85.8 KWh
Safe Energy Storage (Esafe)	$\mathrm{E_{Safe}} = \frac{E_{stored}}{DOD}$	171.6 KWh = 171600Wh
Total Capacity of Battery Bank ($\mathrm{C_{tb}}$)	$\mathrm{C_{tb}} = \frac{\mathrm{E_{Safe}}}{V_b}$	14299.33 Ah
Total Number of Batteries in Bank ($\mathrm{N_{tb}}$)	$\mathrm{N_{tb}} = \frac{\mathrm{C_{tb}}}{C_{batt}}$	72
Number of Batteries in Series ($\mathrm{N_{sb}}$)	$\mathrm{N_{sb}} = \frac{V_{dc}}{V_b}$	4
Number of Batteries in Parallel (N_{pb})	$N_{pb} = \frac{N_{tb}}{N_{sb}}$	18
Total voltage across connected (V_{total})	$V_{total} = \mathrm{N_{sb}} \times V_{batt}$	48 V
Current produced per each battery (I_{batt})	$I_{batt} = \frac{\mathrm{C_b}}{V_{batt}}$	16.67 A
Total current produced per capacity (I_{total})	$I_{total} = \mathrm{N_{pb}} \times I_{batt}$	300 A
Total power delivered as per capacity	$P_{del} = V_{total} \times I_{total}$	14.4 kW
Cost of Battery Bank (B_{b_cost})	$B_{b\_cost} = N_{tb} \times B_{cost}$	$28800

The stand-alone PV system battery bank will consist of 72 total batteries configured with 18 strings of 4 series connected batteries. Each of 18 strings are connected in parallel with each other. That means Battery Bank described as total batteries configured with 18 strings of 4 in series consists of 72 connected batteries.

3.5.4 Charge Controller Sizing

Sizing an appropriate, charge controller starts by determining the required total current that the controller should withstand. From the results of the required current, the total number of charge controllers can then be determined and once the cost of a single charge controller known, the total cost of the controllers can then be determined. Table 3.11 described the summary of the Charge Controller sizing procedure and its cost estimate.

Table 3.11 Sizing and Cost Estimate of Charge Controller Summary

Required Information		
Charge Controller: SB3048L -MPPT, Vcc= 24, V_{oc} = 37.3V, Icc= 30 A (dc), C_{cost} = \$500 **Safety Factor (F_{safe})** = 1.25		
Parameter Being Determined	**Working Formula**	**Computed Parameter Value**
Required Charge Controller Current (I_{r_cc})	$I_{r\_cc} = I_{sc\_m} \times N_{pm} \times F_{safe}$	127.8 A
Number of Charge Controllers (N_{cc})	$N_{cc} = \frac{I_{r\_cc}}{I_{cc}}$	4
Cost of Charge Controllers (C_{t_cost})	$C_{t\_cost} = N_{cc} \times C_{cost}$	\$2000
Array maximum voltage (V_{A_max})	$V_{A\_max} = F_{safe}\, N_{sm} \times V_{oc}$	94V

3.5.5 Inverter Sizing

The inverter is a device, which converts DC electrical sources from PV array to AC source of electricity. Photovoltaic modules always produce DC electricity. Most loads are design to operate on AC electrical power. Inverters are a very essential part of PV array systems where alternating current output power is required. The number of inverter-required, which obtained by dividing total, connected AC watts to chosen inverter wattage. To give the battery longer lifetime it should be charged safely and the charge controller protects the battery from over charging and under charging. It has to be capable of carrying the short circuit current of the PV array. Finally, based on the cost of an individual, the total cost of the inverter obtained.

Input power: The input power fed to the inverter can be given in terms of input DC current and input DC voltage.

$$P_{DC} = V_{DC} \times I_{DC} \tag{3.31}$$

Output power: The output of the inverter is can be given in terms of RMS value of voltage, RMS value of current and Power Factor (PF).

$$P_{AC} = V_{rms} \times I_{rms} \tag{3.32}$$

Efficiency of inverter: The efficiency of an inverter can be given in terms of output power and input power, and can be written in the following way:

$$Efficency\ of\ converter = \frac{P_{AC}}{P_{DC}} \times 100\% \tag{3.33}$$

$$Efficency = \frac{V_{rms} \times I_{rms} \times PF}{V_{DC} \times I_{DC}} \tag{3.34}$$

Three-phase inverter is usually used to supply three-phase loads. Figure 3.11 shows the basic circuit of the three-phase VSI inverter. The output voltage waveform is displaced by 120^0 concerning each other. The magnitude of the output voltage of each leg depends on the input voltage or Vdc and switch status. Per each cycle, two switches are always on and the result of the output voltage is independent of the output load current.

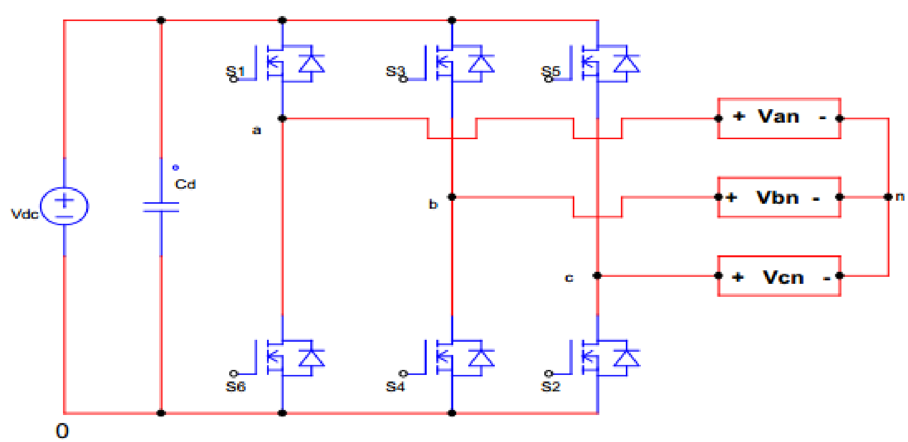

Figure 3.11 Three phase full bridge VSI inverter

The result of the output line voltage consists of discrete values, those Vdc, -Vdc , and zero. The state of generating the output waveform of voltage is done by modulation index equated by

$$\frac{V_{dc}}{2} M_1 = V_{an} + V_{n0} \tag{3.35}$$

$$\frac{V_{dc}}{2} M_2 = V_{bn} + V_{n0} \tag{3.36}$$

$$\frac{V_{dc}}{2}M_3 = V_{cn} + V_{n0} \qquad (3.37)$$

Where, M is the modulation index which varies between 0 and 1. Generally modulation index of the fundamental is given by equation

$$M = m_\alpha \cos(\omega_t - \alpha) \qquad (3.38)$$

$$\frac{V_{dc}}{2}\{(S_1 + S_3 + S_5 - (S_6 + S_4 + S_2)\} = V_{an} + V_{bn} + V_{bn} \qquad (3.39)$$

For the balanced voltage the equation become

$$V_{an} + V_{bn} + V_{bn} = 0 \qquad (3.40)$$

$$\frac{V_{dc}}{6}(2S_1 + 2S_3 + 2S_5) = V_{n0} \qquad (3.41)$$

Then, substituting for V_{n0} the each phase voltage become

$$\frac{V_{dc}}{3}(2S_1 - S_3 - S_5) = V_{an} \qquad (4.42)$$

$$\frac{V_{dc}}{3}(2S_3 - 2S_1 - S_5) = V_{bn} \qquad (4.43)$$

$$\frac{V_{dc}}{3}(2S_5 - S_1 - S_3) = V_{cn} \qquad (4.44)$$

Then, the RMS value can be calculate as

$$V_{rms} = V_{ratio}V_{dc} \qquad (4.45)$$

Where, Vrms is depending on the different types of mechanism applying to control the parameter.

The value of the line voltage is equal to root three times that of the phase voltage. The line to line peak voltage is expressed

$$V_{L-L} = \sqrt{3}[\frac{2}{2\pi}\int_0^{\frac{2}{3}\pi}(V_{dc})^2 d(\omega t)]^{\frac{1}{2}} \qquad (4.46)$$

$$V_{L-L} = \frac{\sqrt{3}}{2}V_{dc}m \qquad (4.47)$$

Table 3.12 Sizing and Cost Estimation Summary of inverter

Required Information		
Inverter: XW6000**,** DC Voltage = 24 V, AC Voltage = 230 V, E_T = 17582.14W, P_{inv} = 6000W, Icost = $5000		
Parameter Being Determined	**Working Formula**	**Computed Parameter Value**
$No.of\ inveretr\ neede$ (N_{inv})	$N_{inv} = \frac{E_{T\_AC}}{P_{inv}}$	3
Cost of Inverter (I_{cost})	$\mathrm{I_{t\_cost}} = N_{inv} \times \mathrm{I_{cost}}$	$15000

Chosen inverter wattage (P_{inv}) = 6000W

$$No.of\ inveretr\ neede\ (N_{inv}) = \frac{total\ connected\ AC\ load\ in\ watts\ (E_{T\_AC})}{choosen\ inverter\ wattage\ (P_{inv})}$$

$$= \frac{17582.1\ Wh/day}{6000W} = \mathbf{2.93 \cong 3}$$

Or

$$Surge\ capacity\ needed = 2.5 \times total\ connected\ AC\ load\ in\ watt \qquad (3.47)$$

$$= 2.5 \times 17582.14\ W = \mathbf{43955.35}$$

$$choosen\ inverter\ Surge\ capacity = 12{,}000$$

$$No.of\ inveretr\ neede = \frac{Surge\ capacity\ needed}{choosen\ inverter\ Surge\ capacity}$$

$$= \frac{43955.35}{12{,}000W} = \mathbf{3.4 \cong 3}$$

3.5.6 Cable Sizing

For stand-alone solar PV system (from panel array to controller, the controller to the battery, and a controller to the inverter to sub distribution box, from sub distribution box to load) can be determined.

Table 3.13 Suggested maximum permissible cable voltage drops [40]

Parameters	**Value**
Battery to charge controller	< 1%
Battery to inverter	< 1%
Solar module to charge controller	< 3%
Charge controller to loads	< 5%
Inverter to loads	< 5%

- Assume that 5% voltage drop in distribution system AC side
- 3% voltage drop in DC side
- 1% drop from charge controller to battery

To estimate the cross-sectional area cable size, first, the current that generated from PV solar has to be calculated.

$$Area\ of\ the\ wire\ (A) = \frac{2\times\rho\times L\times I_{tsc}}{\%\,V_{drop}} = \frac{2\times L\times I_{tsc}}{R\times\%\,V_{drop}} \qquad (3.19)$$

Where R is resistance of the wire, which is equal to 56 Ω/m and ρ is the resistivity of the wire, which the value is the reciprocal of resistance.

Table 3.14 Wire Sizing Summary

Required Information		
$\mathbf{V_{dc\_modu}}$ = 48V, L = 15m, $\rho = 0.01786\ or\ R = 56\Omega/m$, $\%\ V_{drop} = 3\%$, Npm =12		
Parameter Being Determined	**Working Formula**	**Computed Parameter Value**
PV array to battery bank through charge controller current (I_{t_sc})	$I_{t\_sc} = I_{sc\_m} \times N_{pm} \times F_{sa}$	127.8 A
Wire size PV array to battery bank through charge controller (A_1)	$A_1 = \dfrac{2 \times \rho \times L \times I_{t\_sc}}{\%\ V_{drop}}$	48 mm^2
P_{DG} = 6500 W, V_{dc} = 48V, L = 8m, V_{oper} = 230V, $V_{drop} = 0.9\%$, pf = 90%		

Maximum current in (I_{DG}) Amps	$I_{DG} = \frac{P_{DG}}{\text{pf} \times V_{oper}}$	31.4 A
Wire size from diesel generator to inverter (A_2)	$A_2 = \frac{2 \times \rho \times L \times I_{DG}}{\% V_{dc\_drop}}$	20 mm^2
V_{dc_modu} = 48V, L = 7m, $\rho = 0.01786\ or\ R = 56\Omega/m$, % $V_{drop} = 3\%$		
$V_{drop} = 0.9\%$, Icc =30 A, L = 4m, $N_{p\_cc} = 2$, V_{cc}= 24		
Maximum input charge controller to battery (I_{t_cc}) Amps	$I_{t\_cc} = I_{cc} \times N_{p\_cc}$	60 A
Wire size from charge controller to battery (A_3)	$A_3 = \frac{2 \times \rho \times L \times I_{CC}}{\% V_{drop}}$	35 mm^2
P_{inv} = 6000W, pf = 0.9, L = 15m, $\rho = 0.01786\ or\ R = 56\Omega/m$, $V_{drop} = 5\%$, V_{dc} = 24V, V_{oper} = 230V,		
Current produced by inverter output (I_{inv_out}) Amps	$I_{inv\_out} = \frac{P_{inv}}{pf \times V_{opera}}$	29 A
Wire size from inverter to sub distribution box (A_4)	$A_4 = \frac{2 \times \rho \times L \times I_{in\_m}}{\% V_{dc\_drop}}$	13 mm^2

3.6 Energy Management system using PSIM PLC Simulator

Programmable logic control, are also called programmable controller or PLCs, are solid-state member, of computer family, using integrated circuits instead, of electromechanical devices to impalements control functions. PLC are the ability to store commands or instructions, such as timing, sequences, counting, data manipulation, arithmetic and communications to control industrial machines and processing. A programmable controller, as illustrated in below Figure 3.12 a, consists of two basic, the input/output interface system and the central processing unit (CPU) in figure 3.12 b, The (CPU) consists of three components, the processor, the memory system, and the power system supply which governs all PLC activities.

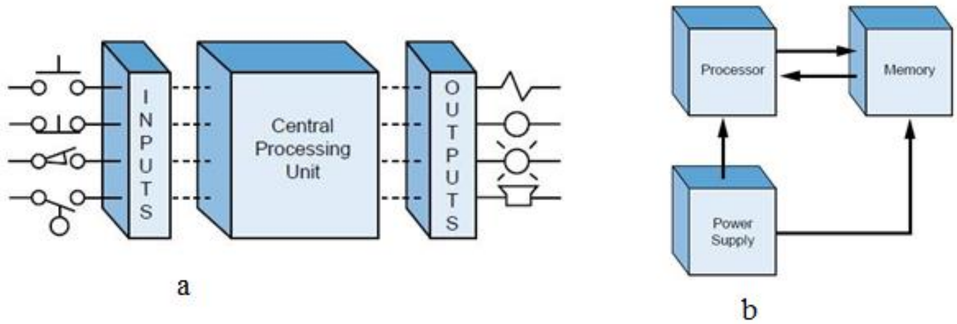

Figure 3.12 PLC conceptual application diagram

- **Operation of PLC**

The operation of the PLC controller is relatively simple. The input/ output (I/O) system physically connected to the field devices that encountered in the machine or that utilized in the control of a process. These field devices may be analog or discrete input/output devices, for example, limit switches, pressure transducers, motor starters, pushbuttons, solenoids, etc. The input/output interfaces associated the connection between the information providers (inputs), the CPU and controllable devices (outputs). Figure 3.13 below shown the I/O system forms the interface by which field devices connected to the controller.

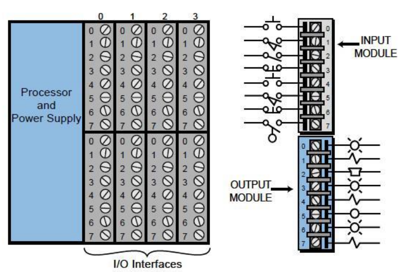

Figure 3.13 The I/O system with interface

The main purpose of the interface is to condition, different signals received from or sent to external field devices. Incoming signals from sensors (e.g., push buttons, analog sensors, selector switches, limit switches, and thumb-wheel switches) to wired to terminals on the input interfaces. Devices that will be controlled, like motor starters, pilot lights, solenoid valves, and position valves, connected to the terminals of the output interfaces. The power system supply provides all the voltages required for the proper operation of the various central processing unit sections [78]

When a system has more than two sources, it is necessary to have an energy management system, which expected to optimize the power-sharing among resources, the cost production, and emission. In this thesis, the main purpose of PSIM PLC simulator is to control the EMS of the system.

PLC used in this thesis has three inputs (Solar PV (SPV), Diesel generator (DG) and Storage Battery and load based on the load required.

- Load control (switching) – ON/OFF loads to achieve economic and effective energy use.
- Source control (switching) – which types of a source at what time (SPV, DG and EEB) continuous, and reliable operation at best economic level. The PLC controller makes a decision on the output based on the operating state of the input.

Table 3.15 State of power supply units with respect to load demand and operation time in energy management system (EMS) based on PLC control

Operating Time	Load (kW)	SPV		DG		Battery	
		ON	OFF	ON	OFF	ON	OFF
00:00 – 06:00	18.135	OFF		OFF		ON	
06:00 – 08:00	7.161	ON		OFF		ON	
08:00 -18:00	32.015	ON		OFF		OFF	
18:00 -21:00	33.3839	OFF		ON		ON	
21:00 – 00:00	20.8463	OFF		OF		ON	

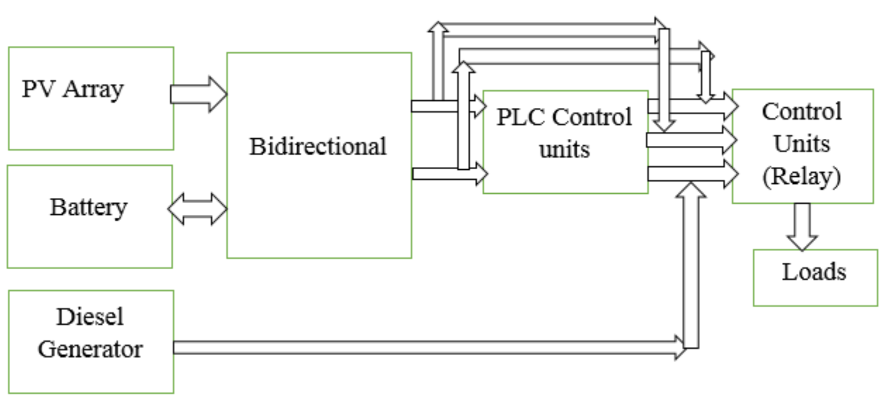

Figure 3.14 Block diagram of hybrid system with using PSIM PLC simulator controller

The ladder program for PSIM PLC simulator shown figure 3.15 below describes the input I:102 is start button and I:103 is stop button and output O:100 is battery supply, O:102 is PV supply and O:103 is diesel generator supply. Finally, by using the F1 button to run a simulation of PLC.

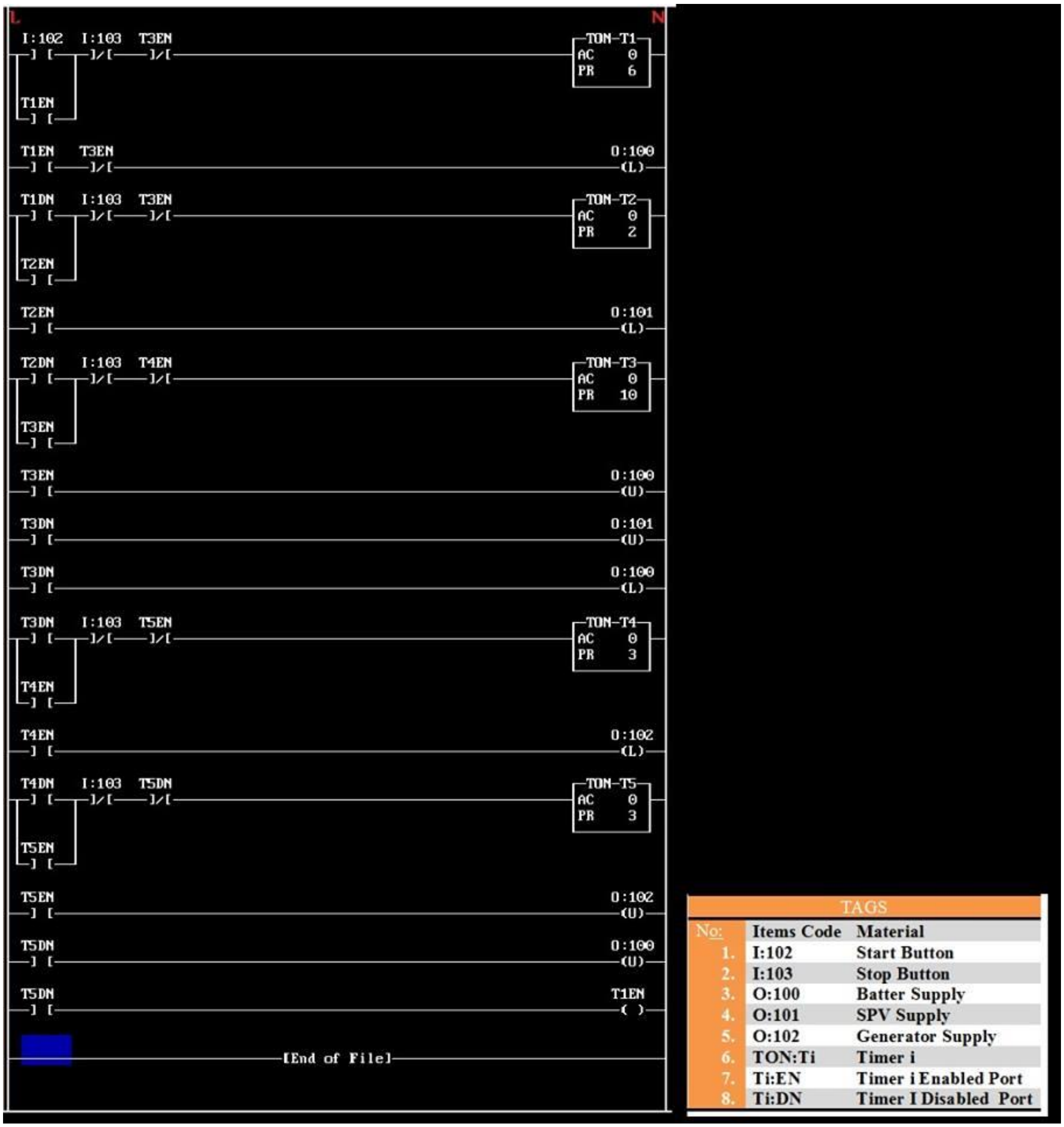

Figure 3.15 Ladder diagram of PSIM for Hybrid system of energy management model

The results are shown in figure 3.16 a) battery and diesel generator supply the community from 18:00 -21:00, b) shows when battery and solar supplying loads from duration of 06:00 – 08:00 and similarly, figure 3.17 a) shows only battery supply from 00:00 – 06:00, b) show only solar PV supply from 08:00 -18:00 for 10 hrs.

a) b)

Figure 3.16 Results of PSIM PLC simulator for a) battery and generator supplying b) battery and solar supplying together

(a) (b)

Figure 3.17 Results of PSIM PLC simulator for a) battery and b) solar PV supplying

CHAPTER 4
MODELING HYBRID SYSTEM

Under this, section each component of the hybrid modeling system includes PV module, diesel generator; battery, converter, and inverter were discussed in detail.

4.1 Modeling hybrid system using MATLAB/Simulink

4.1.1 Model of Diesel Generator Sets

Diesel generator sets convert fuel energy (diesel or bio-diesel) into mechanical energy by means of an internal combustion engine, and then into electric energy by means of an electric machine working as a generator.

- **The mathematical Modeling of a Diesel Generator Set**

The analysis of the complex aspects of a diesel generator set requires the development of reliable mathematical models that necessary for simulation in different operation regimes, specifically in the case as close as possible to the reality of the assembly internal combustion engine – the synchronous generator. The synchronous generator represents the main part of a diesel generator set. It converts the mechanical power produced by the primary mover into electrical power. The mathematical models that be used in the study of the synchronous generator can be classified into circuit models and field models. However, the ones most used in electric drive systems being the circuit models.

The orthogonal model (d-q) of the synchronous machine used based on the decomposition of the three-phase machine in an equivalent bi-phase one, Fig. 4.1. In the way, the phasors system specific to the three-phase machine is decomposed along with the longitudinal axis *d* and transversal axis *q* respectively.

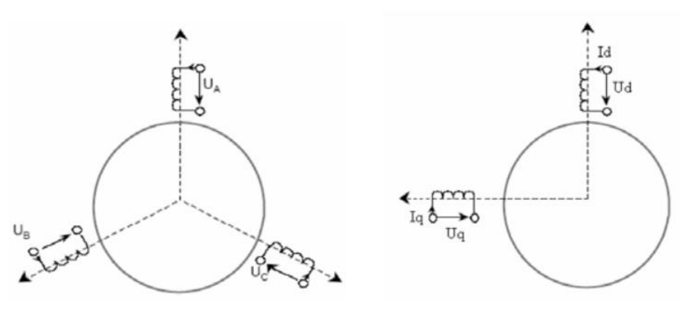

Figure 4.1 Transformation of a three-phase machine in an equivalent bi-phase one [79]

The voltage equations of the synchronous generator written in a coordinate system $d\theta$ - $q\theta$ situated at the electric angle θ with respect to the fixed coordinate system $d - q$ is as follows [79]:

$$V_{s\theta} = R_s I_{s\theta} + \frac{d\Psi_{s\theta}}{dt} + j\omega_{s\theta} \quad (4.1)$$

$$V_{r\theta} = R_r I_{r\theta} + \frac{d\Psi_{r\theta}}{dt} \quad (4.2)$$

Where: $V_{s\theta}$ & $V_{r\theta}$ = are the stator and rotor voltage phasors, R_s and R_r = are the stator and rotor resistances, $I_{s\theta}$ and $I_{r\theta}$ = are the stator and rotor current phasors, $d\Psi_{s\theta}$ and $\Psi_{r\theta}$ = are the stator and rotor magnetic flux phasors, $\omega_{s\theta}$ = is the stator pulsation.

The numerical modeling scheme used for the simulation of a diesel generator set in an isolated regime presented in Fig. 4.2, where we can distinguish: the generator set, the electric load, the normally open switch S1, and the measurement blocks.

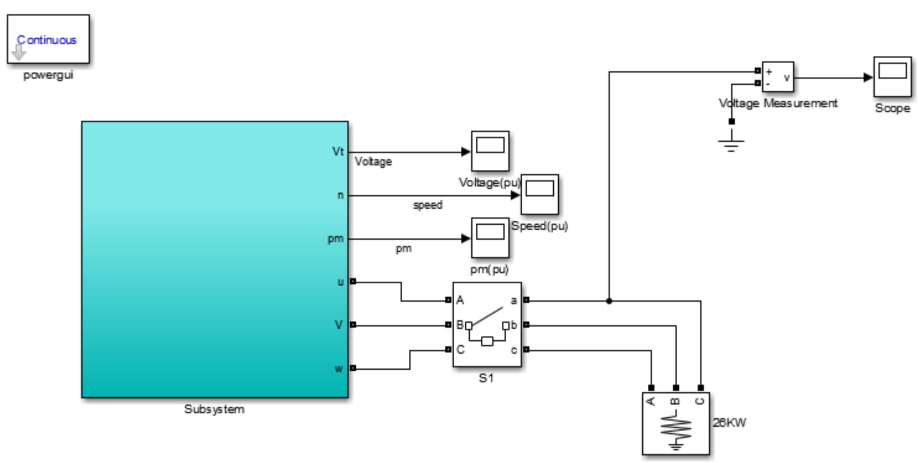

Figure 4.2 Simulink model of a generator set

The generator set block composed of the diesel internal combustion engine model and the synchronous generator model. The internal combustion engine consists of the voltage and speed regulation systems, Fig.4. 3. The main data of the simulated generator set are as follows: rated apparent power 8.5 KVA, real power rated 6.5Kw, rated voltage 400 V, rated frequency 50 Hz.

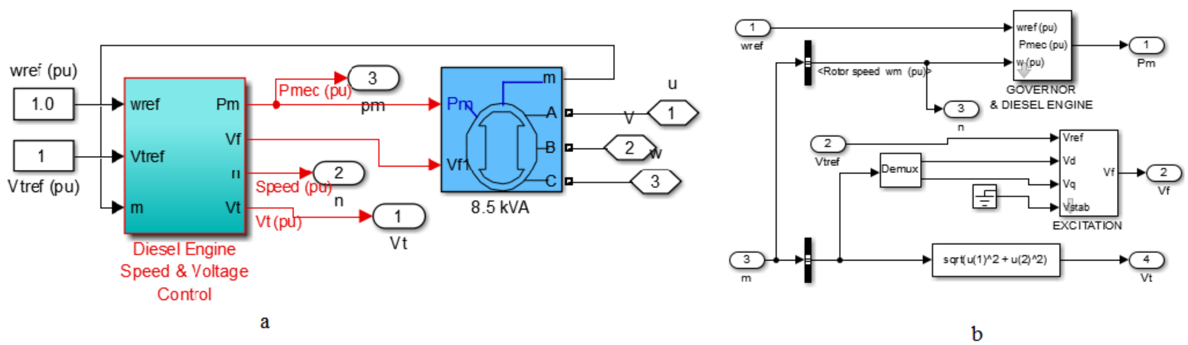

Figure 4.3 Simulink model of a generator set with voltage and speed regulation systems a) global scheme of the generator set b) Diesel engine and regulation systems

4.1.2 Model of PV module Simulink

A generalized PV model built using Matlab/Simulink to illustrate and verify the nonlinear I-V and P-V output characteristics of the PV module. The behavior of photovoltaic (PV) cells can be modeled with an equivalent circuit that includes a photocurrent source, a single diode junction, and a series resistance and a shunt resistance, [80].

The fill factor is useful parameters for quality control test. It is obtained by dividing the peak power of the PV by its short circuit current.

$$FF = \frac{P_{max}}{V_{OC} \times I_{sc}} \tag{4.3}$$

PV panel fill factor is usually between, 0.7 and 0.8 ideal PV panel has 1.0[49]

Table 4.1 Module data sheet value of SCHOTT PERFORM POLY 240W solar array at 25^{0}C, 1,000 W/m^2

Parameters	Values
Nominal power [Wp] Pmpp	>240W
Voltage at nominal power [V] Vmpp	30.4V
Open-circuit voltage [V] Voc	37.3V
Current at nominal power [A] Impp	7.9A
Short-circuit current [A] Isc	8.52A
Cells per module N_S	60
Module Efficiency [%] η	14.3%

Power [%/ºC]	-0.44
Open-circuit voltage [%/ºC]	-0.32
Short circuit current [%/ºC]	0.04

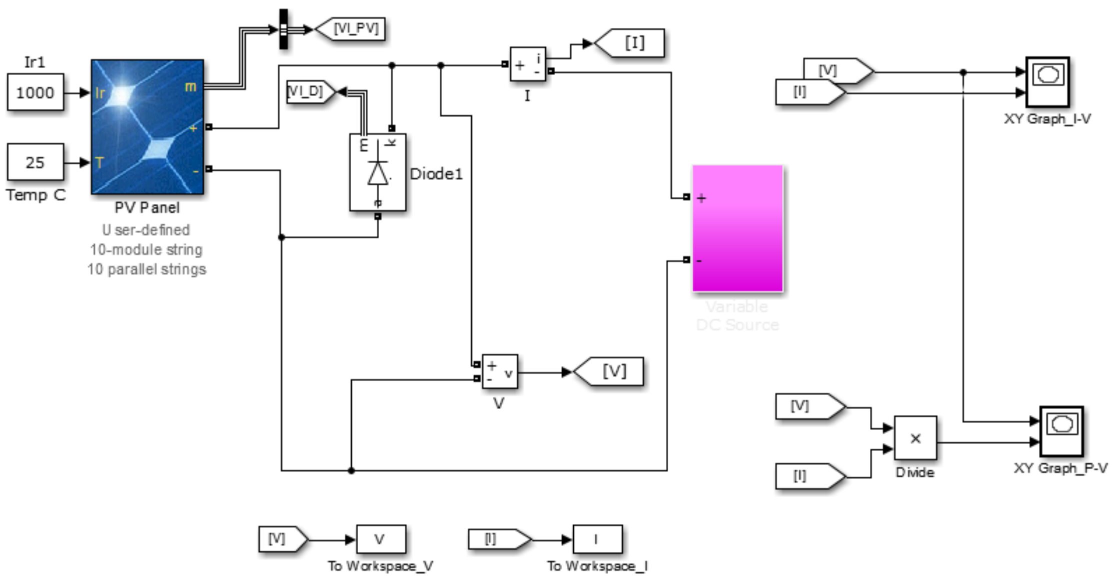

Figure 4.4 Matlab/Simulink model of the PV array

In this model, 60 PV cells interconnected in series to form one module. As a result, the module voltage is obtained by multiplying the cell voltage by the cells number while the total module current is the same as the cell's current.

Table 4.2 Parameters of POLY SCHOTT PERFORM 32000W solar array at 25 C, 1,000 W/m^2

Number of parallel modules (Npm)	12
Number of series modules (Nsm)	11
Output voltage (Vout)	410.3V
Output current (Iout)	102.24A
Maximum output power (Pmax)	32000W

4.1.3 Model of PV DC-DC Boost Converter

The boost converter is a type of DC–DC converter that, the magnitude of the output voltage is always greater than the input voltage magnitude. DC-DC boost converter model designed and applied using MatLab/Simulink as illustrated in Figure 4.5.

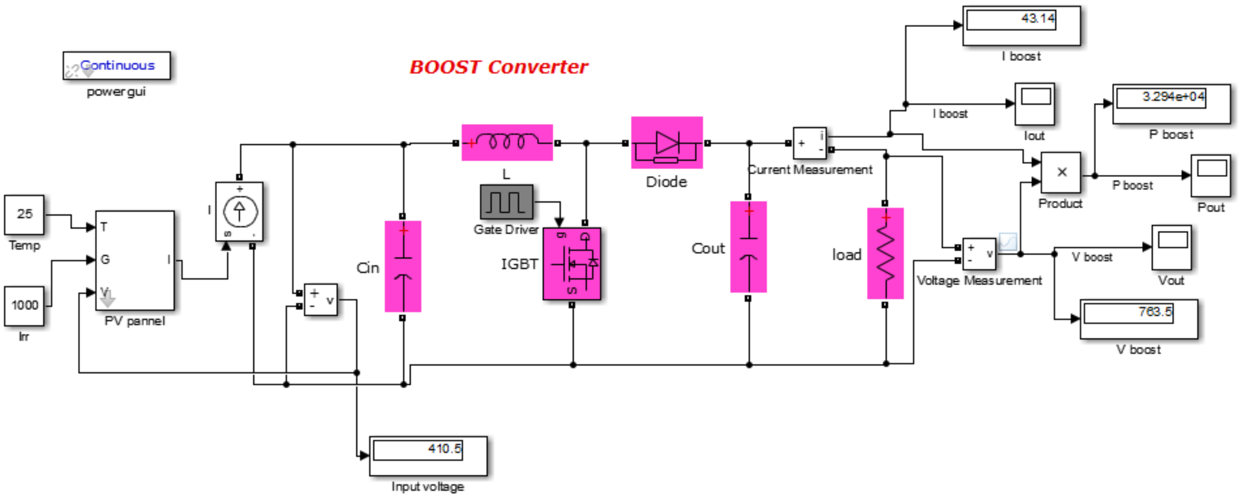

Figure 4.5 Simulink model of Boost converter

DC-DC converters used to interface the photovoltaic module with the inverter, in order to ensure the photovoltaic module is always operating at the maximum PowerPoint. This is done by controlling the converter duty ratio (D) with maximum power point tracking algorithms (MPPT).

shows the circuit of the boost converter where the (conversion ratio between input and output voltage) is [35]

$$\mu = \frac{V_{out}}{V_{in}} = \frac{1}{1-D} = \frac{T}{t_{off}} \tag{4.4}$$

Where t_{off} is the duration that the switch is not active.

The design specifications of the boost converter shown in Table 4.3. The specifications are for a variable value of the input voltage of the boost converter where the input voltage comes from the solar energy source and the output voltage of the boost converter fixed to 760V DC. The inductor, capacitor, load resistance & IGBT values must work out for this circuit to build. Determining the value of the filter inductor and capacitor to operate the converter in the conduction of continues that the output voltage is a key step in finding the value of components required.

Table 4.3 Parameter of DC – DC boost converter

Required Information		
Input voltage range (Vin=Vpv) = (78-410) V Pmax = 32KW Output voltage (Vout) =760V Switching frequency (fs) = 5kHz	Vout ripple (ΔVout) = 1% -5% Iin ripple (ΔIin) = 20% -40% Efficiency (η) = 0.9	
Parameter Being Determined	**Working Formula**	**Computed Parameter Value**
Minimum Duty ratio (Dmin)	$D_{min} = 1 - \eta \times \frac{V_{in\_max}}{V_{out}}$	0.52
Maximum Duty ratio (Dmax)	$D_{max} = 1 - \eta \times \frac{V_{in\_min}}{V_{out}}$	0.91
Max, input current ($I_{\max\_in}$)	$I_{\max\_in} = \frac{P_{max}}{V_{in}}$	78A
Max. load current ($I_{\max\_load}$)	$I_{out} = I_{\max\_load} = \frac{P_{max}}{V_{out}}$	42A
Ripple current (ΔI_{in})	$\Delta I_{in} = 20\% I_{\max\_in}$	15.6A
Ripple Voltage (ΔV_{out})	$\Delta V_{out} = 5\% V_{\text{out}}$	38V
Inductance (L)	$L = \frac{(1-D)DV_{in}}{\Delta I_{in} f}$	$\geq$ 0.13Mh
Input capacitance (C_{in})	$C_{in} = \frac{I_{\max\_load} Dmin^2}{0.02(1-D_{min}) f V_{in\_max}}$	≥1.1mF
Output capacitance (C_{out})	$C_{out} = \frac{(1-D)DV_{in}}{8Lf^2 \Delta V_{out}}$	≥1µF
Load resistance (R_{load})	$R_{\text{load}} = \frac{V_{out}}{I_{\text{out}}}$	17.7Ω

4.1.4 Bidirectional DC-DC Converter Battery

The bidirectional DC-DC converter alongside energy storage has turned into a promising alternative for some, power-related systems, consisting solar and wind system, electric vehicles, energy component vehicles, etc. It minimizes the cost and improves performance, additional, improves the efficiency of the systems [81]. In the off-grid solar system, the bidirectional battery DC-DC converter is often used to transfer the solar energy to the capacitive (battery) energy source during the times when the solar irradiation are sufficient levels, while to deliver energy to the load when the DC bus voltage is low. A battery buck-boost type high-performance bidirectional converter, as shown in Figure 4.6, used to charge and discharge the battery.

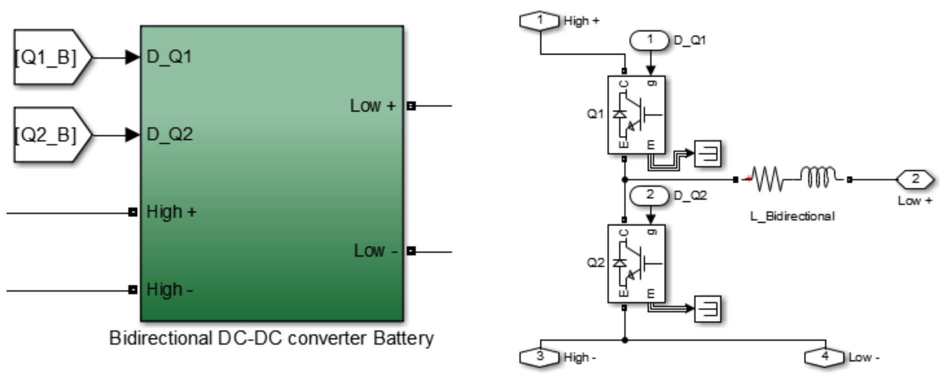

Figure 4.6 Bidirectional DC-DC converter Battery circuit.

As shown in Figure 4.6 the DC-DC (buck-boost) bidirectional converter consists of two main switches (Q1, Q2) with an inductor. Q1 and Q2, once activated, are responsible for maintaining the buck mode and boost mode, respectively.

4.1.5 Model of Lead-Acid battery storage

As seen in section 3.5.3 based on the design of battery size. The stand-alone PV system battery bank will consist of 72 total batteries configured with 18 strings of 4 series-connected batteries. The total required capacity of the battery bank is 14299.33Ah. The model of the Lead –Acid battery storage in the Matlab Simulink is implemented using different standard Simulink blocks and some of the Simpower system blocks in a library as shown in fig 4.7 below. The output of the model is containing a three vector signal: State of Charge (SOC), Battery current and Battery voltage.

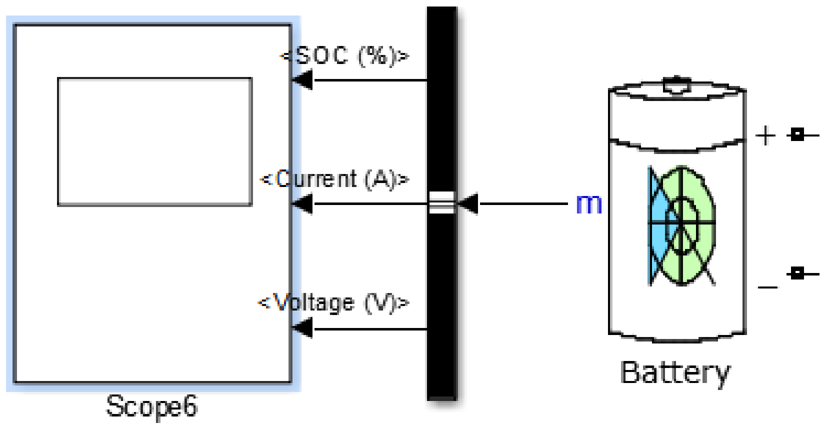

Figure 4.7 Simulink battery model

4.1.6 Modeling of the three-phase inverter

The simulation model of the three-phase photovoltaic system realized by adding a three-phase full-bridge inverter from the Simulink block toolbox. A pulse generator block used to generate the PWM signal of the inverter. Figure 4.7 shows the settings of the pulse generator. The carrier frequency, sampling time and modulation index, can be set up with the pulse generator block.

The three-phase universal inverter circuit takes the output of DC–DC boost voltage as an input and the gate signal generated by SPWM generator. The output voltage of the inverter (V_{rms}) calculated as

$$V_{inv\_out} = \sqrt{\frac{3}{2}} \times m \times \frac{V_{out}}{2} = V_{LL} = 0.6124mV_{out} \qquad (4.5)$$

As a result, the inverter input DC voltage converted in to (456±5%) AC voltage to supply loads. When the value of the modulation index (m) is 0.98 considered for this thesis. Figure 4.8 shows the Simulink modeling block of the inverter

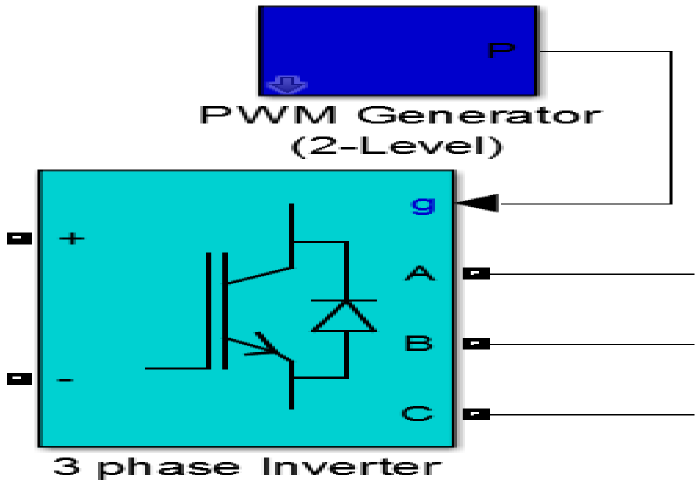

Figure 4.8 Simulink models of 3-phase inverter with pulse generator

Where, $V_{out} = V_{dc}$ is the output voltage of the boost converter, m is the modulation index in rage between 0 and 1 which for this case assumed to be 0.98, f is the fundamental AC frequency, and fs is the PWM frequency.

Table 4.3 Three phase H –bridge Inverter parameters designs based on section 3.5.5

m = 0.98, $P_{inv} = 6000W$, $V_{out} = 540V$, f = 50Hz, fs = 5000Hz		
Parameters	**Formula**	**Value**
Inverter power P_{inv_total}	$P_{inv\_total} = N_{inv} \times P_{inv}$	18Kw = 18000W
Output AC voltage (V_{rms})	$V_{rms} = V_{LL} = 0.6124mV_{out}$	(456∓5%) V
Output AC current (I_{rms})	$I_{rms} = \frac{P_{inv-total}}{\sqrt{3}V_{rms}}$	22.7A

The figure 4.9 shows Simulink model circuit of the inverter based on the parameter.

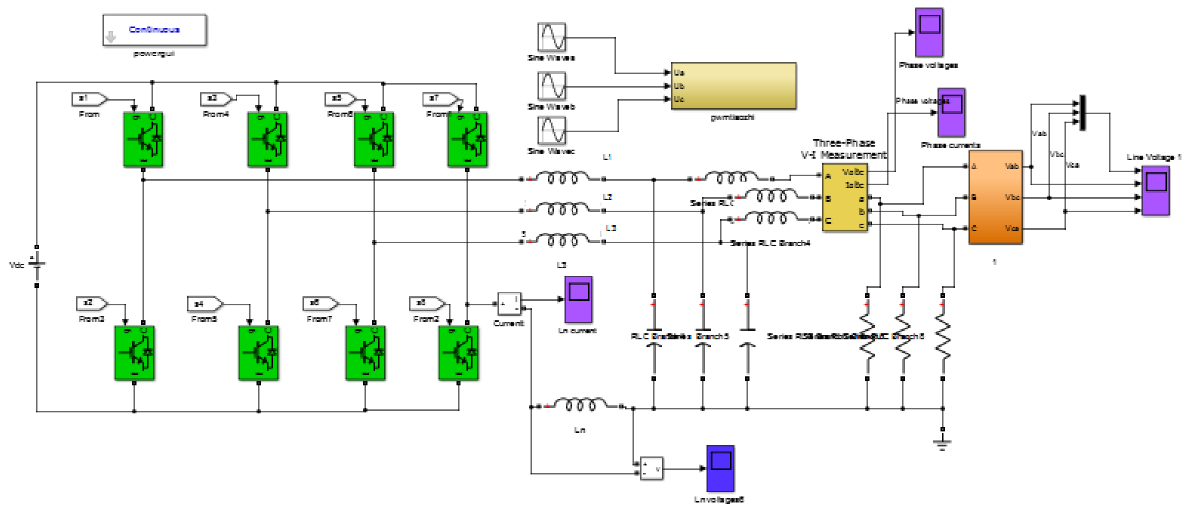

Figure 4.9 Simulink models of three phase VSI

4.1.7 Modeling of LCL low pass filters

The output AC voltage of the inverter is not purely sinusoidal, but by applying the low pass filters which minimizes the value of the harmonic value of the output voltage to supply pure sinusoidal sources to the required load. Inverter contains both input and output inductor, capacitor filter and the appropriate damping resistor with scale.

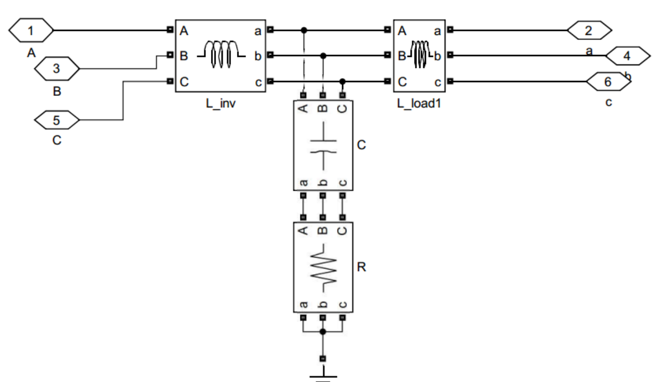

Figure 4.10 Simulink models of LCL low pass filters

The parameter of low pass filter inverter side inductor (Linv), load side inductor (L_{loa}), filter capacitance (C) and damping resistance can be calculated as the following equations in table : The output ripple current (ΔI_l) in the design of L_{inv} was considered up to 15% of the rated output current of the inverter $I_{inv.}$ Where r is constant the ratio of two inductors which is assumed the value of 0.8, ΔI_l is 10% I_{inv} for this thesis work [82] [83].

Table 4.4 LCL parameters designs

Parameters	**Formula**	**Value**
Inverter side inductor L_{inv}	$L_{inv} = \frac{V_{inv\_peak}}{16 \times f_s \times \Delta I_{inv}}$	6.1mH
Load side inductor L_{load}	$L_{load} = r \times L_{inv}$	4.9mH
Capacitance of the filter C_f	$C_f = 5\%Cb = 0.05 \frac{P_{inv}}{2\pi f_s Vin^2}$	3µF
Resonant frequency f_o	$f_o = \frac{1}{2\pi}\sqrt{(\frac{(L_{inv} + L_{load})}{(L_{inv} \times L_{load} \times C_f)})}$	1763Hz = 1.76kHz
Damping resistance	$R_{dam} = \frac{1}{3}\left(\frac{1}{2\pi f_o C_f}\right) = \frac{1}{6\pi f_o C_f}$	10Ω

Even if non-linear loads are at low power, they distort sinusoidal current and voltage waveforms in off-grid power systems. There are odd and even harmonics in off-grid PV systems. The simulation results show that the odd harmonic components contribute more to harmonics as compared to even harmonics. As a result, it has been observed that the LCL filter provides a high performance, taking into account some risky points.

4.1.8 Model of the MPPT controller for solar PV system based on the optimal power

The output of the PV module is nonlinear due to the variables temperatures and variables of irradiance supplied as an input to the PV module. Therefore, the maximum power point of the PV module also varies.

Under this project thesis, by using Perturb and observer (P&O) techniques for tracking the maximum output power of the PV module to command the DC–DC boost converter.

- **Model of MPPT using Perturb and Observe Method**

In this method, the controller adjusts the voltage by a small amount from the array and measures power, if the power increases, further adjustments in the direction tried until power no longer increases. This called P&O method. Due to ease of implementation, it is the most commonly used MPPT method. The model of P&O as shown in figure 4.10 below

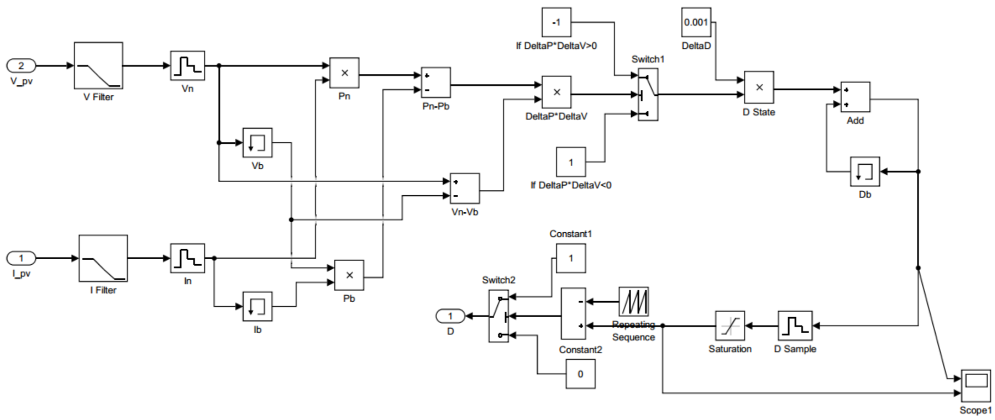

Figure 4.11 Simulation models of P&O

4.1.9 Modeling of the complete system for electrification

The total model of the system as shown below in fig 4.12

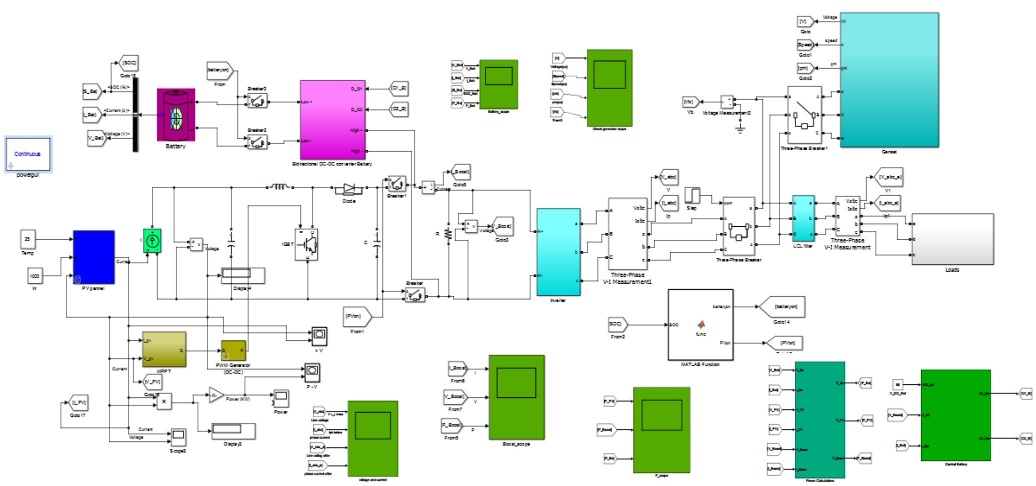

Figure 4.12 General Simulink model of the system for the electrification with P&O MPPT.

4.2 Modeling of the Hybrid system using Homer software

The hybrid system model for electrification, which consists of Solar PV, diesel generator, battery, and converter to simulate on the Homer software as shown in figure 4.13. Solar PV array produced DC power, which converted into AC to fed AC bus to supply AC load. The diesel generator generated AC power directly fed AC bus and supply AC load. Excess energy goes to the battery storage bank and used by the system if Solar PV sources do not have enough energy.

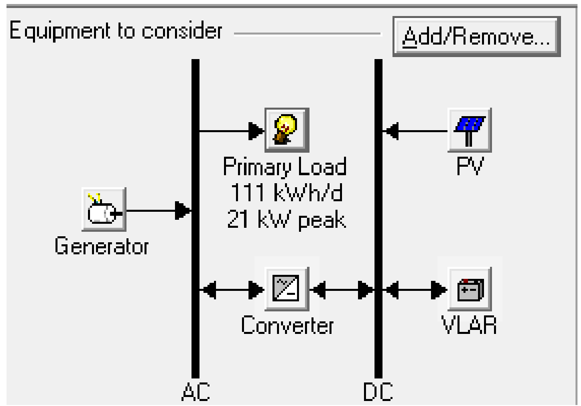

Figure 4.13 The hybrid system Homer Configuration model

Figure 4.14 below shows solar energy status of Konso town using Homer software with latitude of 5^0 North and longitude of 37^0 East. The scaled annual average solar radiation was found to be 5.899 kWh/m^2/day and scaled annual average clearness index was found to be 0.592.

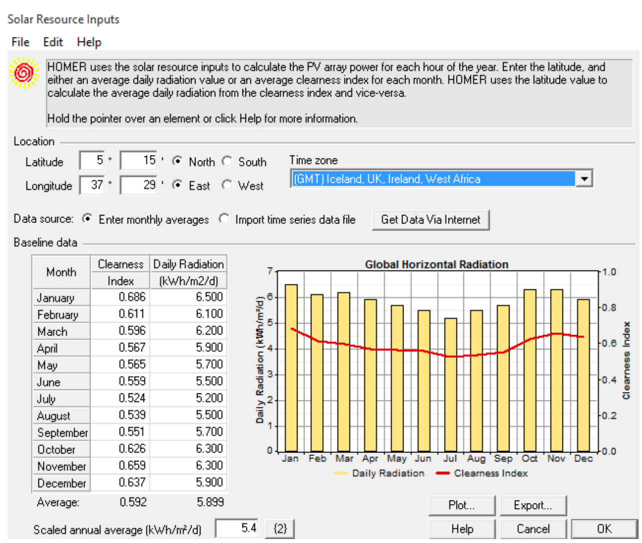

Figure 4.14 Solar energy profile input in to Homer software

4.2.1 The Optimization Method

When different sizes or quantities of parts chosen, there will be different schemes of the system. The following two steps have been used to select the best scheme.

Step 1: filter the qualified schemes that meet the electric requirements. The constraint conditions of the hybrid power system are as follows.

I. Power balance constraints

$$P_{pv} + P_{DG} + P_{bat} = P_{load} + P_{um} + p_{loss} + P_{exc} \quad (4.6)$$

The output power of the battery, P_{load} is the power of load consumption, P_{um} is the unmated a power, P_{loss} is power loss, and finally, P_{exc} is the excess power. Where P_{pv} is the output power of PV array, P_{DG} is the power of diesel generator, P_{bat} is the

II. Power reliability constraints

$$\frac{W_{um}}{W_{cons}} \leq 0.1\% \quad (4.7)$$

Where W_{nm} is the unmet work per year and W_{cons} is load consumption work per year.

Step 2: Rank of the qualified configuration with NPC (net present cost)

The economic consideration under homer simulations

NPC is the present value of all the costs of installing and operating that component over the project lifetime, minus the present value of all the revenues that it earns over the project lifetime. In this thesis, the NPC been calculated by the following equation.

$$NPC = C_i + f_d \times C_r + f_d \times C_{o\&m} + f_d \times C_f - f_d \times S \quad (4.8)$$

Where, C_i is the initial capital costs, C_r is the replacement cost, $C_{o\&m}$ is the operation and maintenance cost, C_f is the fuel cost, S is the salvage value and f_d is the discount factor.

The discount factor is a ratio used to calculate the present value of a cash flow that occurs in any year of the project lifetime. In this thesis, the f_d is calculated by the following equation:

$$f_d = \frac{1}{(1+n)^i} \quad (4.9)$$

Where: n = real interest rate, for this thesis is 6%, i = number of years.

Salvage (S) value is the value remaining in a component of the power system at the end of the project lifetime. This thesis assumes linear depreciation of components, meaning that the salvage value of a component is directly proportional to its remaining life. This thesis calculates salvage value using the following equation:

$$S = C_{rep} \times \frac{R_{rem}}{R_{comp}} \tag{4.10}$$

Where, $R_{rem} = R_{comp} - (R_{project} - R_{rep})$

Where, C_{rep} is the replacement cost, R_{rem} is the remaining life of the component at the end of the time (year), R_{comp} is the component life time (year), R_{proj} is the project life time (year) and R_{rep} is the replacement duration time (year).

Another economic indicator used in this thesis is the Levelized cost of energy (COE). COE is the average cost per kWh of useful electrical energy produced by the system. To calculate the COE, this thesis divides the annualized cost of producing electricity by the total electric load served, using the following equation [84]:

$$COE = \frac{C_{ann\_total}}{W_{consumption}} \tag{4.11}$$

Where$C_{ann_total} = NPC \times CRF, W_{consumption} = E_{pirm} + E_{defer}$

$$CRF\ (I, N) = \frac{i(1+i)^N}{i(1+i)^N - 1} \tag{4.12}$$

Where C_{ann_total} is the total annualized cost of the system ($/year), E_{pirm} is primary load served (kWh/year), E_{defer} is deferrable load served (kWh/year), i is the real interest rate, N is the number of years for this thesis the project lifetime is 25 year.

4.2.2 Cost analysis of hybrid system

The inputted data treated by the software describe renewable energy availability, load demand, hybrid system component costs (PV array, diesel generator, battery, and converter) and sizes as mentioned in table 4.5 below.

Table 4.5 Hybrid system for electrification cost, size and technical parameter summary

System Parameters	**PV-panel**	**Diesel Generator**	**Battery**	**Converter**
Size (kW)	1	25	14299.33Ah	1
Capital cost($)	1520	8599	18000	833
Replacement cost ($)	0	0	0	333
O&M ($/yr)	10	10	10	208
Size (kW) considered	0, 5, 10, 15, 20, 24, 30, 32, 36, 40, 50, 60,	0, 6, 8, 12, 18, 24, 26	---	0, 5, 10, 15, 20, 25, 30
Quantities considered	-------	---------	0, 64, 72, 88, 96	------
Life time	25 yrs.	20000 hrs.	10 yrs.	15 yrs.

CHAPTER 5

SIMULATION RESULTS AND DISCUSSION

5.1 MATLAB simulation result

The PV model simulator implemented in MATLAB/SIMULINK as shown in appendix (A). The PV array used in the simulation is a 32kW power that eleven strings with twelve modules of 240W power. Or 12*11 elements are combined to generate the desired power at standard conditions specified at irradiation of (G = 1000kW/m^2) and temperature of (T =25^{0}C).

As seen in section 3.5.2 the design PV array, the PV model simulator implemented in MATLAB/SIMULINK as shown in parameters required for simulation is initialized by the following script as shown in Appendix (A). The PV array used in the simulation, which required for daily energy, is 85.5kWh/day energy that 12 string with 11 modules of 240W power. On the other hand, 11x12 elements are combined to generate the desired power at standard conditions specified at irradiation of (G = 1000kW/m^2) and temperature of (T =25^{0}C). For the solar PV of 32Kw is the combination of the Poly 240W with 11 modules in series and 12 modules in parallels.

Figure 5.1 shows the output curve of current versus voltage and power versus voltage of the single module of SCHOTT PERFORM 240W respectively.

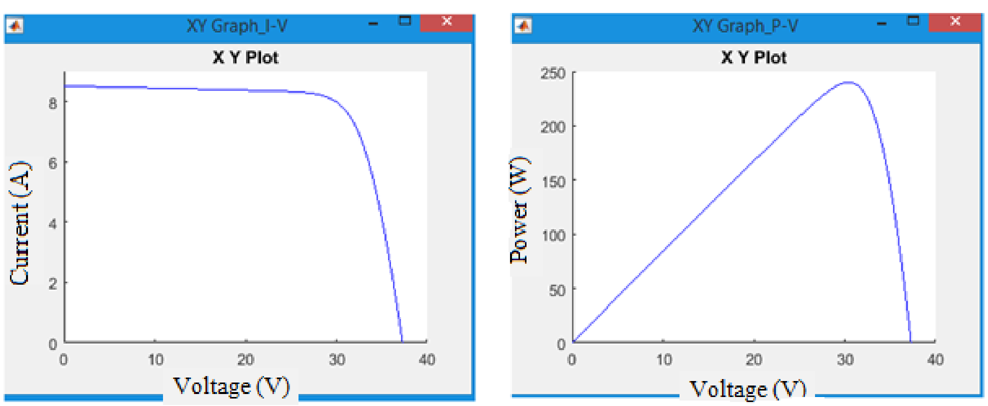

a b

Figure 5.1 a) I – V and b) P – V characteristics curve of the PV module at T = 25^{0}C and G = 1000w/m^2

The value of the shunt resistance connected in parallel to the cells selected as 1,000 Ω and the value of series resistance connected in series with the solar cell as 0.001 Ω. The constant 1,000 given as input to the sun is the irradiation considered in W/m^2. The system is simulated with various range of resistors connected to it, in this condition. A single solar PV module parameters values written in MATLAB M-File coding shown in appendix (A) and get the following output characteristics. I–V characteristic of the photovoltaic device depends on the internal characteristics of the device (*Rs*, *Rp*) and an external influence such as irradiation level and temperature.

I-V and P-V characteristics of the solar panel for irradiance values of 200, 400, 600, 800 and 1000 W/ m^2 shown in Fig 5.2.

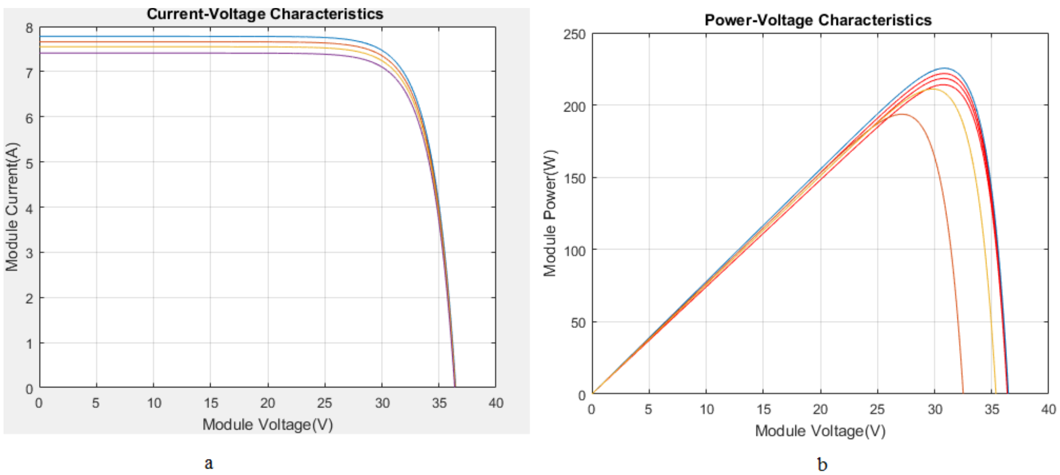

Figure 5.2 Characteristic of solar panel with varying irradiance (a) I – V (b) P – V

Operating temperature affects the electrical output of the solar module. Then, I-V and P-V characteristics with varying operating temperatures are shown in Fig 5.3 based on appendix (A). The module is set to operate with an irradiance value of 1000 W/ m^2. The operating temperatures are set at 25^{0}C, 40^{0}C, 50^{0}C and 60^{0}C. The x-axis is the module's voltage while the y-axis is the module's current.

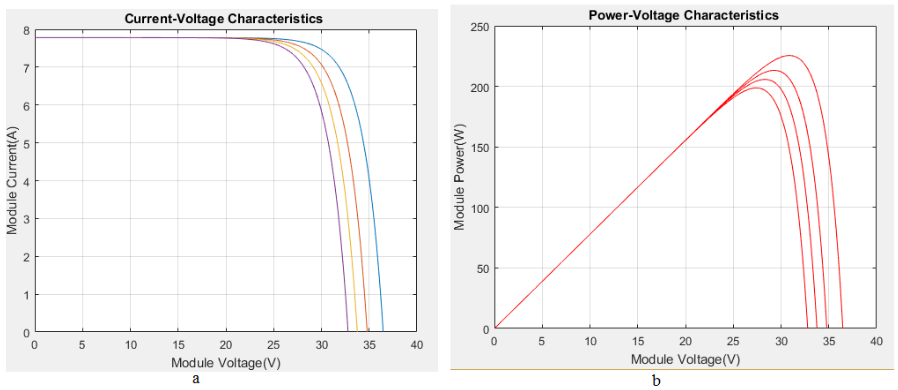

Figure 5.3 Characteristic of solar panel with varying temperature (a)I – V (b)P – V

Figure 5.4 shows the characteristics of the PV array of 32kW. The values of the current and voltage are 102.3A and 410.3V at maximum power respectively with the array PV array 32kW in 12 times to 11 the PV modules of 240W.

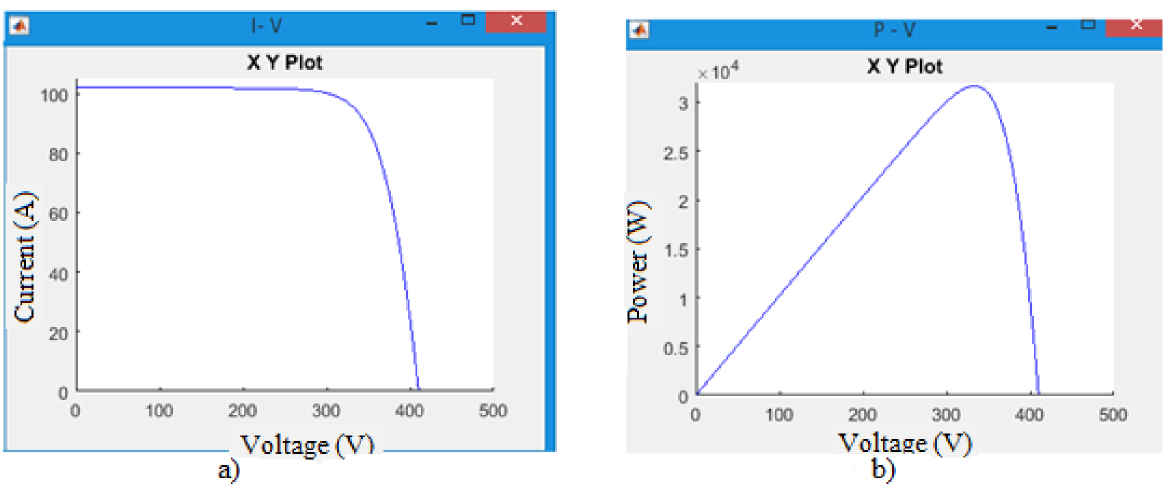

Figure 5.4 a) I – V and b) P – V characteristics curve of the PV array at T = 25^{0}C and G = 1000w/m^2

The output current and output voltage of the solar PV array are 102.3A and 410.3V as shown in figure 5.5 at T = 25^{0}C and G = 1000 w/m^2

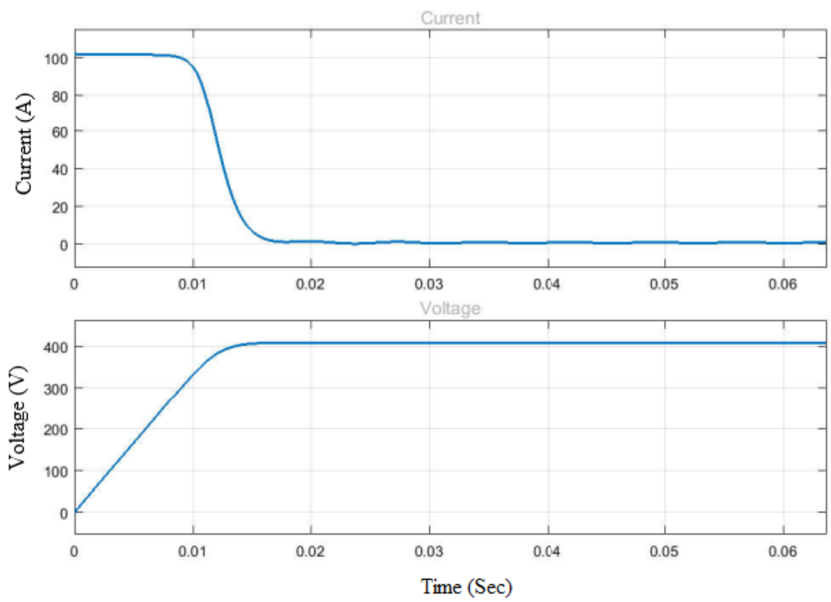

Figure 5.5 output current and output voltage of the PV array at T = 25^0C and

G = 1000w/m^2

Figure5.6 shows output voltage of PV array and output voltage of direct boost converter under normal condition (1KW/m^2 and 25^0C).

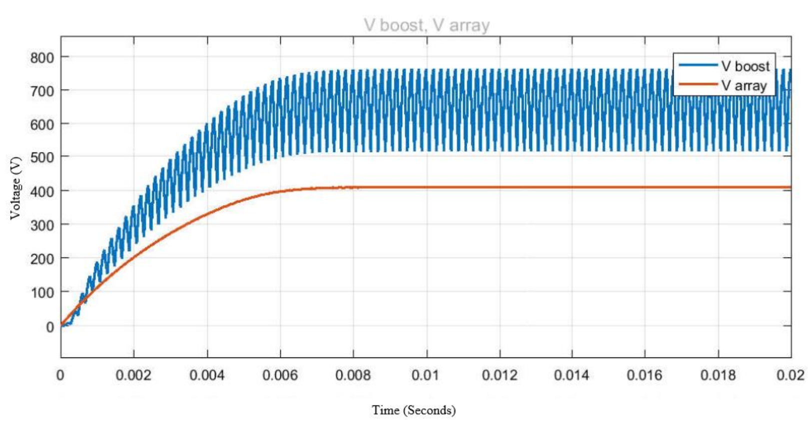

Figure 5.6 Output voltage of direct PV array and output voltage of direct boost converter at normal condition.

The value of the battery's SOC varies as the value of the DC voltage changes, so that if the DC voltage is more than the nominal voltage of the battery, then the SOC will remain the same. However, if the DC voltage is less than the nominal voltage of the battery then the SOC will decrease. Figure 5.7 shows the output of the state of charge (SOC), output current, and output voltage of the battery.

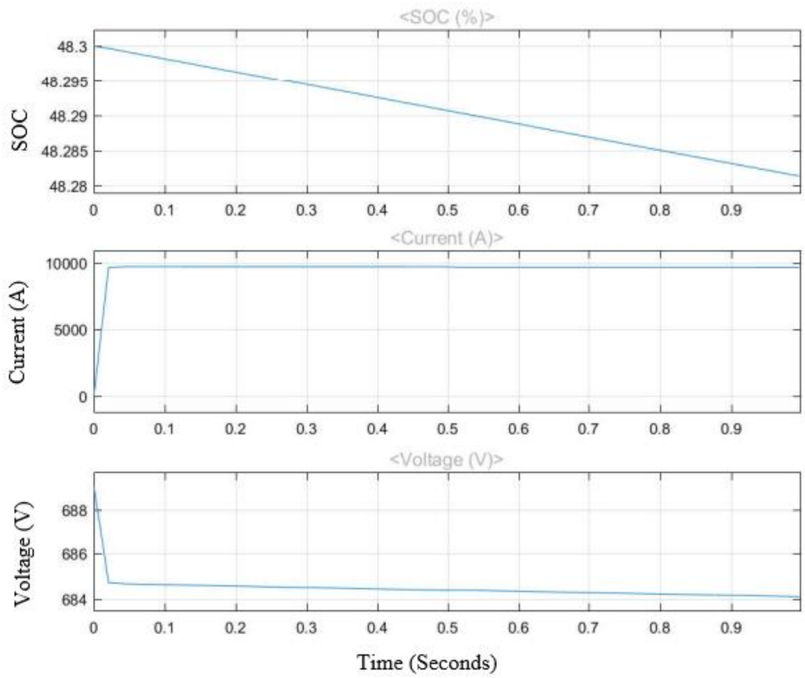

Figure 5.7 The results of the output of SOC, output current and output voltage of battery at standard condition.

From the above figure 5.7, when the output current of the battery increases then, the output of the voltage of the battery is decreased and the state of charge become discharging of the battery.

The figures 5.8 and figure 5.9 showed below that the outputs result of the inverter line to line voltage and phase to phase voltage.

Figure 5.8 Line to line voltages of output three phase inverter

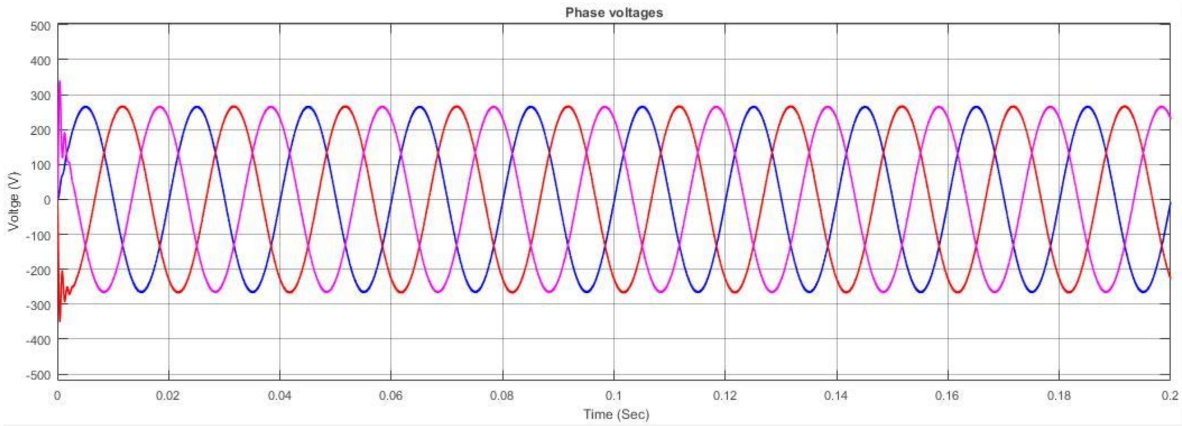

Figure 5.9 Phase to phase voltages of output three phase inverter

The simulation results of the AC output of voltage before low pass filter and after the filter circuit at standard irradiation of G = 1000W/m^2 and temperature of T = 25^0c of the hybrid system as shown in figure 5.10.

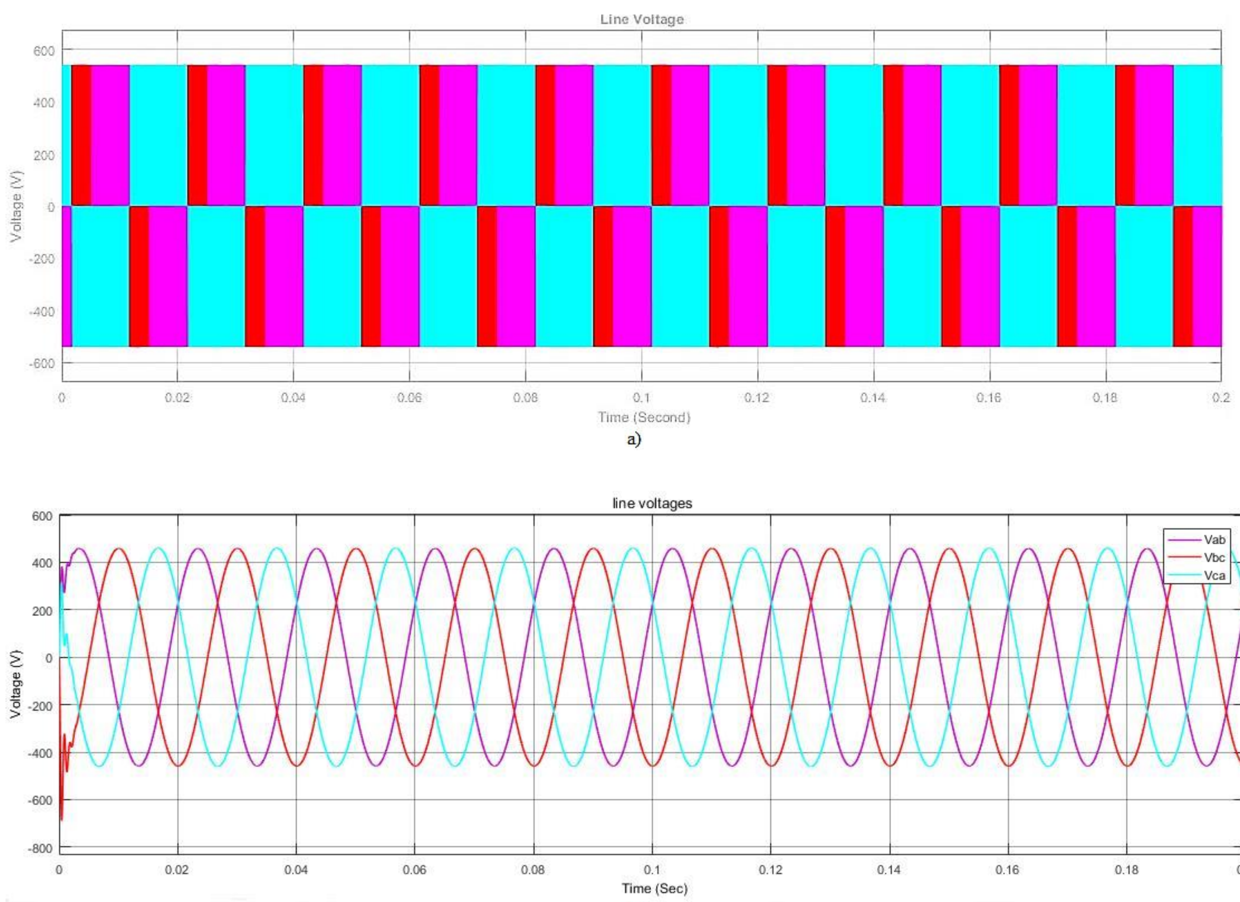

Figure 5.10 Line to line voltage a) before and b) after the LCL low pass filter

The harmonic results have been simulated using Matlab/Simulink software. From the results of harmonic orders filters, the 3rd, 5th, and 7th, harmonics filters are simulated to analysis if they are effectively reduced the distortion level to acceptable values as per IEEE standard. The output phases current waveform of before and after filters are presented for comparing results.

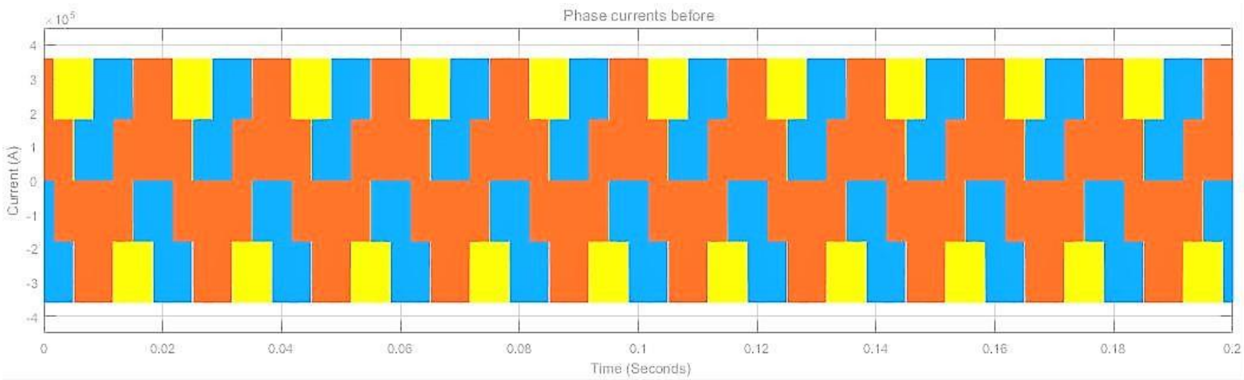

Figure 5.11 Phase current waveform without filter

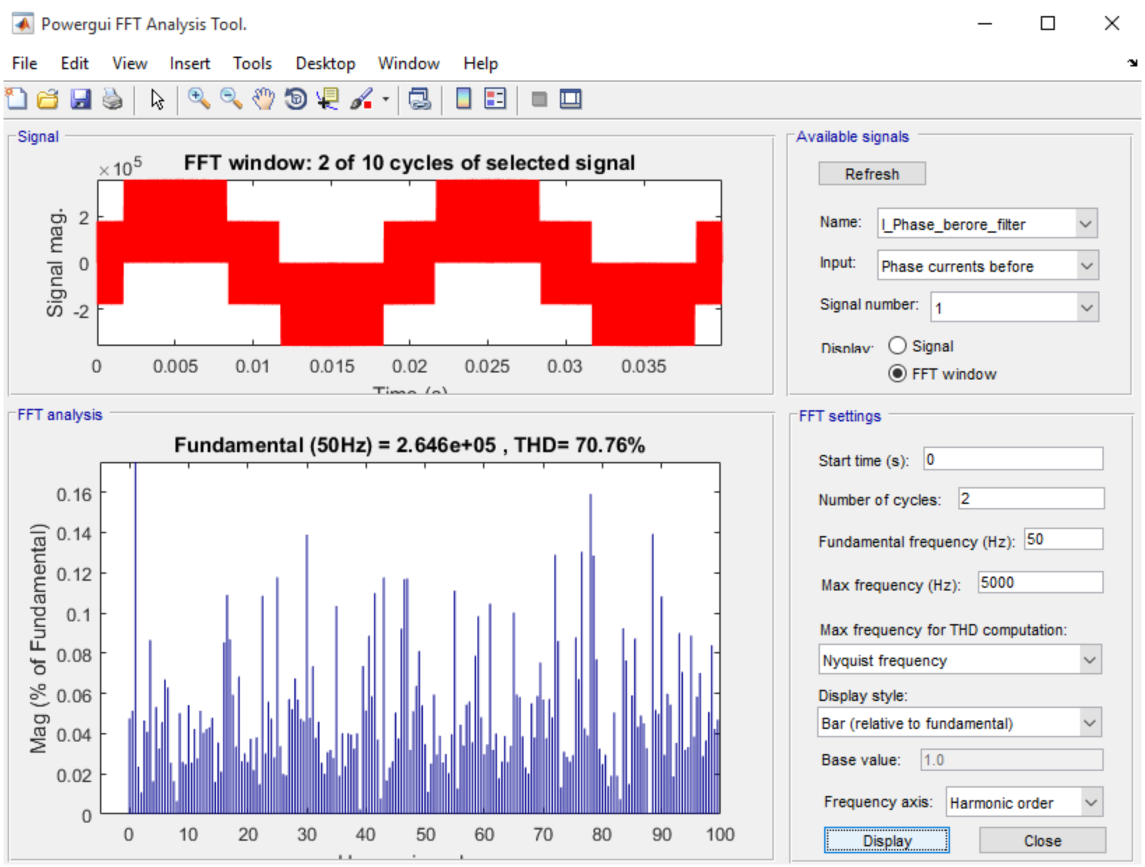

Figure 5.12 FFT Analysis phase current before filter

Figure 5.11 result shows the produced output waveform phase current is distorted due to harmonics and in figure 5.12 form the Fast Fourier Transform (FFT) analysis the values of the Total Harmonics Distortion (THD) are 70.98% for 1st, 5% for 3rd, 25% for 5th, and 35% for 11th harmonic order which is not acceptable as IEEE standard of 5%. Therefore, in order to solve the problem of harmonics, low pass filter LCL are used, and consequently, the resulting output waveform to become pure sinusoidal.

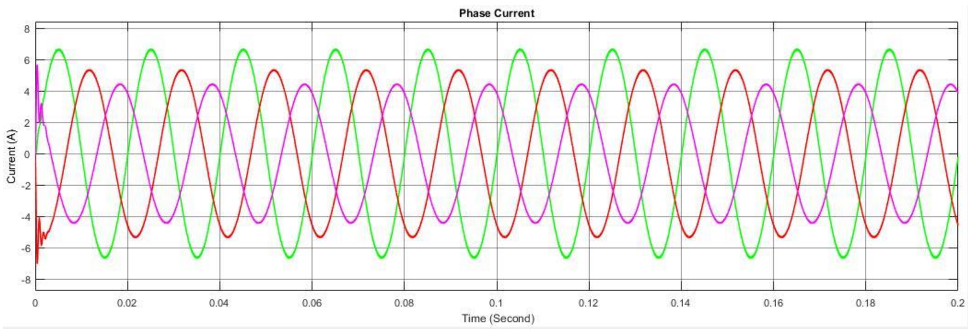

Figure 5.13 Output phase current waveform with filter

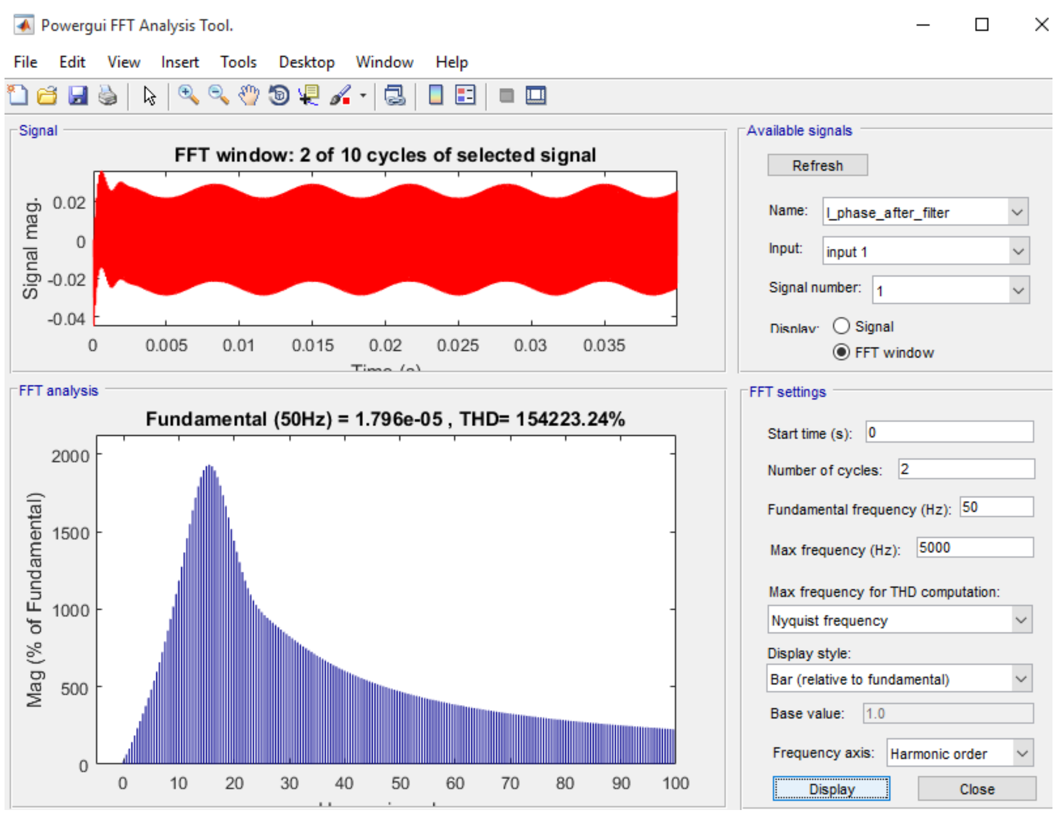

Figure 5.14 FFT Analysis phase current after filter

The obtained result in figure 5.13 is pure sinusoidal and in figure 5.14 shows the FFT analysis the value of THD is reduced from 70.97 % to 15%, which is more acceptable.

Comparing the analysis PV system model simulation results without and with MPPT controller tested at normal operating temperature and irradiance condition (25^0C and 1000W/m^2) and variable or at nonlinear conditions. Figure 5.15 shows output voltage, figure 5.16 output current, and figure 5.17 output powers with and without a controller at the normal operating condition. The output power of PV model system simulation were performance under varying irradiance and temperature with and without MPPT as shown below from figure 5.18 to figure 5.20.

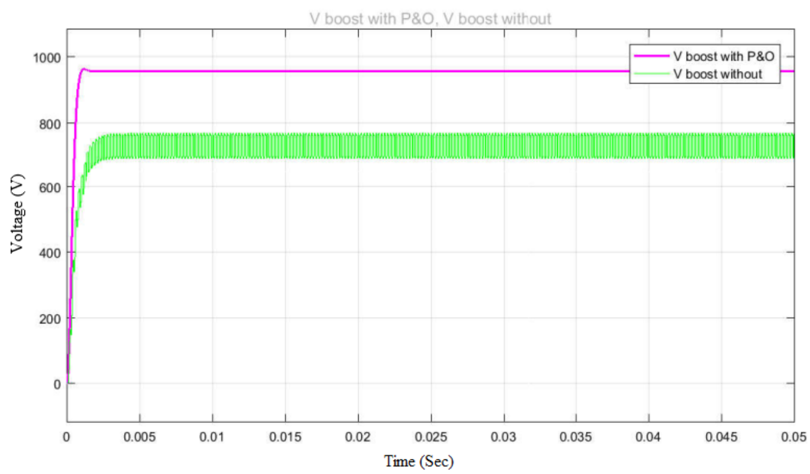

Figure 5.15 Output voltage with and without controller at normal condition

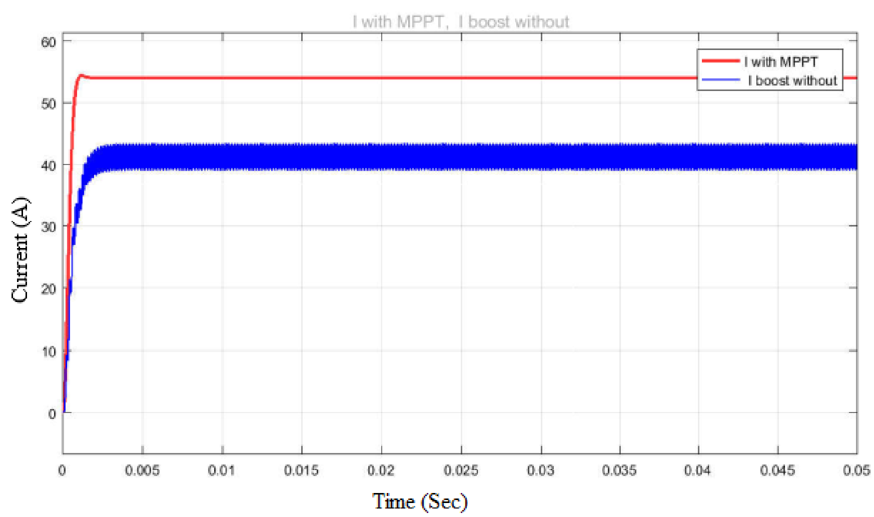

Figure 5.16 Output current with and without controller at normal condition

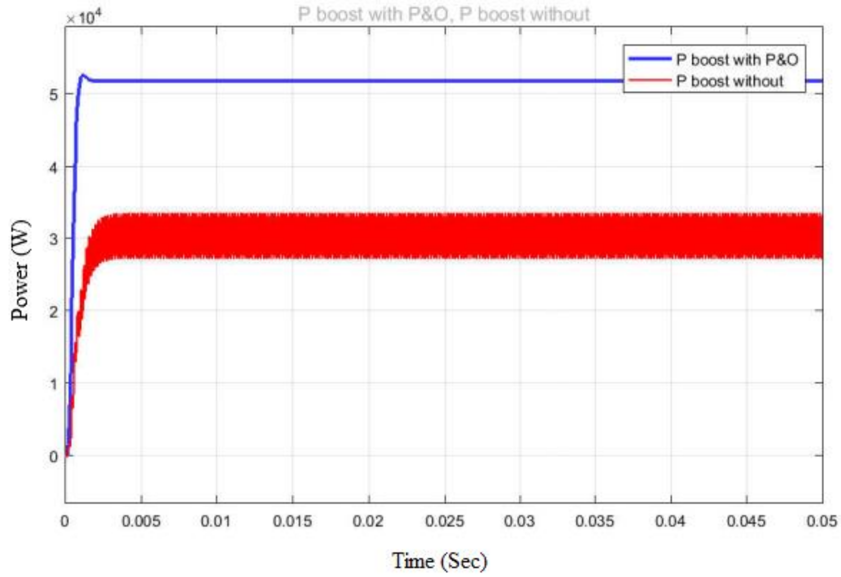

Figure 5.17 Output power with and without controller at normal operating condition.

Figure 5.18 shows Output power for variable irradiation 200 W/m^2, 400W/m^2, 600W/m^2, 800W/m^2, 1 000W/m^2, and constant temperature 25˚C.

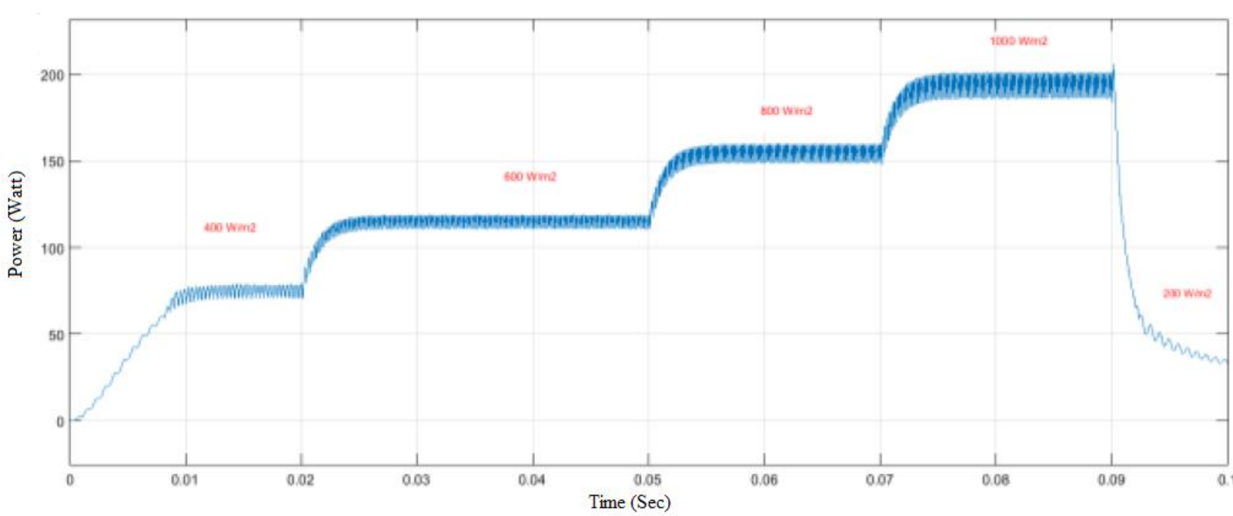

Figure 5.18 Output Power for MPPT system with P&O with variable irradiation and constant temperature (25^0C).

Figure 5.19 is shown Output power for constant irradiation (1000 W/m^2) and different temperatures 25^0, 50^0, 75^0 and 100^0 C.

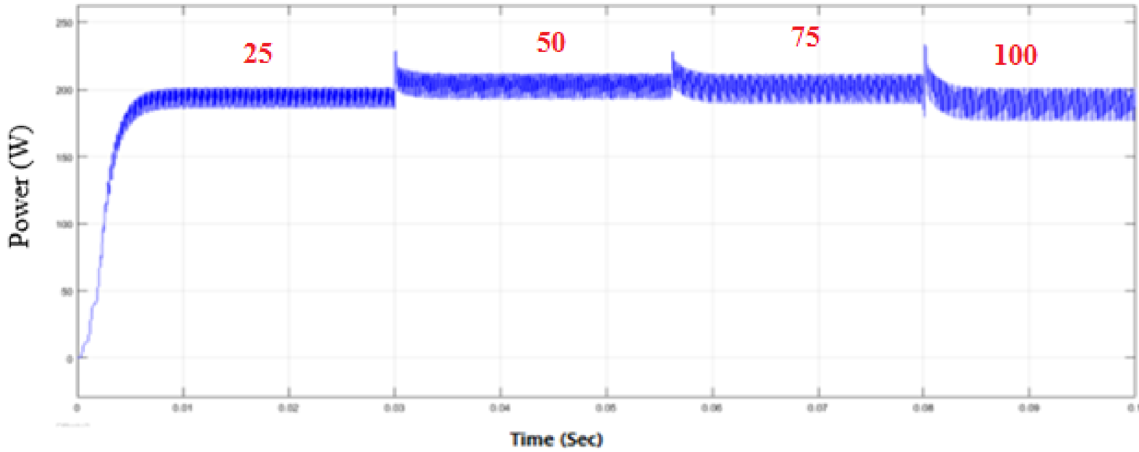

Figure 5.19 Output Power for MPPT system with P&O with variable temperature and constant irradiation 1000 W/m^2.

Figure 5.20 is shown Output power for variable irradiation and variable temperature.

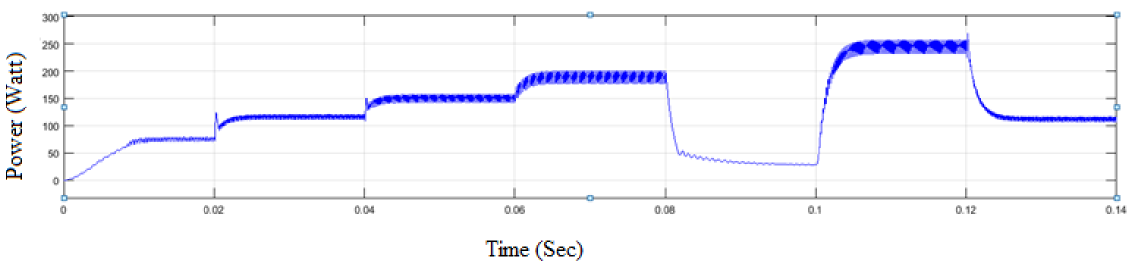

Figure 5.20 Output Power for MPPT system with P&O with variable temperature and variable irradiation.

Figure 5.21 simulation results show diesel generator output values of voltage (pu), rotor speed (pu), mechanical power (per unit) and output of line voltage. The mechanical power is initially drawn is very small because synchronous generator coupled with the engine running with no load, but after suddenly connecting to RL load, the mechanical power draws by an engine which increases immediately from 0.05 up to 0.08 seconds. Then, starts to decrease to reach the stability regime. The voltage (per unit) at the generator terminals also demonstrates a significant decrease for a short time, after which it stabilizes in less than 0.05 sec. These are because of the action voltage regulation system.

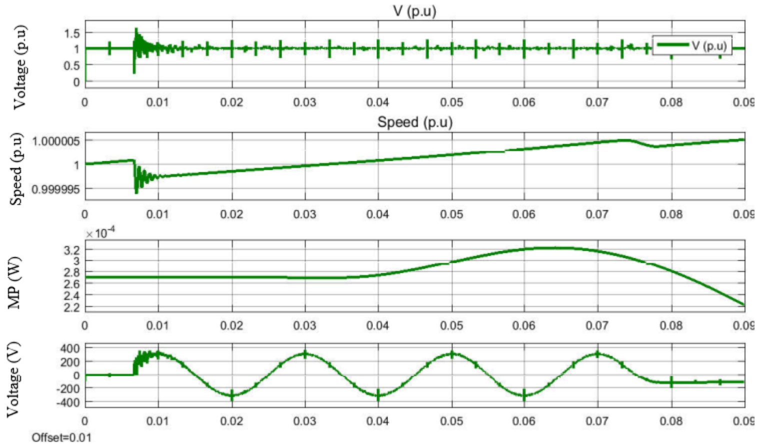

Figure 5.21 Show the output value of time variation of generator set parameters, output voltage (pu), rotor speed (pu), mechanical power (pu), and terminal output voltage.

An analysis of the solar PV cell is followed by the development of the simulation model using Matlab/Simulink software. The model developed has been depending on the effect of irradiation and ambient temperature on the system performance studied. From the simulation results studied solar PV generation are mainly varied due to the changing of irradiation and ambient temperature effects. Thus, the output voltage of the PV module is inversely proportional to the ambient temperature, the output current of the module is directly proportional to the solar intensity available, and the output power of module is a direct positive relationship with irradiation and an inverse relationship with ambient temperature on the system performance. An improved MPPT method based on the P&O technique has been proposed for studied. The result shows that the system with the tracking system is more effective and more accurate as compared with direct solar PV model under different solar irradiation changes and ambient temperature changes.

5.2 Simulation result of Homer software

5.2.1 Optimization Result

Different combinations of hybrid systems with solar PV, diesel generator, batteries, and converters acquired from the HOMER Optimization simulation for off-grid electrification of the study region.

After the simulation, HOMER provides several combinations of available power sources with their total net present worth, initial capital cost, energy per kWh cost, the total system configuration and component sizes that meet the load requirement. The simulation results, which include each component size, each system configuration's costs and total net present worth, as shown below.

And by comparing soar tracking system with no tracking system simulation results, of categorized simulation results of table 5.1 with tacking and table 5.2 is the overall simulation results with tracking, and similarly, table 5.3 shows categorized simulation results without solar tracking and table 5.4 shows overall simulation results without solar tracking simulations as shown below.

The categorized table displays only the most cost-effective configuration from each system type. From the categorized result of the simulation as shown in Table 5.1 and 5.3 the first optimal result is the combination of PV, diesel generator, battery and converter, the second system configuration is the combination of battery, converter and diesel generator. The diesel generator in this combination can be utilized only during peak time, and the third system configuration is the combination of diesel generator, battery, and convertor. The third system configuration is a combination of PV, diesel generator and converter. Finally, the fourth system configuration only contains diesel generator.

Table 5.1 Categorized optimizations results with tracking

PV	Gen	Batte	Conv	Disp.	Initial capital cost		Operating cost		Total NPC		COE		Ren.	Diesel
KW	KW	KW	KW	Strat	$/yr.	ETB/yr.	$/yr.	ETB/yr.	$	ETB	$/KWh	ETB/kWh	Fra	L/yr.
32	12	72	20	CC	99,315	2,864,245	4,285	123,579	154,090	4,443,956	0.298	8.594	0.98	314
0	16	72	10	CC	42,884	1,236,775	44,512	1,283,726	611,893	17,646,994	1.181	34.06	0	16,987
32	20	0	10	CC	59,662	1,720,652	75,585	2,179,871	1,025,894	29,586,783	1.981	57.13	0.58	18,441
0	20	0	0	CC	2,692	77,637	121,459	3,502,878	1,555,349	44,856,265	3.003	86.61	0	29,134

Table 5.2 Top ranked overall optimizations results using with tracking

PV	Gen	Battery	Conv.	Dispatch	Initial capital cost		Operating cost		Total NPC		COE		Ren.	Diesel
KW	KW	KW	KW	Strategy	$/yr.	ETB/yr	$/yr.	ETB/yr	$	ETB	$/KWh	ETB/KWh	Fra	L/yr.
32	12	72	20	CC	99,315	2,864,245	4,285	123,579	154,090	4443955.6	0.298	8.594	0.98	314
32	16	72	20	CC	99,854	2,879,789	4,329	124,848	155,190	4475679.6	0.3	8.652	0.98	320
32	12	72	20	LF	99,315	2,864,245	4,448	128,280	156,175	4504087	0.302	8.71	0.99	270
32	20	72	20	CC	100,392	2,895,305	4,380	126,319	156,378	4509941.5	0.302	8.71	0.98	330
32	8	80	20	CC	102,377	2,952,553	4,299	123,983	157,334	4537512.6	0.304	8.767	0.99	256
32	24	72	20	CC	100,931	2,910,850	4,437	127,963	157,650	4546626	0.304	8.767	0.98	343
32	8	72	25	CC	102,942	2,968,847	4,318	124,531	158,137	4560671.1	0.305	8.796	0.99	277
32	26	72	20	CC	101,200	2,918,608	4,478	129,146	158,450	4569698	0.306	8.825	0.98	353
32	12	80	20	CC	102,915	2,968,069	4,401	126,925	159,180	4590751.2	0.307	8.854	0.99	283

Table 5.3 Categorized optimizations results without tracking

PV	Gen	Batte	Conv	Disp.	Initial capital cost		Operating cost		Total NPC		COE		Ren.	Diesel
KW	KW	KW	KW	Strat	$/yr.	ETB/yr.	$/yr.	ETB/yr.	$	ETB	$/KWh	ETB/kWh	Fra	L/yr.
32	12	72	20	CC	98,777	2,848,729	5,160	148,814	164,745	4,751,246	0.318	9.17112	0.96	671
0	16	72	10	CC	42,884	1,236,775	44,512	1,283,726	611,893	17,646,994	1.181	34.06004	0	16,987
32	20	0	10	CC	59,662	1,720,652	77,230	2,227,313	1,046,924	30,193,288	2.022	58.31448	0.56	18,813
0	20	0	0	CC	2,692	77,637	121,459	3,502,878	1,555,349	44,856,265	3.003	86.60652	0	29,134

Table 5.4 Top ranked overall optimizations results without tracking

PV	Gen	Battery	Conv.	Dispatch	Initial capital cost		Operating cost		Total NPC		COE		Ren.	Diesel
KW	KW	KW	KW	Strategy	$/yr.	ETB/yr	$/yr.	ETB/yr	$	ETB	$/KWh	ETB/KWh	Fra	L/yr.
32	8	72	20	CC	98,777	2,848,729	5,160	148,814	164,745	4751245.8	0.318	9.17112	0.96	671
32	12	72	20	CC	99,315	2,864,245	5,269	151,958	166,674	4806878.16	0.322	9.28648	0.96	711
32	16	72	20	CC	99,854	2,879,789	5,339	153,977	168,103	4848090.52	0.325	9.373	0.96	735
32	20	72	20	CC	100,392	2,895,305	5,385	155,303	169,230	4880593.2	0.327	9.43068	0.96	744
32	24	72	20	CC	100,931	2,910,850	5,427	156,515	170,301	4911480.84	0.329	9.48836	0.96	748
32	8	72	25	CC	102,942	2,968,847	5,291	152,592	170,575	4919383	0.33	9.5172	0.96	664
32	26	72	20	CC	101,200	2,918,608	5,468	157,697	171,097	4934437.48	0.33	9.5172	0.96	759
32	12	80	20	CC	102,915	2,968,069	5,403	155,823	171,979	4959874.36	0.332	9.57488	0.96	685
32	12	72	25	CC	98,777	2,848,729	5,363	154,669	172,039	4961604.76	0.332	9.57488	0.96	708

Exchange rate to convert USD to Eth Birr is (1USD=28.84Birr), Source: commercial Bank of Ethiopia, June 28, 2019.

Based on the above Tables 5.1 up to 5.4 the first optimization result the most feasible hybrid configuration is 32kW PV, 72 VRLA batteries, 12kW of diesel generator for table 5.1 to 5.3 and 8kW, for table 5.4, and 20kW of the converter. Table 5.2 shows the overall optimization result of using horizontal axis, continuous adjustment solar tracking system, the initial capital cost was observed to in the range of 2,864,245 Birr/yr. to 2,968,069 ETB, the operating cost is in the range of 123,579 ETB/year to 126,925 ETB/year, the total net percent cost (NPC) is in the range of 4,443,956 ETB to 4,590,751 ETB, and the Levelized cost of energy (COE) is in the range of 8.59432 ETB/kWh to 8.85388 ETB/kWh. Both LF and CC dispatch strategy is feasible. While table 5.5 shows the overall optimization result without using tracking, the initial capital cost obtained more compare with tracking in the range of 2,848,729 Birr/yr. to 2,848,729 Birr/yr., the operating cost is in the range of 148,814 ETB to 154,669 ETB, the total NPC is in the rage of 4,751,245.8 to 4,961,604.76 ETB, and the Levelized cost of energy (COE) is in the range of 9.17112 ETB/kWh to 9.57488 ETB/kWh, which is more cost. And only cycling charge (CC) dispatch strategy is feasible.

Table 5.5 Comparison of overall optimizations results with and without tracking

Parameters	**Overall optimization with solar tacking**	**Overall optimization without solar tacking**
Initial capital cost	2,864,245 Birr/yr. to 2,968,069 ETB.	2,848,729 Birr/yr. to 2,848,729 Birr/yr.
Operating cost	123,579 ETB/year to 126,925 ETB/year	148,814 ETB to 154,669 ETB
Total NPC	4,443,956 ETB to 4,590,751 ETB	4,751,245.8 to 4,961,604.76 ETB
COE	8.59432 ETB/kWh to 8.85388 ETB/kWh.	9.17112 ETB/kWh to 9.57488 ETB/kWh
dispatch strategy	Both LF and CC are feasible	Only CC is feasible

In categorized simulation result Table 5.1, the fourth rank is containing only diesel generator system which only the initial cost is lower but both the NPC and COE cost is very high as compared to the remain options. Generally, the only diesel generator supply system is not cost-effective as compared to the other rank. The electrical production as shown in figure 5.22 below

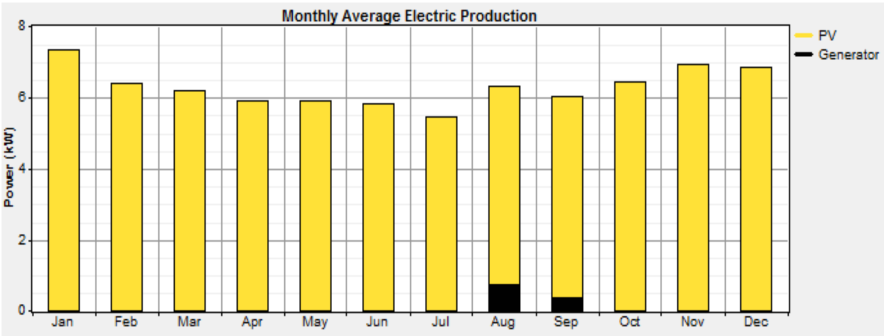

Figure 5.22 Monthly average electric productions

As seen the electrical output there are three things are commonly to considered as follows:

I. Energy production
II. Energy consumption and
III. Excess electricity

For the first rank, the solar PV production covered by 98% and found of the generator covered 2%. For this case of electrification, there is no consideration of the deferrable load. Therefore, the AC primary load consumes all 100%. There is no unmated load is found in the result and there is found 5.12% of excess electricity, this result may arise from the unequal distribution of the resources throughout the month. The value of excess as shown in figure 5.23 below, the excess electricity is small from April to October and higher in January, December, and February as in accordance of the input solar radiation to the Homer software.

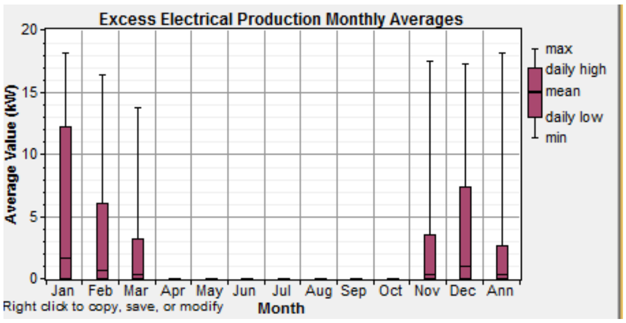

Figure 5.23 Monthly Excess Electrical production

The capacity shortage of the output system is zero because the input capacity shortage to the software considered zero. Therefore, the system conformation condition can support all the demand without the shortage at any time.

Table 5.6 System report for selected of most cost effective hybrid system

System architecture		**Annual electric energy production (KWh/year)**			**Annual electric energy consumption (KWh/year)**			**Emission (kg/year)**	
PV	32kW	PV	54,257	98%	Primary load	40,513	100%	Carbon dioxide (CO2)	826
DG	12kW	DG	897	2%	Total	40,513	100%	Carbon monoxide (CO)	2.04
Battery	72	Excess electricity	2,826	5.12%	**Cost summary**			Unburned hydrocarbons	0.226
Rectifier	20kW	Unmet load		0%	NPC	4,443,956 ETB		Particulate matter	0.154
Inverter	20kW	Capacity shortage	0	0%	COE	8.59432 ETB/kWh		Sulfur dioxide (SO2)	1.66
Dispatch strategy	CC				Operating cost	123,579 ETB/yr.		Nitrogen Oxide (NOx)	18.2

Figure 5.24 displays yearly cash flow throughout the system's lifetime. Replacements of the charging batteries and converters mostly take places in 12th, 15th, 20th, and 24th year of the system.

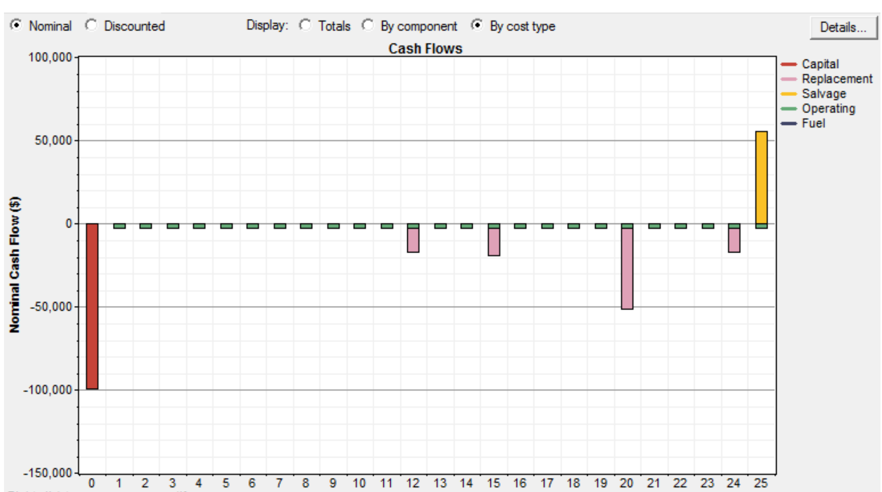

Figure 5.24 Nominal cash flows

The cash flow of the system is also included in $ 61,442 NPC for PV, $ 12,651 NPC for Gen, $53,843 net present cost for BESS, $26,153 net present cost for converter respectively. The total system cost about $ 154,090 for the hybrid system, as shown in Figure 5.25.

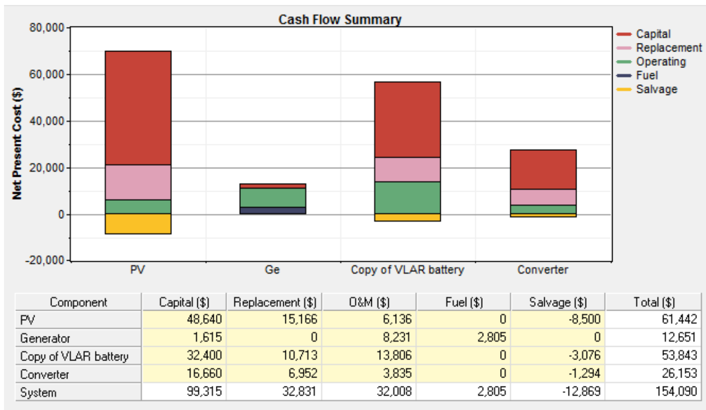

Component	Capital ($)	Replacement ($)	O&M ($)	Fuel ($)	Salvage ($)	Total ($)
PV	48,640	15,166	6,136	0	-8,500	61,442
Generator	1,615	0	8,231	2,805	0	12,651
Copy of VLAR battery	32,400	10,713	13,806	0	-3,076	53,843
Converter	16,660	6,952	3,835	0	-1,294	26,153
System	99,315	32,831	32,008	2,805	-12,869	154,090

Figure 5.25 Cost summary for the most cost effective system

5.2.2 Sensitivity Analysis

The optimization of the combination of the components parameters changes of the project lifelong of the system measured by the sensitivity. Sensitivity analysis was also carried out to analyze the dynamic behavior of exist on the input variable change due to various reasons. During the input parameter is changed, it is better to estimate how much the system optimum change with the variation of the variables. In this thesis, work the diesel price from a range of $0.6/L to $1.4/L and solar radiation range from 5.2 kWh/d/m^2 to 5.6 kWh/d/m^2 used for sensitivity analysis parameters. Based on the diesel consumption, level of cost of energy dependence on the total net present cost, the total net present cost and level cost of energy depended on the diesel consumption, and examine how Total Net Present Cost and Level Cost of Energy. Figure 5.26 Show sensitivity analysis carried out at fixed average solar radiation of 5.2 kWh/d/m^2 and average diesel price $0.7/L, PV/Gen/Battery system is the best cost-effective for total NPC, which as diesel price increases the total NPC are also increased.

Figure 5.26 Show the diesel price variation and global solar radiation variation draws along y-axis and x-axis respectively. The result, when the diesel is equal to $0.7/L the total NPC is equal to $154,090 and when the diesel price is equal to $1.2/L then total NPC is equal to $156,094 at fixed global solar radiation of 5.2 kWh/m^2/day. Similarly, the result, when the diesel is equal to $0.7/L the total NPC is equal to $146,237 and when the diesel price is equal to $1.2/L then total NPC is equal to $146,705 at fixed global solar radiation of 5.4 kWh/m^2/day.

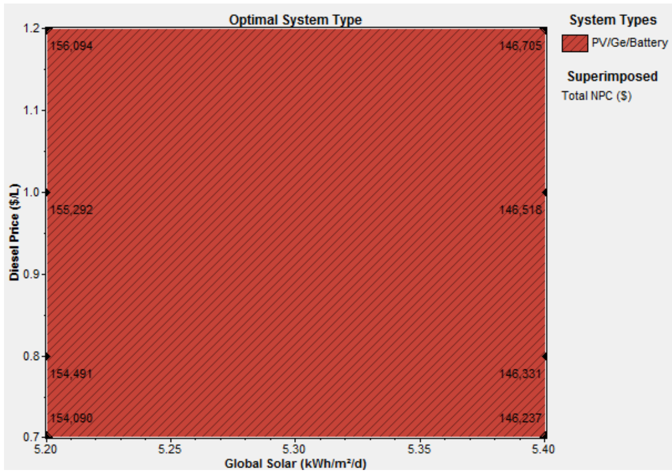

Figure 5.26 Sensitivity of total diesel to solar radiation with some important NPCs labeled

In figure 5.27 a) shows the variation of diesel consumption and fraction relative to diesel prices by fixing the global solar radiation 5.4 kWh/m^2/day. The diesel consumption is varying from $0.7/L to $1.2/L and the renewable fraction constant at 100%, the NPC varies from $146,250 to $146,700.

Finally, in figure 5.27 b) is show the Total NPC and Levelized cost of energy concerning the variation of the diesel prices in $/L. As diesel price varies from $0.7/L to $1.2/L both the value of the total NPC and levelized COE varied, which of total NPC varies from $146,200 to $146,700 and levelized COE varies from $0.2824 to $0.2834/kWh.

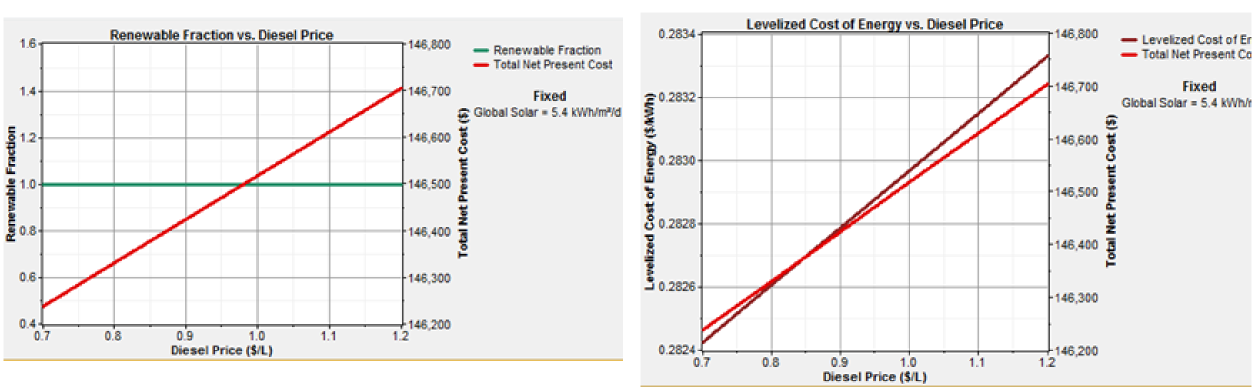

a)

b)

Figure 5.27 a) Renewable Fractions and Diesel Consumption with Respect to Total NPC b) COE and Total NPC with respect to Diesel price $/L

CHAPTER 6
CONCLUSION and RECOMMENDATIONS

6.1 Conclusions

Under this thesis works the solar radiation data was collected from Meteorological agency station and from NASA and based on the data load estimation of the community for electrification systems, the economic feasibility of the hybrid power system consisting of solar PV, diesel generator, battery storage, and converter by using Homer software simulation compotes studied. Secondly, the photovoltaic system maximum power tracking had developed based on the theory and mathematical model. The PV model with P&O controller were designed to supply the load. The output of the boost converter is supplied to the bidirectional DC–DC converter in order to storage energy to the battery when availability power is high and lower power is required to the load else directly supplied to inverter during low power. The battery is charged during the high potential of solar power and discharge during the lower value of solar PV generating. The output of voltages, currents and the state of charging of the battery has tested under MATLAB simulations. By using the three-phase breaker the solar PV with battery storage – diesel generator has connected to supply the three load. Lowe pass filter has also designed to reduce the line harmonics contents. The result before the filter and after the filter had analyzed through simulations.

Optimization and sensitivity of the Solar PV – Diesel generator of the hybrid system had analyzed by Homer software for economic estimation. Comparing the Homer simulation optimization results solar power tracking system more feasible compared to no tracking system. The best - optimized result was to be selected from the arrangement of the simulated. The feasibility study for the hybrid setup has based on the outcome of the potential of solar energy for the case study. In the results, different options of alternative feasibility hybrid schemes, with almost the same by the renewable resource and different total NPC cost obtained.

The range of the Levelized cost of energy (COE) of the overall simulation results is in between $0.298/KWh to $0.31/KWh or 8.594ETB/KWh to 8.854ETB/KWh. Therefore, this result is the less effective as compared to the $0.06/KWh current energy tariff of the country. But, by considering the current problem of the community, and taking this in consideration of the high potential of renewable demand to minimize the impact of the effect of the global warming of the environment, deforestation and changing the lives of the rural community.

6.2 Recommendations

The following recommendations have been considered based on this research work basic findings.

- The artificial intelligence control system such as fuzzy logic control (FLC), artificial neural network (ANN) and genetic algorithm (GA) can be used for improving the performance to generate power from the PV panel.
- Automation studio is the most effective for the energy management system to analyze the effect of the realization of the different sources.
- Better optimization of the economic analysis can be achieved by integrating Homer software with MATLAB/Simulink.
- Thus, the researcher of this thesis recommends that all the private sectors, government, and non-governmental organizations should cooperate to overcome these problems by utilizing more flexible approaches to improve the extremely poor status profile of rural electrification in Ethiopia.
- In this thesis only considered the specific village of SNNP, Konso, Jarso Kebele thus further study should make consideration for those who do not ever get electricity form diesel generator.
- Similarly solar and other renewable energy potentials can be studied for other sites in the rural community of the country.

References

[1] "Ethiopia trade and investment," www.ethioembassy.org.uk/trade and investment, January 2012.

[2] García-Valverde.et.al, "Life cycle assessment study of a stand-alone photovoltaic system," *Sol Energy,* vol. 83(9), p. 1434–45., 2009.

[3] e. Rehman S, "Cost of solar energy generated using PV panels," *Renew Sustain Energy* , vol. 11(8), p. 1843–57., 2007.

[4] D. D. Guta, "Assessment of Biomass Fuel Resource Potential And Utilization in Ethiopia: Sourcing Strategies for Renewable Energies," *INTERNATIONAL JOURNAL of RENEWABLE ENERGY RESEARCH,* vol. 2, 2014.

[5] "World Bank report of 2012. http://www.worldbank.org/".

[6] "The Ethiopian Power Sector: A Renewable Future," Berlin Energy Transition Dialogue, March 2017.

[7] Ethiopia enrgy sector program for sustainable development and security of supply to end poverty, "Ministry of Water, Irrigation and Energy/ www.moie.gov.et," March 2017.

[8] S. Tsegaye, "Highlights of The Ethiopian Energy Sector Solar Energy Foundation," June 27/29/2016.

[9] W. Byrd, Solar Electric System Basics, http://lacleantech.net/solar_electric_systems.pdf, 2007.

[10] *working principle of photovoltaic cell or solar cell,* https://www.electrical4u.com/working-principle-of-photovoltaic-cell-or-solar-cell, May 15, 2018.

[11] S. Pukhrem, *How Solar Cells Work Components and Operation of Solar Cells,* https://solarlove.org/how-solar-cells-work-components-operation-of-solar-cells/, May 13, 2013.

[12] e. a. Andrej Cotar, "photovoltaic systems, commissioning party: IRENA- Istrian regional energy," January 2012.

[13] A. Goetzberger, Photovoltaic Solar Energy Generation, Springer, 2005.

[14] H. a. D. Zhang, "The stand alone PV generation System with Parallel Battery Chareger," in *International conference on electrical and control enginerring,* pp 4450 – 4453, 2010.

[15] B. K. S. a. A. L. D'Agostino, "A comparative analysis of solar home system programmes in China, Laos, Mongolia and Papua New Guinea,," *Prog. Dev. Stud,* Vols. 12, no. 4, p. 315–335, Oct. 2012.

[16] S. R. a. Bhattacharya, "Off-grid electricity generation with renewable energy technologies in India: an application of HOMER," *Renewable Energy,* vol. vol. 62(0), pp. 388-398, Sep, 2014.

[17] "Solar Cell Characteristics," available:http://shodhganga.inflibnet.ac.in/bitstr.

[18] M. S. K. et.al, "Comparison of P&O and Improved IC MPPT Controller Boost Converter for Solar PV Standalone and grid Connected Mode Operation," *Pramana Research Journal,* vol. 9, no. 2, pp. 257-267, 2019.

[19] M. A., "Comparative study chain of energy conversion dedicated to a small wind turbine," PhD from the Institute National Polytechnique de Toulouse, France, 2005.

[20] V. A. Ani, "Design of a Reliable Hybrid (PV/Diesel) Power System with Energy Storage in Batteries for Remote Residential Home," *Journal of Energy,* 2016.

[21] M. e. al, "Coupling PV and CAES power plants to transform intermittent PV electricity into a dispatchable electricity source," *Progress in Photovoltaics: Research and Applications,* vol. 16, p. 649–668, 2008.

[22] e. Anca D. Hansen, Models for a Stand-Alone PV System, Risø National Laboratory, Roskilde, December 2000.

[23] M. Rivera, "Small Wind / Photovoltaic Hybrid Renewable Energy System Optimization, MSc Thesis," *University of Puerto Rico,* 2008.

[24] http://batteryuniversity.com/learn/article/whats_the_best_battery, Writer, *Battery University [BU].* [Performance]. Retrieved Nov 11, 2012, from.

[25] N. Albuquerque, Maintenance and Operation of Stand-Alone Photovoltaic Systems, Sandia National Laboratories: Photovoltaic Design Assistance Center, December 1991.

[26] C. S. Solanki, Solar Photovoltaic Technology and Systems: A Manual for Technicians, Trainers and Engineers, Delhi: PHI Learning Private Limited, 2013.

[27] R. A. M. .. J. Ventre, Photovoltaic Systems Engineering Third Edition, Taylor & Francis: CRC Press, 2010.

[28] Vince Lombardi, "practical guid to solar power system design for Homer owners," B.S./M.S. Engineering Mechanics, Virgnia Tech, 1988/1990.

[29] M. Hankins, stand-alone solar electric systems the earthscan expert handbook for planning, design and installation, London • Washington, DC: Earthscan, 2010.

[30] A. Oi, *Design and simulation of photovoltaic water pumping system,* California : Master Thesis, 2009.

[31] M. L. a. C. Greenwood, *"Green investing: Towards a clean energy infrastructure,* Polytechnic State University: World Economic Forum USA Inc, January 2009.

[32] A. Oi, "Design and Simulation of Photovoltic Water Pumping System," Thesis,California Polytechnic State University, San Luis Obispo, September 2005.

[33] M. K. et.al, "LCL filter design for photovoltaic grid connected systems," *Revue des Energies Renouvelables SIENR'14 Ghardaïa,* p. 227 – 232, 2014.

[34] P. S. B. M. Reddy, "Analysis of Isolated Bi-Directional dc-dc Converters for Performance Enhancement of PV System and Energy Storage System," Bikaner, India, 2016.

[35] H. Q. a. J. S. L. W. Yu, "Design of high-efficiency bidirectional DCDC converter and high-precision efficiency measurement," *IEEE Trans. Power Electron,* Vols. 25, no. 3, p. 650–658, 2010.

[36] C. K. Y. S. H. P. B. K. a. D. K. T. Kang, "A design and control of bi-directional non-isolated DC-DC converter for rapid electric vehicle charging system," in *IEEE Applied Power Electronics Conferenceand Exposition and APEC*, 2012.

[37] S. F. a. A. R. C. D. R. Northcott, "Design of a bidirectional buck-boost dc-dc converter for a series hybrid electric vehicle using PSCAD/EMTDC," in *in 5th IEEE Vehicle Power and Propulsion Conference, VPPC*, 2009.

[38] R. M. S. a. J. C. Balda, "Comparing DC-DC converters for power management in hybrid electric vehicles," in *IEEE Int. Electr.Mach. Drives Conf, IEMDC*, 2003.

[39] D. Ravi.et.al, "Bidirectional dc to dc Converters: An Overview of Various Topologies, Switching Schemes and Control Techniques," *International Journal of Engineering & Technology,* pp. 360-365, 2018.

[40] M. Hankins, Stand-Alone Solar Electric Systems The Earthscan Expert Handbook for Planning, Design and Installation, London • Washington, DC: Earthscan, 2010.

[41] M. A, "Technoeconomic Assessment of Wind Energy to Supply the Demand of Electricity for a Residential Community in Ethiopia," KTH School of Industrial Engineering and Management ,Master thesis for Energy Technology, August 2011.

[42] K. G. et.al., "Feasibility of Solar Wind Renewable Energy in India," *International Journal of Engineering and General Science,* vol. 5, no. ISSN:2091.730, 2017.

[43] K. R. K. Chaitanya Marisarla, ""A Hybrid Wind and Solar Energy System with Battery Energy Storage for an Isolated System",," *International Journal of Engineering and Innovative Technology (IJEIT),,* vol. 3, no. ISSN: 2277-3754, pp. 99 - 104, September 2013,.

[44] A. e. al, "Off-Grid Renewable Hybrid Power Generation System for a Public Health Centre in Rural Village," *International Journal of Renewable Energy Research,* vol. 6, pp. 282-288, No.1, 2016.

[45] A. A. e. al, "Simulation and design of wind-PV hybrid power generation systems," *International Journal of Enhanced Research in Science Technology & Engineering,,* vol. 3, no. 1, pp. (340-345),, January-2014,.

[46] M.-A. Yazdanpanah, "Modeling and sizing optimization of hybrid photovoltaic/wind power generation system," *Springer*, 5 March 2014.

[47] Z. Girma, "Hybrid renewable energy design for rural electrification in Ethiopia," *Journal of Energy Technologies and Policy*, vol. 3, pp. ISSN 2224-3232 (Paper) ISSN 2225-0573 (Online), No.13, 2013.

[48] B. Tudu, ""Stand-alone Hybrid Renewable Energy System-An Alternative to Increased Energy Demand",," in *International Conference on Control, Instrumentation, Energy & Communication*, Kolkata, 2014.

[49] Chowdhury.et.al, "Economic analysis of PV/diesel hybrid power systems in different climatic zones of South Africa," *Electrical Power and Energy Systems*, vol. 40, p. 104–112, March 2012.

[50] Md Saleh.et.al, "Design, Simulation and Stability Analaysis of Wind - PV - Diesel Hybrid Power System using EPAP," *American Jornal of Modern Energy*, vol. 3, no. doi:10.11648/J.ajme.20170306.12, pp. 121-130, 2017.

[51] R. Conno, "“The United Nation World Water Development Report,”," United Nationals Educational Scientific and Cultural Organization,, Paris,, 2014..

[52] R. Manavala, "Analaysis of Hybride Renewable Energy System Using NPC Inverter," *International Electrical Engineering Journal (IEEJ)*, vol. 4, no. ISSN:2078-2365, pp. PP.864-868, 2013.

[53] G. B. a. G. Bekele, "Design of a Photovoltaic-Wind Hybrid Power Generation System for Ethiopian Remote Area," no. doi:10.1016/j.egypro.2011.12.1164, p. 1760 – 1765, 2012.

[54] E. e. al, "Design and Implementation of a Renewable Energy Monitoring System," in *IEEE*, Istanbul, Turkey, May 2013.

[55] T. K. a. R. Segal, "Designing rural electrification solutions considering hybrid energy systems for Papua New Guinea," in *1st International Conference on Energy and Power*, RMIT University, Melbourne, Australia:Available online at www.sciencedirect.com, 2017.

[56] "Renewable Energy Potential in Ethiopia," Available From, http://www.afribiz.info/content/2013/.

[57] E. R. Group, "Diversity and Security for Ethiopian power system preliminary assessment of risk and opportunities for a power sector," Heinrich boll foundation, Addis Ababa, August 2009.

[58] M. Y. Drake F. and, "Assessment of solar and wind energy in Ethiopia I," *Solar Energy*, Vols. 57, No. 3, pp. 205-217, 1996.

[59] T. J. A. W. T, Renewable Energy Resources”, 2nd Edn, London: Taylor & Francis, 2006.

[60] J. a. B. W. Duffie, Solar Engineering of Thermal Processes. 3rd ed, New Jersey: John Wiley and Sons, Inc, 2006.

[61] A. V., Fundamentals of Renewable Energy processes, Elsevier Inc., 2005.

[62] M. Y. a. D. F., "Assessment of solar and wind energy resources in Ethiopia: II. Wind energy," *Solar Energy*, Vols. 57, No. 4, pp. 323-334, 1996.

[63] B. W. .Duffie J.A., Solar Engineering of Thermal Processes, 3rd Edition, New York: Wiley, 1991.

[64] G. T. .. A. T. Shyam, Handbook of Solar Energy Theory, Analysis and Applications, Singapore: Springer, 2016.

[65] *List of the Power Consumption of Typical Household Appliances available on: https://www.daftlogic.com/information appliance power consumption,* @09:55, on 26/03/2019.

[66] "how to design solar pv system. available on http://www.leonic.com @11:03, on 08/03/2019".

[67] A. J. Kaller R, Electric Traction 1, Lausanne: Polytechnic and university pressesRomande, 1995.

[68] e. a. Dakyo B, "Control strategy for stand alone wind-diesel hybrid system using a speed model," in *In: 7th International ELECTRIMACS Congress*, Montréal, 2005.

[69] G. M. Masters, Renewable and Efficient Electric Power Systems, Hoboken, New Jersey: John Wiley & Sons, Inc, 2004.

[70] G. Fletcher, The Electrician's Guide To Photovoltaic System Installation, Canada, 2013.

[71] S. C. Krauter, Solar Electric Power Generation - Photovoltaic Energy Systems, Berlin Heidelberg : Springer, 2006.

[72] M. R. SUNNY, Sizing An Energy Storage To Be Used In Parallel With PV Inverter To Balance The Fluctuations In Output Power From PV Generator Msc, Thesis, Tampere University of Technology, 2014.

[73] R. M. a. A. Abtahi, Photovoltaic Systems Engineering, 4th edition, CRC Press, 2017.

[74] M. R. Patel, Spacecraft Power Systems, CRC Press, 2004.

[75] M. A. G. M. E. W. a. S. R. W. R. Corkish, Applied Photovoltaics, 2nd ed., Earthscan, 2007.

[76] B. e. a. Ali, "Hybrid Photovoltaic Diesel System in a Cable Car Resort Facility," *European Journal of Scientific Research,* vol. 26 No.1, 2010.

[77] G. Fletcher, The Electrician's Guide To Photovoltaic System Installation, USA, 2014.

[78] *Operation of PLC . available on: https://mohandseeen.blogspot.com/2012/02/principles-of-plc-operation-cpu-inputs.html.*

[79] C. Ghiţă, Electrical Machines, Matrix-Rom: House, Bucharest, 2005.

[80] W.D.Soto, "Improvement and Validation of a Model for Photovoltaic Array Performance," M.Sc. Thesis, Solar Energy Laboratory, University of Wisconsin Madison, 2012.

[81] R. J. a. R. Y. D. Wai, "High-efficiency bidirectional converter for power sources with great voltage diversity," *IEEE Trans. Power Electron,* vol. 22, pp. 1986-1996, Sep. 2007.

[82] M. H. Rashid, "Pulse-Width-Modulation Inverters," *Upper Saddle River, NJ: Prentice-Hall,* p. 237–248, 2004.

[83] A. K. e. al, "LCL filter design for photovoltaic grid connected systems," *Revue des Energies Renouvelables SIENR,* p. 227 – 232, 2014.

[84] P. Cilman, "Hybrid Optimization Model of Electric Renewable," Available:www.homerenergy.com., March 2013.

[85] M. Ibrahim, "Decentralized Hybrid Renewable Energy Systems," Dissertation, Kassel, Germany, 2002.

[86] O. O. E. O. R. Saiju, A Simulation Model for Expandable Hybrid Power, Systems, Kasseler Symposium, 2002, Kassel, Germany.

[87] "Ministry of Water, Irrigation and Energy. www.moie.gov.et".

[88] G. mengstie, "Ethiopia- The case of small scale Renewable Energy for all financing access for the poor," Oslo, 11 October 2011.

[89] P. Cook, "Infrastructure, rural electrification and development," *Energy Sustain*, pp. vol. 15, no. 3, pp. 304–313, Sep. 2011.

[90] H. W. a. B. LI, "The cooperated MPPT Control of stand-alone PV power Generation System," in *Proceedings of the 8th world congress on intellignet Control and Automation*, China, pp 2228 – 2231, 2010.

[91] C. J. a. L. Q. Guo X. Yun, "Real-Time and grid-connected control of PV power system," in *The international conference on advanced power systesm automation and protection*, pp 923 – 92, 82011.

[92] P. L. a. P. Gilman, "Micro power System Modeling With HOMER," 2006.

[93] D. Linden, Handbook of Batteries, New York: McGraw-Hill, 1995.

[94] M. R. Patel, Wind and Solar Power Systems, Boca Raton, FL: CRC Press, 1999.

[95] L. V. O. a. A. V. Loon, "Facts & Figures Solar Energy Eastern Africa," Solarplaza, 2017.

[96] S. e. Krishnaa., "Modeling and Simulation of Grid Connected PV/WT Energy System Using Super-Capacitor," *IOSR Journal of Engineering (IOSRJEN),* pp. 01-07, Apr. 2008.

Appendix-A

```
%program for I-V and P-V Characteristics curve of a PV array:

% function Ia = poly240i (Va,Suns,Tac)
% % model for the Poly240 solar array
% current given voltage, illumination, and temperature
% Ia=poly240(Va,G,T)=array voltage
% Ia,Va=array current,voltage
% G=num of Suns (1 Sun=1000 w/m^2)
% T=Temp in Deg C
K=1.38e-23;%Boltzman's const
 q=1.60e-19;%charge on an electron
% enter the following constants here and the model will be
%calculated based on these. for 1000w/m^2
 Tac=30
 Suns=1000
 A = 1.3; % "diode quality" factor,=2 for crystalline, <2 for amorphous
 Vg = 1.12; %band gap voltage, 1.12 for Xtal Si, ~1.75 for amorphous Si
Ns=60;%number of series connected cells
T1 = 273+25;
Voc_T1 = 37.1/Ns % open circuit voltage per cell at temperatureT1
Isc_T1 = 8.42;% short circuit current  per cell at Temperature T1
T2 = 273+75;
Voc_T2 = 37,3/Ns% open circuit voltage per cell at temperature T2
Isc_T2 = 8.52;% Short circuit current per cell at temperature T2
TaK = 273+Tac; % array temperature
TrK = 273+25;% Reference Temperature
Iph_T1 = Isc_T1*Suns;
a = (Isc_T2-Isc_T1)/Isc_T1*1/(T2-T1);
Iph = Iph_T1*(1+a*(TaK-T1))
  Vt_T1 = K*T1/q;% =A*KT/q
Ir_T1 = Isc_T1/(exp(Voc_T1/(A*Vt_T1))-1);
Ir_T2 = Isc_T2/(exp(Voc_T2/(A*Vt_T1))-1);
b = Vg*q/(A*K);
Ir = Ir_T1*(T1/TaK.^(3/A).*exp(-b.*(1./TaK-1/T1))
X2V = Ir_T1/(A*Vt_T1)*exp(Voc_T1/(A*Vt_T1));
dVdI_Voc = -1.15/Ns/2; %dV/dI at Voc per cell from manufacturers graph
Rs = -dVdI_Voc-1/X2V% series resistance per cell
dVdI_Isc = -1.45/Ns/2; %dV/dI at Isc per cell from manufacturers graph
X3V = Ir_T1/(A*Vt_T1)*exp(Isc_T1/(A*Vt_T1));
 Rp = -dVdI_Isc-1/X3V % Shunt resistance per cell
%  Ia = 0:0.01:Iph;
Vt_Ta = A*1.38e-23*TaK/1.60e-19;   % =A*KT/q
 % Ia1= Iph-Ir.*(exp((Vc+Ia.*Rs)./Vt_Ta)-1);
% solve for Ia:f(Ia) = Iph-Ia-Ir.*(exp((Vc+Ia.*Rs)./Vt_Ta)
%  Newton's method: Ia2 = Ia1-f(Ia1)/f'(Ia1)
Va=37.1;
Vc=Va/Ns;
Ia=zeros(size(Vc));
%Iav=Ia;
for j=1:20;
    Ia=Ia-[(Iph-Ia-Ir.*(exp((Vc+Ia.*Rs)./Vt_Ta)-1))-((Vc+Ia.*Rs)./Rp)]...
        ./(-1-(Ir.*(exp((Vc+Ia.*Rs)./Vt_Ta)-1)).*Rs./Vt_Ta)-
((Vc+Ia.*Rs)./Rp)
% Iav=[Iav;Ia]  %to observe convergence for debugging.
```

```
  end
p=Va.*Ia
I=0
for Ir = 9.7926e-008
    for Iph = 7.78
            V = ((A*K*T1*Ns)/q)*log((Iph+Ir-I)/Ir);
             v = [0:0.001:V]
              i = (Iph-(Ir*exp((q*v)/(A*K*T1*Ns)))+Ir);
              p = v.*i;
            figure(1)
            plot(v,i,'-');
            hold on
            xlabel('Module Voltage(V)')
            ylabel('Module Current(A)')
            title('Current-Voltage Characteristics ');
            grid on
            figure(2)
            plot(v,p,'-');
            hold on
            xlabel('Module Voltage(V)')
            ylabel('Module Power(W)')
             title('Power-Voltage Characteristics ');
             grid on
            end
   end

%Program for various irradiance:

 I = 0;
 Ir = 9.7926e-008;
   for  Iph = [7.78  7.66 7.55 7.41]
           V = ((A*K*T1*Ns)/q)*log((Iph+Ir-I)/Ir);
             v = [0:0.01:V]
             i= (Iph-(Ir*exp((q*v)/(A*K*T1*Ns)))+Ir);
              p=v.*i
              figure(3);
              plot(v,i,'-');
              hold on
              xlabel('Module Voltage(V)')
              ylabel('Module Current(A)')
              title('Current-Voltage Characteristics ');
              grid on
              figure(4)
              set(gcf,'Color', 'w')
              plot(v,p,'r-');
              hold on
              xlabel('Module Voltage(V)')
              ylabel('Module Power(W)')
              title('Power-Voltage Characteristics ');
              grid on
         end

%Program for different temperatures:

   Iph = 7.78;
   I = 0;
```

```
for  Ir = [9.7926e-008 2.2607e-007 3.7821e-007 6.1348e-007]
              V = ((A*K*T1*Ns)/q)*log((Iph+Ir-I)/Ir);
               v = [0:0.001:V]
                i = (Iph-(Ir*exp((q*v)/(A*K*T1*Ns)))+Ir);
                p = v.*i;
                figure(5)
                plot(v,i,'-');
                hold on
                xlabel('Module Voltage(V)')
                ylabel('Module Current(A)')
                 title('Current-Voltage Characteristics ');
                grid on
                figure(6)
                plot(v,p,'r-');
                hold on
                xlabel('Module Voltage(V)')
                ylabel('Module Power(W)')
                title('Power-Voltage Characteristics ');
                 grid on
           end

%Program for both varying irradiance and temperature:

I = 0
for Ir = 9.7926e-008
    for Iph = 7.78
          V = ((A*K*T1*Ns)/q)*log((Iph+Ir-I)/Ir);
          v = [0:0.001:V]
           i = (Iph-(Ir*exp((q*v)/(A*K*T1*Ns)))+Ir);
           p = v.*i;
           figure(7)
           plot(v,i,'-');
           hold on

    for  Ir = 6.9399e-007
        for  Iph = 7.66
                V = ((A*K*T1*Ns)/q)*log((Iph+Ir-I)/Ir);
                v = [0:0.001:V]
                i = (Iph-(Ir*exp((q*v)/(A*K*T1*Ns)))+Ir);
                p = v.*i;
                plot(v,i,'-');
                hold on
    for  Ir = 1.6385e-007
        for  Iph = 1.8790
                 V = ((A*K*T1*Ns)/q)*log((Iph+Ir-I)/Ir);
                  v = [0:0.001:V]
                  i = (Iph-(Ir*exp((q*v)/(A*K*T1*Ns)))+Ir);
                  p = v.*i;
                  plot(v,i,'-');
                  hold on
                  xlabel('Module Voltage(V)')
                  ylabel('Module Current(A)')
                 title('Current-Voltage Characteristics ');
                   grid on
                           end
                       end
```

```
                  end
            end
      end
end
for Ir=9.7926e-008
    for Iph=7.78
   %Ir=9.7926e-008;
   V=((A*K*T1*Ns)/q)*log((Iph+Ir-I)/Ir);
    v=[0:0.001:V]
    i=(Iph-(Ir*exp((q*v)/(A*K*T1*Ns)))+Ir);
    p=v.*i;
    % subplot(2,1,1);
    figure(4)
    plot(v,p,'-');
    hold on
    for Ir=6.9399e-007
        for Iph=7.66
            V=((A*K*T1*Ns)/q)*log((Iph+Ir-I)/Ir);
    v=[0:0.001:V]
    i=(Iph-(Ir*exp((q*v)/(A*K*T1*Ns)))+Ir);
    p=v.*i;
    plot(v,p,'-');
    hold on
    for Ir=1.6385e-007
        for Iph=7.55
            V=((A*K*T1*Ns)/q)*log((Iph+Ir-I)/Ir);
    v=[0:0.001:V]
    i=(Iph-(Ir*exp((q*v)/(A*K*T1*Ns)))+Ir);
    p=v.*i;
    plot(v,p,'-');
    hold on
     xlabel('Module Voltage(V)')
    ylabel('Module Power(W)')
    title('Power-Voltage Characteristics ');
    grid on;
        end
    end
    end
    end
    end
```